DAVID MENOTTI GOMES

Orientador: Arnaldo de Albuquerque Araújo
Co-orientador: Laurent Najman

REALCE DE CONTRASTE EM IMAGENS DIGITAIS USANDO EQUALIZAÇÃO DE HISTOGRAMA

Belo Horizonte
Abril de 2008

Universidade Federal de Minas Gerais
Instituto de Ciências Exatas
Programa de Pós-Graduação em Ciência da Computação

REALCE DE CONTRASTE EM IMAGENS DIGITAIS USANDO EQUALIZAÇÃO DE HISTOGRAMA

Tese apresentada ao Curso de Pós-Graduação em Ciência da Computação da Universidade Federal de Minas Gerais como requisito parcial para a obtenção do grau de Doutor em Ciência da Computação.

DAVID MENOTTI GOMES

Belo Horizonte
Abril de 2008

Federal University of Minas Gerais
Instituto de Ciências Exatas
Graduate Program in Computer Science

CONTRAST ENHANCEMENT IN DIGITAL IMAGING USING HISTOGRAM EQUALIZATION

Thesis presented to the Graduate Program in Computer Science of the Federal University of Minas Gerais in partial fulfillment of the requirements for the degree of Doctor in Computer Science.

DAVID MENOTTI GOMES

Belo Horizonte
April 2008

UNIVERSIDADE FEDERAL DE MINAS GERAIS

FOLHA DE APROVAÇÃO

Realce de Contraste em Imagens Digitais usando Equalização de Histograma

DAVID MENOTTI GOMES

Tese defendida e aprovada pela banca examinadora constituída por:

Dr. Arnaldo de Albuquerque Araújo – Orientador
Universidade Federal de Minas Gerais

Dr. Laurent Najman – Co-orientador
Université Paris-Est

Dr. Mario Fernando Montenegro Campos
Universidade Federal de Minas Gerais

Dr. Alexei Manso Corrêa Machado
Pontifícia Universidade Católica de Minas Gerais

Dr. Jacques Facon
Pontifícia Universidade Católica do Paraná

Dr. Ricardo da Silva Torres
Universidade de Campinas

Belo Horizonte, Abril de 2008

Resumo

Dispositivos para aquisição e processamento de imagens podem ser encontrados em sistemas complexos de monitoração de segurança ou simples aparelhos celulares. Em certas aplicações, o tempo necessário para processar uma imagem não é tão importante quanto a qualidade das imagens processadas (por exemplo, em imagens médicas), mas em alguns casos a qualidade da imagem pode ser sacrificada em favor do tempo. Essa tese foca-se no nesse último caso, e propõe dois tipos de métodos eficientes para o realce de contraste de imagens. Os métodos propostos são baseados em equalização de histograma (EH), e alguns focam imagens em tons de cinza e outros imagens coloridas.

Os métodos baseados em HE atualmente utilizados para processar imagens em tons de cinza tendem a mudar o brilho médio da imagem para o tom médio do intervalo de tons de cinza. Essa mudança não é desejavél em aplicações que visam melhorar o contraste em produtos eletrônicos utilizados pelo consumidor, onde preservar o brilho da imagem original é necessário para evitar o aparecimento de artefatos não exitentes na imagem de saída. Para corrigir esse problema, métodos de bi-equalização de histogramas para preservação do brilho e contraste de imagens foram propostos. Embora esses métodos preservem o brilho da imagem original na imagem processada com um realce significante do contraste, eles podem produzir imagens que não parecem naturais. Esse novo problema foi resolvido por uma nova tecnica chamada Equalização de Multi-histogramas, que decompõe a imagem original em várias sub-imagens, e aplica o método de EH clássico em cada uma delas. Essa metologia execute um relace de contraste menos intenso, de forma que a imagem processada parece mais natural. Essa tese propõe duas novas funções de discrepância para decomposição de imagens, originando dois novos métodos de Multi-EH. Além disso, uma função de custo é utilizada para determinar em quantas sub-imagens a imagem original será dividida. Experimentos mostraram que os métodos propostos são melhores que outros EH estudados, uma vez que eles preservam o brilho e produzem imagens com uma aparência mais natural.

Em relação aos métodos para realce de contraste em imagens coloridas, essa tese propõe um método genérico e eficiente de EH baseado no espaço de cores RGB que preserva a tonalidade da cor, e implementa duas instâncias desse método genérico. A primeira instanciação utiliza os histogramas $1D$ *R-red*, *G-green* e *B-blue* para estimar um histograma $3D$ *RGB*, que é então equalizado. A segunda instanciação, por sua vez, utiliza os histogramas $2D$ *RG*, *RB*, e *GB*.

A EH é executada utilizando transformadas de deslocamento que preservam a tonalidade da cor, evitando o aparecimento de cores não realistas. Os métodos propostos tem complexidade linear no espaço e no tempo em relação ao tamanho da imagem, e não usam nenhuma conversão de um espaço de cores para outro. As imagens produzidas foram avaliadas subjetiva e objetivamente, comparando os métodos propostos com outros estudados. A avaliação objetiva foi feita utilizando medidas de contraste e de qualidade da cor da imagem, onde a qualidade foi definida como uma função ponderada dos índices de naturalidade e coloridade. Um conjunto de 300 imagens extraídas da base de dados da Universidade de Berkeley foram analisadas. Os experimentos mostratam que o valor do contraste das imagens produzidas pelos métodos propostos é em médias 50% maior que o valor do contraste na imagem original, e ao mesmo tempo a qualidade das imagens produzidas é próxima a qualidade da imagem original.

Abstract

Today, devices able to capture and process images can be found in complex surveillance monitoring systems or simple mobile phones. In certain applications, the time necessary to process the image is not as important as the quality of the processed images (*e.g.*, medical imaging), but in other cases the quality can be sacrificed in favour of time. This thesis focus on the latter case, and proposes two types of fast image contrast enhancement methods. The proposed methods are based on histogram equalization (HE), and some target gray-level images while others target color images.

Regarding HE methods for gray-level images, current methods tend to change the mean brightness of the image to the middle level of the gray-level range. This is not desirable in the case of image contrast enhancement for consumer electronics products, where preserving the input brightness of the image is required to avoid the generation of non-existing artifacts in the output image. To surmount this disadvantage, Bi-histogram equalization methods for brightness preserving and contrast enhancement have been proposed. Although these methods preserve the input brightness on the output image with a significant contrast enhancement, they may produce images which do not look as natural as the input ones. In order to overcome this drawback, we propose a technique called Multi-HE, which consists of decomposing the input image into several sub-images, and then applying the classical HE process to each one of them. This methodology performs a less intensive image contrast enhancement, in a way that the output image presents a more natural look. We propose two discrepancy functions for image decomposing, conceiving two new Multi-HE methods. A cost function is also used for automatically deciding in how many sub-images the input image will be decomposed on. Experiments show that our methods are better in preserving the brightness and producing more natural looking images than the other HE methods.

In order to deal with contrast enhancement in color images, we introduce a generic fast hue-preserving histogram equalization method based on the RGB color space, and two instantiations of the proposed generic method. The first instantiation uses R-red, G-green, and B-blue $1D$ histograms to estimate a RGB $3D$ histogram to be equalized, whereas the second instantiation uses RG, RB, and GB $2D$ histograms. The histogram equalization is performed using shift hue-preserving transformations, avoiding the appearance of unrealistic colors. Our methods have linear time and space complexities with respect to the image dimension, and do

not need to apply conversions from a color space to another in order to perform the image contrast enhancement. Subjective and objective assessments comparing our methods and others are performed using a contrast measure and a color image quality measure, where the quality is established as a weighed function of the naturalness and colorfulness indexes. We analyze 300 images from a dataset of the University of Berkeley. Experiments show that the value of the image contrast produced by our methods is in average 50% greater than the original image value, keeping the quality of the produced images close to the original one.

Résumé

Aujourd'hui, des appareils capables de capter et de traiter les images peuvent être trouvés dans les systèmes complexes de surveillance ou de simples téléphones mobiles . Dans certaines applications, le temps nécessaire au traitement de l'image n'est pas aussi important que la qualité du traitement des images (par exemple, l'imagerie médicale), mais dans d'autres cas, la qualité peut être sacrifiée au profit du temps . Cette thèse se concentre sur ce dernier cas, et propose deux types des méthodes rapides pour l'amélioration du contraste d'image . Les méthodes proposées sont fondées sur l'égalisation d'histogramme (EH), et certaines s'adressent à des images en niveaux de gris, tandis que d'autres s'adressent à des images en couleur .

En ce qui concerne les méthodes EH pour des images en niveaux de gris, les méthodes actuelles tendent à changer la luminosité moyenne de l'image de départ pour le niveau moyen de la bande de niveau de gris . Ce n'est pas souhaitable dans le cas de l'amélioration du contraste d'image pour les produits de l'électronique grand-public, où la préservation de la luminosité de l'image de départ est nécessaire pour éviter la production d'artefacts non-existant dans l'image de sortie . Pour éviter cet inconvénient, des méthodes de Bi-égalisation d'histogrammes pour préserver la luminosité et l'amélioration du contraste ont été proposées . Bien que ces méthodes préservent la luminosité de l'image de départ tout en améliorant fortement le contraste, elles peuvent produire des images qui ne donnent pas une impression visuelle aussi naturelle que les images de départ . Afin de corriger ce problème, nous proposons une technique appelée multi-EH, qui consiste à décomposer l'image en plusieurs sous-images, et à appliquer le procédé classique de EH à chacun d'entre eux . Cette méthode, bien qu'elle offre une amélioration du contraste moins marquée, produit une image de sortie d'une apparence plus naturelle . Nous proposons deux fonctions de décalage pour découpage d'histogramme, concevant ainsi deux nouvelle méthodes de multi-EH . Une fonction de coût est également utilisé pour déterminer automatiquement en combien de parties l'histogramme de l'image d'entrée sera décomposé . Les expériences montrent que nos méthodes sont meilleures pour la préservation de la luminosité et produisent des images plus naturelles que les autres méthodes de EH .

Pour améliorer le contraste dans les images en couleur, nous introduisons une méthode générique et rapide, qui préserve la teinte. L'égalisation d'histogramme est fondée sur l'espace couleur *RGB*, et nous proposons deux instanciations de la méthode générique . La première instanciation utilise des histogrammes $1D$ *R-red*, *G-green*, et *B-bleu* afin d'estimer l'histogramme

$3D$ RGB qui doit être égalisé, alors que le deuxième instanciation utilise des histogrammes $2D$ RG, RB, et GB . L'égalisation d'histogramme est effectué en utilisant des transformations de décalage qui preserve la teinte, en évitant l'apparition de couleurs irréalistes . Nos méthodes ont des complexités de temps et d'espace linéaire, par rapport à la taille de l'image, et n'ont pas besoin de faire la conversion d'un espace couleur à l'autre afin de réaliser l'amélioration du contraste de l'image . Des évaluations subjectives et objectives comparant nos méthodes et d'autres sont effectués au moyen d'une mesure de contraste et de couleur afin de mesurer la qualité de l'image, où la qualité est établi comme une fonction pondérée d'un indice de "naturalité" et d'un indice de couleur . Nous analysons 300 images extraites d'un base de données de l'Université de Berkeley . Les expériences ont montré que la valeur de contraste de l'image produite par nos méthodes est en moyenne de 50% supérieure à la valeur de contraste de l'image original, tout en conservant une qualité des images produites proche de celle des images originales .

To my father. I believe he is gardening in heaven.

Publications

The list of works published (and submitted) during the doctorate study is shown in the followings. The publications related to the thesis are marked with stars (*). At the end of this document, we briefly describe the works not directly related with the thesis.

Articles in Journals

1. (*) Menotti, D., Najman, L., Facon, J., and de Albuquerque Araújo, A. (2007c). Multi-histogram equalization methods for contrast enhancement and brightness preserving. *IEEE Transaction on Consumer Electronics*, 53(3):1186–1194.

2. (*) Menotti, D., Najman, L., de Albuquerque Araújo, A., and Facon, J. (2008). Fast hue-preserving histogram equalization methods for color image contrast enhancement. *IEEE Transaction on Consumer Electronics* submitted on January 15, 2008.

3. Menotti, D. and Borges, D. L. (2007). Segmentation of envelopes and address block location by salient features and hypothesis testing. *INFOCOMP Journal of Computer Science*, 6(1):66–79.

Papers in Conferences

1. (*) Menotti, D., Najman, L., de Albuquerque Araújo, A., and Facon, J. (2007b). A fast hue-preserving histogram equalization method for color image enhancement using a bayesian framework. In *14th International Workshop on Systems, Signals and Image Processing (IWSSIP 2007)*, pages 414–417, Maribor, Slovenija. IEEE Catalog Number: 07EX1858C, ISBN: 978-961-248-029-5, CIP 621.391(082).

2. Menotti, D., Najman, L., and de Albuquerque Araújo, A. (2007a). 1d component tree in linear time and space and its application to gray-level image multithresholding. In *8th International Symposium on Mathematical Morphology (ISMM)*, pages 437–448, Rio de Janeiro, Brazil.

3. (*) Menotti, D., Melo, A. P., de Albuquerque Araújo, A., Facon, J., and Sgarbi, E. M. (2006). Color image enhancement throught 2D histogram equalization. In *13th International Conference on Systems, Signals and Image Processing (IWSSIP 2006)*, pages 235–238, Budapest, Hungry.

4. Melo, A. P., Menotti, D., Facon, J., Sgarbi, E. M., and de Albuquerque Araújo, A. (2005). Realce de imagens coloridas através da equalização de histogramas 2D. In *Workshop of Undergraduate Students - XVIII Brazilian Symposium on Computer Graphics and Image Processing (SIBGRAPI 2005)*, pages 1–8, Natal, Brazil.

5. Menotti, D., Borges, D. L., and de Albuquerque Araújo, A. (2005). Statistical hypothesis testing and wavelets features for region segmentation. In *10th Iberoamerican Congress on Pattern Recognition (CIARP 2005), LNCS 3773*, pages 671–678, Havana, Cuba.

6. Facon, J., Menotti, D., and de Albuquerque Araújo, A. (2005). Lacunarity as a texture measure for address block segmentation. In *10th Iberoamerican Congress on Pattern Recognition (CIARP 2005), LNCS 3773*, pages 112–119, Havana, Cuba.

7. Menotti, D., Facon, J., Borges, D. L., and de Souza Britto-Jr, A. (2004b). Segmentacao de envelopes postais para localizacao do bloco endereco: uma abordagem baseada em selecao de caracter1sticas no espaco *Wavelet*. In *III Workshop of Theses and Dissertations on Computer Graphics and Image Processing (WTDCGPI), part of SIBGRAPI'2004*, page 8, Curitiba, Paraná, Brazil.

8. Menotti, D., Facon, J., Borges, D. L., and de Souza Britto-Jr, A. (2004a). A quantitative evaluation of segmentation results through the use of ground-truth images: an application to postal envelope segmentation. In *Eletronical (CD-ROM) Proceedings of SIBGRAPI'2004, Technical Poster IEEE Brazilian Symposium on Computer Graphics and Image Processing*, page 1, Curitiba, Paraná, Brazil.

9. Eiterer, L. F., Facon, J., and Menotti, D. (2004b). Postal envelope address block location by fractal-based approach. In *XVII Brazilian Symposium on Computer Graphics and Image Processing, (SIBGRAPI 2004)*, pages 90–97, Curitiba, PR, Brasil.

10. Eiterer, L. F., Facon, J., and Menotti, D. (2004a). Envelope address block segmentation through fractal-based approach. In *9th Iberoamerican Congress on Pattern Recognition (CIARP 2004), LNCS 3287*, pages 454–461, Puebla, Mexico.

11. Eiterer, L. F., Facon, J., and Menotti, D. (2004c). Segmentation of envelope address blocks through fractal-based approach. In *Iberoamericam Meeting on Optics (RIAO) and Optics Lasers and Their Aplications (OPTILAS)*, pages 1–6, Porlamar, Venezuela.

Technical Reports

1. Botelho, F., Menotti, D., and Ziviani, N. (2004). A new algorithm for constructing minimal perfect hash functions. Technical Report TR004/04, Department of Computer Science, Universidade Federal de Minas Gerais.

Contents

List of Figures

List of Tables

List of Algorithms

Chapter 1

Introduction

Nowadays digital cameras are certainly the most used devices to capture images. They are everywhere, including mobile phones, personal digital assistants (PDAs - a.k.a. pocket computers or palmtop computers), robots, and surveillance and home security systems. There is no doubt that the quality of the images obtained by digital cameras, regardless of the context in which they are used, has improved a lot since digital cameras early days. Part of these improvements are due to the higher processing capability of the systems they are built-in and memory availability. However, there are still a variety of problems which need to be tackled regarding the quality of the images obtained, including:

1. contrast defects,
2. chromatic aberrations,
3. various sources of noises,
4. vignetting,
5. geometrical distortions,
6. color demosaicing and
7. focus defects.

Among the seven problems related above, some are more dependent on the quality of the capture devices used (like 2-7), whereas others are related to the conditions in which the image was captured (such as 1). When working on the latter, the time required to correct the problem on contrast is a big issue. This is because the methods developed to correct these problems can be applied to an image on a mobile phone with very low processing capability, or on a powerful computer.

Moreover, in real-time applications, the efficiency of such methods is usually favored over the quality of the images obtained. A fast method generating images with medium enhancement on image contrast is worth more than a slow method with outstanding enhancement.

With this in mind, this work proposes two types of methods based on histogram equalization (HE) to enhance contrast in digital images. Although there has been a lot of research in the image enhancement area for 40 years (Graham, 1962; Rosenfeld and Kak, 1976; Wang et al., 1983; Zhu et al., 1999; Wang and Bovik, 2006), there is still a lot of room for improvement concerning the quality of the enhanced image obtained and the time necessary to obtain it.

HE is a histogram specification process (Zhang, 1992; Kundu, 1998; Coltuc et al., 2006) which consists of generating an output image with a uniform histogram (*i.e.*, uniform distribution). In image processing, the idea of equalizing a histogram is to stretch and/or redistribute the original histogram using the entire range of discrete levels of the image, in a way that an enhancement of image contrast is achieved. Figure 1.1 shows an illustrating example of using HE for image contrast enhancement.

The first type of proposed methods, which deals with gray-level images, works on a multi-HE (MHE) framework for image contrast enhancement. These MHE methods are especially useful for applications where the brightness (*i.e.*, the mean gray-level) of the processed images must be preserved, and real-time processing is required (*e.g.*, digital cameras and video surveillance systems).

On the other hand, the second type of proposed methods concentrates on color images, and also focus the improvement of image contrast. They implement HE methods based on the *RGB* color space[1] (Kuehni and Schwarz, 2008) which are hue-preserving (Naik and Murthy, 2003), *i.e.*, neither new nor unrealistic colors are produced. In other words, these methods prevent the appearance of new and unrealistic colors in the enhanced image, and are linear in time (with respect to the image dimension). Because this second type of method is linear in time, it is indicated to enhance images in real-world applications, such as natural images acquired by mobile phones and PDAs.

Remark that the first type of methods can be seen as a more elaborated version of the existing methods for brightness preserving in gray-level image contrast enhancement through HE. The second type of methods, in contrast, is a simplified, fast and hue-preserving color image contrast enhancement method with respect to the proposed existing ones. The next section describes the main motivations to use the two types of methods just described.

[1]The color space which is composed of R-red, G-green and B-blue color channels

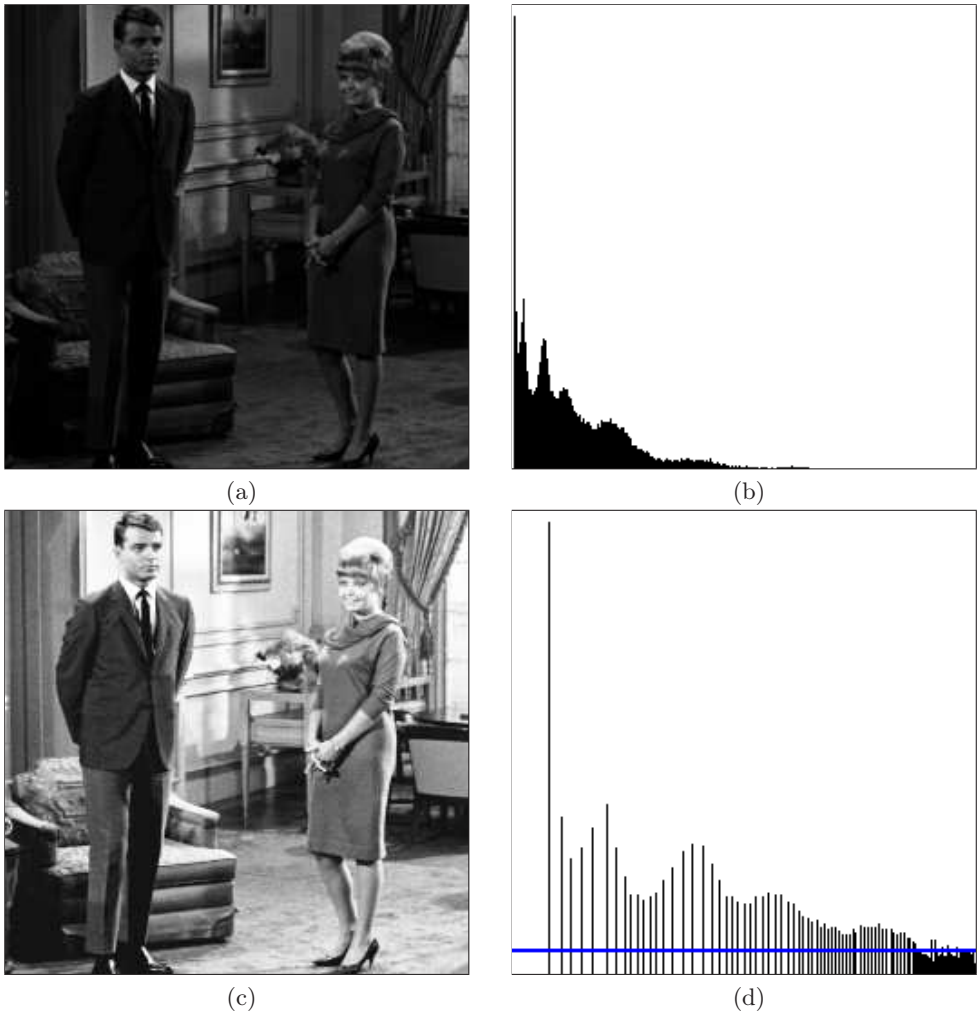

Figure 1.1: Illustration of HE. (a) Original image. (b) Histogram of the original image. (c) Processed image. (d) Histogram of the processed image.

1.1 Motivation

Image enhancement methods based on improvements of contrast and avoidance of the appearance of unrealistic colors are really useful in applications where an image with more distinguished texture details and perceptually better colors are required. As explained before, these applications include surveillance system based on images or simply better image visualization in mobile phones and PDAs. Although there are a lot of techniques available to perform these tasks, all of them have advantages and drawbacks.

HE is a technique commonly used for image contrast enhancement, since it is computationally fast and simple to implement. Our main motivation is to preserve the best features the HE methods have, and introduce some modifications which will overcome the drawbacks

associated with them.

In the case of **gray-level image contrast enhancement**, methods based on HE (Castleman, 1979; Pizer et al., 1984, 1987; Zuiderveld, 1994; Ibrahim and Kong, 2007) have been the most used. Despite its success for image contrast enhancement, this technique has a well-known drawback: it does not preserve the brightness of the input image on the output one. This drawback makes the use of classical HE techniques (Gonzalez and Woods, 2002) not suitable for image contrast enhancement on consumer electronic products, such as video surveillance, where preserving the input brightness is essential to avoid the generation of non-existing artifacts in the output image.

To overcome such drawback, variations of the classic HE technique, such as Kim (1997); Wang et al. (1999); Chen and Ramli (2003b), have proposed to first decompose the input image into two sub-images, and then perform HE independently in each sub-image. For the decomposition, these methods use some statistical measures of the image, which consider the value of the image gray-levels. These methods based on Bi-HE perform image contrast enhancement with success while preserving the input brightness in some extend, but they might generate images which do not look as natural as the input ones. Such result is unacceptable for consumer electronics products.

Hence, in order to enhance contrast, preserve brightness and produce natural looking images, we propose a generic MHE method which first decomposes the input image into several sub-images, and then applies the classical HE process to each of them. We present two discrepancy functions to decompose the image, conceiving two variants of that generic MHE method for image contrast enhancement, *i.e.*, Minimum Within-Class Variance MHE (MWCVMHE) and Minimum Middle Level Squared Error MHE (MMLSEMHE). A cost function, taking into account both the discrepancy between the input and enhanced images and the number of decomposed sub-images, is used to automatically make the decision of in how many sub-images the input image will be decomposed on.

Regarding the **color image contrast enhancement**, the classical image enhancement methods are also based on HE. The extension of these methods to color images is not straightforward. This is because there are some particular properties of color images which need to be properly taken into account during image contrast enhancement.

Among these properties are the luminance (L) (or intensity (I)), saturation (S) and hue (H) attributes of the color (Berns et al., 2000). Color spaces such as *HSV*, *HSI*, *CIELUV* and *CIELAB*[2] were conceived based on these three attributes (Kuehni and Schwarz, 2008). Whereas the luminance represents the achromatic part of the color (*e.g.*, it can be defined as a weighted function of the R, G, and B color channels), the saturation and hue refer to the chromatic part of the image. The saturation can be seen as measure of how much white is

[2] *CIELUV* and *CIELAB* are two uniform color spaces developed by the *Commission Internationale de l'Eclairage - CIE*, where L stands for the luminance and A, B, U and V stand for the color channels.

present in the color, and the hue is the attribute of the color which decides its "real color", *e.g.*, red or green. For the purpose of enhancing a color image, the hue should not be changed for any pixel, avoiding output images with unnatural aspect.

However, color images in digital devices, such as mobile phones, cameras and PDAs, are commonly transmitted, displayed and stored in the RGB color space (*i.e.*, R-red, G-green, and B-blue). This color space is not the most appropriated one for image processing tasks, since the meaning of the attribute colors is not explicitly separated as it would be in other color spaces. The conversion from the RGB color space to a Luminance-Hue-Saturation (LHS)-based color space is trivial, but can be both not suitable for real-time applications and the digital devices referred above. Moreover, working on a LHS-based color space requires tackling the well-known gamut problem (Naik and Murthy, 2003).

The literature of HE methods for color image contrast enhancement presents works based on the RGB, LHS, $CIELUV$ and other color spaces. Both the methods based on the RGB color space and the ones based on other color spaces do not present all the characteristics required for use in portable devices: to be fast, improve the images contrast and still preserve the hue. The formers because the hue is not preserving, and the latter methods due the time required for conversions among color spaces and maybe the same reasons pointed for the former methods. In order to achieve that, this work presents a generic fast hue-preserving HE method based on the RGB color space for image contrast enhancement.

From the generic method we create two variants, which are characterized by the histograms dimension they use, *i.e.*, $1D$ or $2D$. The equalization is performed by hue-preserving transformations directly in the RGB color space, avoiding the gamut problem, keeping the hue unchanged[3] and the requirement of conversion between color spaces. Moreover, our methods improve the image contrast (*i.e.*, improve the variance on the luminance attribute) and, simultaneously, the saturation is modified according to the equalization of the RGB histogram. The methods estimate the RGB $3D$ histogram to be equalized through R, G and B $1D$ histograms and RG, RB, and GB $2D$ histograms, respectively, yielding algorithms with time and space complexities linear with respect to the image dimension. These characteristics make these methods suitable for real-time applications.

At this point, it is worth noticing that there are several sophisticated color image contrast enhancement methods available in the literature, such as Huang et al. (2006); Luft et al. (2006). However, these methods are so computationally expensive that their use is neither practical for real-time nor real-world applications. This is in contrast with our methods, which are linear in time and space (regarding the image dimension).

[3] In Naik and Murthy (2003), it is shown that a shift transformation on the RGB color space by the same factor in all three channels is hue-preserving

1.2 Objectives

Given the motivations presented above, the main objectives of this work are:

1. Create MHE methods for gray-level image contrast enhancement with constraints to the processed images: brightness preserving and natural looking.
2. Compare the methods developed for gray-level image contrast enhancement with other HE-based methods by means of the $PSNR$ measure, brightness preserving and contrast enhancement.
3. Build fast hue-preserving HE methods for color image contrast enhancement.
4. Compare the methods developed for color image contrast enhancement with existent ones using quantitative measures, such as color naturalness and colorfulness indexes (see (Yendrikhovskij et al., 1998b,a; Hasler and Susstrunk, 2003)).
5. Implement all the proposed methods so that they have linear time complexity with respect to the image dimension, and are suitable for real-time applications.

1.3 Contributions

Achieving the proposed objectives in the image contrast enhancement domain, the principal contributions of this thesis are:

1. MHE methods for gray-level image contrast enhancement with constraints to the processed images such as brightness preserving and natural looking.
2. An analysis of the impact that MHE methods have on gray-level image contrast enhancement, when constraints such as brightness preserving and natural looking are imposed to the processed images.
3. A comparison of the methods conceived for gray-level image contrast enhancement and other HE related methods using objective measures (*e.g.*, $PSNR$, brightness preserving and contrast enhancement).
4. Fast hue-preserving image contrast enhancement methods based on the RGB color space, suitable for real-time applications.
5. A comparison of the methods developed for color image contrast enhancement and other HE based methods using objective measures (*e.g.*, contrast improvement and the color naturalness and colorfulness indexes) by using a database from the University of Berkeley, which is composed of 300 images.

1.4 Organization of the Document

The remainder of this thesis is organized as follows. Chapter 2 presents a bibliography review on methods for image contrast enhancement through histogram specification methods, where histogram equalization which is a histogram specification is included.

Chapter 3 introduces our MHE methods for gray-level image contrast enhancement. Related work is described and definitions for presenting our methods are introduced. Then we describe the proposed methods.

Chapter 4 shows the proposed hue-preserving HE methods to enhance color images based on the RGB color space. Some definitions for presenting our methods are introduced and previous works are presented as well. At the end of the chapter, we introduce our methods.

A set of experiments is reported in Chapter 5, which is divided in two parts. The first part presents results concerning the gray-level image contrast enhancement methods proposed in Chapter 3, whereas the second part reports results concerning the color image contrast enhancement methods presented in Chapter 4.

Finally, Chapter 6 presents final considerations and concluding remarks. Future works and directions are pointed as well.

Chapter 2

Histogram Specification for Image Contrast Enhancement: An Overview

In Chapter 1, we talked about a variety of problems involving the quality of the images obtained by standard capture devices, including problems with contrast, noise and color. Image enhancement is a vast area of study dedicated to improve the quality of an input image, returning an output image which is more suitable than the original image (Hanmandlu, 2006) for simple visualization purposes or for a specific application.

Image enhancement methods and techniques have been studied for more than 40 years, and during this time a vast number of methods were developed (Wang et al., 1983). At first, methods were more concentrated in improving the quality of gray-level images (Hall, 1971; Andrews et al., 1972; Hall, 1974). Later, when the acquisition of color images became more accessible, many of these early methods were adapted to be applied to color images (Pratt, 1978; Castleman, 1979; Niblack, 1986; Jain, 1989). At the same time, methods more suitable for color images, which were tailored to take advantage of their properties, were also developed (Soha and Schwartz, 1978; Bockstein, 1986; Strickland et al., 1987).

In this chapter, we present a categorization of a number of methods and techniques that can be used for contrast enhancement, and then survey one of the presented subcategories named histogram specification transformation, which is the core of methods proposed in Chapter 3 and 4. The first attempt to categorize image enhancement methods was made by Wang et al. (1983) in the early eighties. Wang et al. (1983) classified the methods for image enhancement on the basis of the properties of their operators, since the image enhancement is achieved by image processing through operators. Since 1983, the methods used for image enhancement became much more sophisticated, but their basic structure remained the same. For this reason, their classification scheme is still useful to have a broad view of the type of methods existent in the literature and their characteristics. The classification was based on:

1. The operator sensitivity to the image context;

2. The area of the image which the operation covers;

3. The goals of the operation;

4. The techniques involved in the image enhancement.

According to the operator sensitivity to the image context, enhancement methods can be classified as (a) context-free and (b) context-sensitive. A *context-free* method provides a position-invariant operator, in which all the parameters are fixed *a priori*. A *context-sensitive* method, in contrast, works with a position-variant operator, in which the parameters change in response to local image characteristics. Context-free operators are computationally simpler to apply. However, for images with variable information content, a context-sensitive operator is more suitable.

Regarding the area of the image covered by the operator, the existing methods can be divided into local and global. *Local operators* divide the original image into sub-images (or masks), and take one sub-image into consideration at each time. These operators can be further subdivided into fixed-size and variable-size. For more details see Klette and Zamperoni (1996). In a *global operation*, in turn, the whole image is considered at once. Computationally speaking, the application of a local operator requires less storage space than a global operator does.

Based on their goals, the existing methods can be grouped into (a) noise cleaning, (b) feature enhancement, and (c) noise cleanup plus feature enhancement. The noise-cleaning operator aims to remove random noise from the image. In other words, it disregards the image irrelevant information. The *feature-enhancement* operator attempts to decrease the blurring, and to reveal the image features of interest. These two operators deal with different degradation phenomena. In practice, however, many operators are a combination of both (de A. Araújo, 1989; Mascarenhas and Velasco, 1989).

According to the techniques involved, the published methods can be organized into four approaches. They are:

1. Frequency domain filtering, which utilizes low or/and high-pass filters in the frequency domain.

2. Spatial smoothing, which employs linear or nonlinear spatial domain low-pass filters;

3. Edge-enhancement, which involves linear or nonlinear spatial-domain high-pass filters;

4. Radiometric scale transformation, which manipulates or re-quantizes the levels of a channel (*e.g.*, the gray-level image) for contrast enhancement;

The remainder of this chapter is organized as follows. Section 2.1 describes the radiometric scale transformation, which is directly related to the work proposed in this thesis. Section 2.2

and Section 2.3 present a detailed description of methods developed to enhance gray-level and color images, respectively, and that use a subgroup of radiometric scale transformation: histogram specification transformation.

For the reader interested in works based on the other techniques for image enhancement, we recommend:

- Image Frequency Domain Filtering: (Cooley and Tukey, 1965; Singleton, 1967, 1968; Kober, 2006; Tang, 2003; Duda and Hart, 1973; Huang, 1975; Oppenheim and Schaefer, 1975; Duda and Hart, 1973; Meylan and Süsstrunk, 2004).
- Image Spatial Smoothing: (Prewitt, 1970; Graham, 1962; Brown, 1966; Prewitt, 1970; Kuwahara et al., 1976; Tomita and Tsuji, 1977; Tukey, 1977; Nagao and Matsuyama, 1979; de A. Araújo, 1985; Beghdadi and Le-Negrate, 1989; Anderson and Netravali, 1976; Trusell, 1977).
- Image Edge-enhancement (Prewitt, 1970; Arcese et al., 1970; Rosenfeld and Kak, 1976; Abdou and Pratt, 1979; Gabor, 1965; Prewitt, 1970; Wallis, 1976; Lee, 1980, 1981, 1976; Schreiber, 1990).

2.1 Radiometric Scale Transformation

Methods following the radiometric scale transformation approach propose to re-quantize or map each pixel in the image to a new value, capable of improve the contrast of an image. Image contrast enhancement methods which use radiometric scale transformations are very different from those methods categorized as frequency domain filtering, spatial smoothing, and edge-enhancement methods. This is because, in general, gray-level radiometric scale transformation methods take into account one pixel at a time, and consider each pixel independently of its neighbors. For this reason, we say that the operations performed by these methods are punctual.

Thanks to this property, we can work with the histogram of the image, instead of working with the image itself, because the transformation of any pixels with equal gray-level produce the same output. For this reason, we say that the operations are also global.

The histogram of a gray-level image represents the frequency of occurrence of the levels in the image – for a multi-valued image case, *e.g.*, a color image, we have uni- and multi-dimension histograms. Through a histogram analysis, it is possible to extract some interesting image global features, such as the mode (*i.e.*, the most frequent level) and the distribution of levels.

Radiometric scale transformation methods are mainly used in two situations: 1) When the gray-levels (or the luminance in the case of color images) of the objects in the images are so close to the ones of the background that it is difficult to discriminate them; 2) When the gray-levels of a large percentage of pixels concentrate in a narrow portion of the histogram,

making the the image fine details hardly visible. In the former case, contrast enhancement is needed to increase the gray-level differences between the objects and the background. In the latter case, re-quantization or re-scaling is required to increase the dynamic range and to single out hidden fine structures.

The methods presented in this section can work under a variety of frameworks, performing linear and/or non-linear histogram transformations. These histogram transformations include stretching the histogram (Woods and Gonzalez, 1981), using level slicing (Woods and Gonzalez, 1981), applying gamma function corrections (Gonzalez and Woods, 2002), using histogram equalization (Hall, 1974) and, finally, histogram hyperbolization (Frei, 1977).

In the case of histogram stretching, three basic kinds of stretches can be performed: (1) stretch the dark areas and compress the bright areas; (2) stretch the bright areas and compress the dark areas; (3) stretch the mid-range levels and compress the extreme levels of the histogram of the image.

Concerning level slicing, it is a technique where the histogram of an image is divided into "sliced" intervals. These sliced intervals are put together in only one, *i.e.*, the total dynamic range of the output image. This technique is commonly used for visualization purposes, such as on remote sensing applications (Lillesand and Kiefer, 1994), where the image naturalness is disregarded.

Gamma functions corrections consist of applying non-linear functions, which usually follow a power-law expression of the type $O = I^{\gamma}$ (Gonzalez and Woods, 2002; Serra, 2005), to the image histogram. I and O are the input and output images, respectively, and are composed by non-negative real values, typically in a predetermined range, such as 0 to 1. If $\gamma < 1$, we have what is called gamma compression. If $\gamma > 1$, we have a gamma expansion. These gamma functions corrections are very easy to implement, and usually yield satisfactory results. However, trial and error is needed to obtain the best results. In many cases, the investigator has to provide his own mapping functions.

Histogram equalization takes advantage of the fact that the gray-level histograms of most images (or the luminance histograms of color images), in general, show bright or dark peaks. These peaks represent a large dark or a large bright area in the image, and may contain information regarding fine details of the image. To enhance these areas, a method called histogram equalization (or linearization) was proposed. This method maps the observed gray-level values of the image into new gray-level values (or similarly the observed luminance levels of color image to new levels), in a way that the new image presents a uniform gray-level histogram. This is interesting because, according to the perception performed by the rods and cones of the human retina, the image perceived by humans have a uniform histogram (Wyszecki and Stiles, 1967).

On the other hand, another study about human vision pointed out that the human percep-

tion performs a non-linear transformation of the light intensity (Frei, 1977). To include this characteristics of human perception into image contrast enhancement techniques, histogram hyperbolization was proposed (Pratt, 1978; Frei, 1977). In this framework, the desired histogram of the computer enhanced image has a hyperbolic form, and can be exponential, a cubic root or a logarithm.

The methods based on histogram equalization and hyperbolization are also called histogram specification methods, since an output histogram shape is specified *a priori*. In fact, in the literature, there is a confusion between the terms histogram modification and specification, which are in essence histogram transformations.

The methods proposed in this thesis follow the histogram specification transformation or, more specifically, the histogram equalization framework presented in this section. As we propose two different types of methods, one for gray-level and another for color images, the next sections present, with some more level of detail, previous methods in the literature for contrast enhancement purposes following the histogram specification transformation approach.

2.2 Histogram Specification for Contrast Enhancement of Gray-level Images

The first histogram equalization methods for image contrast enhancement were proposed in the early's seventies (Hall, 1974; Andrews et al., 1972). They were based on the principle that the visual contrast of a digitized image can be improved by adjusting its range of gray-level, so that the histogram of the output image is flat, *i.e.*, a uniform density can be specified from the output histogram. This idea of flattening the image histogram comes from the information theory, which states that the entropy of a signal is maximized when it has a uniform distribution property (Wang et al., 1999).

Since then, histogram specification has been widely used for contrast enhancement in a variety of applications, such as medical image processing and radar signal processing, due to its simple function and effectiveness. Many variations of the standard method were implemented, changing the way the density function is calculated, the density or distribution function to be specified (*e.g.*, a uniform, an exponential), the size of the image being processed each time (*e.g.*, local and adaptive methods),*etc.*, as we will show in this section.

However, many of the proposed methods present one drawback: the brightness of the processed image can be changed after the equalization is performed. This problem appears mainly due to the flattening property of the histogram equalization, and makes it rarely utilized in consumer electronic products such as TV, camcorders, video door phones, security video cameras. This is because, for consumer electronics preserving the original brightness of the image may be necessary in order not to introduce unnecessary visual deterioration. This section is divided in two parts. The first part introduces a variety of methods which do not

preserve the brightness of the processed image, while the second describes some methods that do preserve it. This thesis is more focused on this second type of methods, as will be later showed in Chapter 3.

2.2.1 Non-brightness Preserving Histogram Specification Methods

This section describes a set of methods which perform histogram equalization without worrying about preserving the brightness of the processed image. We start with the work of Hummel (1975), which showed that histogram equalization can be accomplished quite simply by using a look-up table, which is applied to every point of the image. The transformation which comes closer of providing a uniform density can be obtained from a scaled version of the cumulative density function, *i.e.*, the integral of the normalized original histogram. If we require this transformation to be single valued, then gray-level bins of the original histogram can only be merged together, but not broken up. Thus, if the original image has a histogram with large peaks, the transformed histogram will have only a very approximately flat histogram. Nonetheless, contrast is improved because gray-level bins with large numbers of points are moved further apart, increasing the discriminability between the corresponding constant gray-level sets. In Hummel (1977), several techniques were proposed to obtain an exact equalized histogram, *i.e.*, an histogram with an exact uniform density. To achieve that, a multiple-valued transformation was defined, *i.e.*, different pixels with the same gray-level value have different output gray-levels.

In Kim et al. (1999), image contrast enhancement methods based on the piecewise-linear approximation of the cumulative density function (CDF) of the image were proposed. They actually they proposed to approximate the computation of the CDF of an image. This approximate CDF makes methods based on HE faster, and more suitable for real-time applications. Experiments showed the accuracy of the approximated CDF with respect to the original one, and that the approach to approximate the CDF is effective.

In Williams et al. (2001), a modified cosine function and semi-histogram equalization was proposed for contrast enhancement of gray-level images, and an extension of this methodology is suggested to color images by equalizing the three channels (R, G and B) separately. We believe this method has several practical drawbacks, such as the dependency of the image dimension.

The methods just described dealt with the problem of improving global contrast, and were conceived to solve problems such as improper lightning conditions (excessive, poor, *etc.*) in the environment. On the other hand, local contrast enhancement methods, which target the visibility of local details in the image, were also proposed. Within this scope, adaptive histogram equalization (AHE) methods (Pizer et al., 1984) are the most well-known.

AHE works by finding local mappings from a pixel to its equalized version using local histograms. In its basic form, the AHE method consists of performing an histogram equal-

ization at each pixel of the image, based on its pixel neighborhood (its contextual region). An evaluation of the effectiveness of AHE for contrast enhancement in clinical computed tomography (CT) images of the chest is shown in Zimmerman et al. (1988). Although AHE improves contrast locally, its computational complexity may not be acceptable for real-time applications. Another disadvantage of the AHE methods is that they often over-enhance the image, creating the so called contrast objects. Contrast objects are objects which were not visible in the original image. AHE can also be used to enhance noise in relatively homogeneous regions (Pizer et al., 1987). However, image contrast enhancement by AHE methods often does not look natural (Stark, 2000), and also amplifies noise.

To overcome the noise amplification drawback, a contrast limited AHE (CLAHE) method was proposed in Pizer et al. (1990). The noise problem associated with AHE can be reduced by limiting the contrast enhancement specifically to the homogeneous areas of the images. These areas are characterized by a high peak in the histogram associated with the contextual regions, since many pixels fall inside the same gray-level range. A complete description and a implementation of this new method for real-time were presented in Zuiderveld (1994) and Reza (2004), respectively. A wavelet-multi-scale version of CLAHE was also proposed in Jin et al. (2001), and applied to improve the contrast of chest CT images.

Aiming to reduce the high number of operations required by the AHE method, which makes its exact and original conceived forms not suitable for real time applications, various methods have been proposed in the last decade. For instance, in non-overlapped sub-block HE methods, the image plane is divided into a number of sub-regions, and the pixels belonging to a particular sub-region are equalized using the local histogram of the sub-region itself (Jain, 1989; Gonzalez and Woods, 2002). In Kim et al. (1998), a system for enhancing contrast of image sequences using a spatially adaptive histogram equalization with temporal filtering was proposed. A local enhancement is performed by block-overlapped histogram equalization, followed by an efficient temporal filtering method for suppressing over-amplified noise. This local result is combined with the original image (a global result) to obtain the enhanced image. The authors claim that this system is practical for real-time applications. In Kim et al. (2001), an alternative strategy was proposed, relying on partially overlapped sub-block HE (POSHE), and it achieves contrast enhancement rates similar to that of AHE, but at the same time it is capable of maintaining a fine visual quality to the image, by getting rid of the blocking effect. Recently, in Lamberti et al. (2006), a contrast enhancement algorithm which exploits efficient filtering techniques based on cascaded multiple-step binomial smoothing masks HE (CMBFHE) was also introduced, and achieved exactly the same results as POSHE.

A combination of adaptive contrast enhancement algorithm (Beghdadi and Le-Negrate, 1989) and adaptive neighborhood histogram equalization (Paranjape et al., 1992) was proposed in Mukherjee and Chatterji (1995), and called adaptive neighborhood extended contrast enhancement. Besides the combination of techniques, the innovation in this method is that it

defines contextual regions in which it carries out local contrast enhancement. Although this method achieves good results, it requires three parameters to be setup in order to define the contextual region.

A variation of CLAHE method was presented in Zhu et al. (1999), which is named contrast local HE (CLHE). First, the HE process is introduced in a variational framework, where the HE process is viewed as an optimization problem. Then, this framework is extended to a local HE (LHE) directly, and a smoothness constraint term is introduced into the optimization function so that the enhancement result is a balance of the enhancement of details of interest and the maintenance of the original image appearance. Results on common and X-ray images are presented comparing this method with global HE, and LHE or AHE. Although this new method outperform the previous ones regarding the contrast of yielded images, unrealistic images are produced.

In Chang and Wu (1998), another adaptive contrast enhancement algorithm, but this time based on local standard deviation (LSD) distribution was proposed. The innovation of this method consists of using nonlinear functions with local standard deviation to weight it. Once the LSD distribution is estimated, the desired histogram can be specified and the enhancement performed. Note that this method is a histogram transformation one. Experiments were carried out on chest X-ray images, and showed that this method adequately enhances details, and produces little noise over-enhancement and few ringing artifacts. The method also outperforms the ones it was compared with. However, three parameters are set to fit the nonlinear local standard deviation model.

In Stark (2000), a scheme for adaptive image contrast enhancement based on a generalization of the equalized histogram was proposed. In particular, he studied the definition of cumulative density functions, which are used to generate the gray-level mapping from the local histogram. By choosing alternative forms of cumulative density function, one can achieve a wide variety of effects. A signed power-law with local-mean replacement form is proposed, and is dependent on two parameters. Through the variation of these parameters, the method can produce a range of degrees of contrast enhancement, from leaving the image unchanged to yielding full adaptive equalization.

In Ni et al. (1997), a prototype of a system for image contrast enhancement through histogram equalization which uses an adaptive image sensor *in situ* was introduced. This image sensor can automatically adapt to different lighting conditions without frame delay, and provides a constant image signal excursion range. Although some critical problems, such as frame rate, fixed pattern noise, *etc.*, remain opened and need further investigation and experimentation, this sensor has shown very encouraging results. A CMOS[1] prototype chip of 64×64 is showed.

[1]CMOS - complementary metal oxide semi-conductor

2.2.2 Brightness Preserving Histogram Specification Methods

Different from the methods presented in the previous section, this section presents a set of works which aim at improving contrast while preserving the brightness of the image.

We firstly present the bi-histogram equalization methods for image contrast enhancement with brightness preserving proposed by Kim (1997); Wang et al. (1999); Chen and Ramli (2003b). All these methods decompose the original image into two sub-image by using statistical properties of the image, such as the mean gray-level value (Kim, 1997), the level which separates the histogram of the image in equal areas (Wang et al., 1999) and the level which yields the minimum brightness changing in the output image (Chen and Ramli, 2003b). Once the image is decomposed, each sub-image histogram is equalized to produce the output image. It is mathematically shown that these methods keep the brightness of the output image near to the input one. An extension of Kim (1997)'s work was proposed in Chen and Ramli (2003a). This last method proposes to recursively decompose the image into sub-images by using its mean gray-level value, yielding a scalable brightness preservation controlled. All these methods will be detailed in Section 3.2, since they are directly related with this thesis.

In Wang and Ye (2005), an elegant and sophisticated variational framework for image contrast enhancement brightness preserving with maximum entropy was introduced. Although the authors claim that their method is a histogram equalization one, it is, in fact, a histogram specification of an entropy distribution. Numerical results achieved by this method, *i.e.*, the entropy and brightness of the output images, are similar to the ones of Chen and Ramli (2003b)'s method.

2.3 Histogram Specification for Contrast Enhancement of Color Images

This section presents a number of methods for contrast enhancement in color images. In some cases, such as images from mobile phones and digital cameras preserving the hue is essential. In others preserving perceptual attributes is sometimes less important than obtaining the greatest possible color contrast improvement (Mlsna and Rodriguez, 1995) (this is especially true for color composites derived from multi-spectral images such as remote sensing images, which have no significant basis in human perception). These methods can be roughly divided into two classes: non hue-preserving and hue-preserving methods. Section 2.3.1 presents non-hue-preserving methods, while Section 2.3.2 presents hue-preserving ones.

2.3.1 Non-Hue-Preserving Histogram Specification Methods

This section describes histogram specification methods for color images which do not preserve the hue attribute of the color. We start by describing the work of Soha and Schwartz (1978).

They proposed a multi-spectral histogram normalization for effective contrast enhancement in color image by stretching the original *RGB* (Kuehni and Schwarz, 2008) components along the principal component axis, in order to equalize the variance of all components (*i.e.*, channels). This method de-correlates the color channels, and does not take into account perceptual features of the color space. Hence, unrealistic colors may be produced. Either linear or non-linear contrast stretching can be used. If a Gaussian stretch is applied, a symmetrical multidimensional Gaussian histogram is produced. This method implicitly offers a favorable feature, because it offers the opportunity to apply smoothing (low pass filtering) to the low order (poorer signal to noise ratio) principal components, and/or edge sharpening (high frequency boost filtering) to the higher order components, prior to performing the inverse rotation.

In turn, the method proposed in Niblack (1986) stretches iteratively three $2D$ histograms on the *RGB* color space, *i.e.*, *RG*, *GB*, *BR*. For the three $2D$ histograms (*RG*, *GB*, *BR*), the following steps are performed iteratively: (1) In *RG*, stretch the g values for each r value; (2) In *GB*, stretch the b values for each g value; (3) In *BR*, stretch the r values for each b value. This method causes distortion in the color space and it is not hue-preserving (Naik and Murthy, 2003).

In Trahanias and Venetsanopoulos (1992), a direct $3D$ histogram equalization method for color image contrast enhancement based on the *RGB* color system was proposed. This method produces images that are over-enhanced, *i.e.*, the colors are well saturated. However, it is indicated to multi-valued images (or color images) where the channels are well correlated, such as in satellite images. This method has $\bigcirc(L^3)$ time complexity which does not allow its implementation for real-time application. This method is described in details in Chapter 4, Section 4.2, because it is directly related to our proposed method for enhancing the contrast of color images.

In Pitas and Kiniklis (1996), two histogram equalization methods based on the *RGB* and *HSI* color spaces for color image contrast enhancement were proposed. In the first algorithm, a $3D$ histogram based on *RGB* color space is equalized following its joint probability density function in the *RGB* cube. This algorithm and the Trahanias and Venetsanopoulos (1992)'s method differ in the way the output *RGB* histogram is obtained, *i.e.*, the manner which output function transformation is computed. Furthermore, the first algorithm proposed by Pitas and Kiniklis (1996) has $\bigcirc(L^3)$ time complexity. To reduce this complexity, a parallel algorithm was proposed for color image histogram calculation and equalization, scanning the image L times, where L is the number of discrete levels for each component R, G and B (typically $L = 256$). In the second algorithm, a $2D$ histogram to be equalized, built from the combination of saturation and intensity channels of *HSI* color space, is specified following rules based on both saturation and intensity thresholds. Note that this later algorithm is hue-preserving, *i.e.*, the saturation and the intensity (or the luminance) channels are enhanced and the hue is left unchanged, but is described in this section because it is an extension of the

non-hue-preserving method initially proposed.

Chitwong et al. (2000) presented an interesting method for color image contrast enhancement based on region segmentation histogram equalization. The method proposes to initially divide the image into small areas using the principles of graph theory, since the graph theory gives high accurate boundaries for regions. The method is applied to multi-spectral satellite imagery by assigning the colors red, green and blue to three different spectral images. When compared to the traditional histogram equalization method, the proposed method clearly outperforms the latter one when a subjective visual assessment is carried out.

In Pichon et al. (2003), a histogram equalization method which takes into account color channels correlations through mesh deformation, which always generates almost (*i.e.*, discrete) uniform color histograms, is proposed. This algorithm makes an optimal use of the *RGB* color space, and it is appropriated for scientific visualization, but not for image enhancement, because it does not preserve the image natural features.

2.3.2 Hue-Preserving Histogram Specification Methods

This section describes hue-preserving contrast enhancement methods. The most common way to preserve the hue attribute when working with histogram specification is to convert the image from its original color space (*e.g.*, *RGB*) to another one, such as *LHS*, *HSI*, *HSV* - color spaces based on luminance (L - or intensity (I)), saturation (S)and hue (H)attributes, *YIQ*, *etc.* After that the histogram specification is applied to the luminance and/or saturation components, keeping the hue unchanged.

In Bockstein (1986), a histogram equalization method based on luminance, saturation, and hue (*LHS*) color space (Kuehni and Schwarz, 2008) was proposed. The equalization is applied to the luminance (L) and the saturation (S) histograms for the smaller regions, while the hue value (H) is preserved.

In Yang and Rodriguez (1995), a scaling and a shifting operator to be directly applied to the *RGB* color space while preserving the properties of *LHS* and *YIQ* color spaces was proposed. After some analysis, the authors concluded that scaling transformations in luminance preserves the hue and the saturation of the *LHS* color space. However, in the *YIQ* color space, only the hue is preserved. In contrast, shifting transformations in luminance preserve the hue and saturation of the *YIQ* color space, whilst only the hue is preserved in the *LHS* color space.

Weeks et al. (1995) proposed a method which modifies the saturation and intensity components of C-Y color space[2] (Kuehni and Schwarz, 2008). This algorithm partitions the whole C-Y color space into $n \times k$ number of subspaces, where n and k are the number of partition in

[2]The C-Y color space (also called color difference space), composed of luminance (Y) and chromatic information (R-Y) and (B-Y), is implemented as a linear combination of R, G and B channels of the *RGB* color space. This space is the same as the *YIQ* one rotated by 33 degrees (Martin, 1962).

the luminance and saturation components, respectively. Saturation is equalized once for each of these $n \times k$ subspaces, within the maximum realizable saturation of the subspace. Later, the luminance component is also equalized, but considering the whole image. To take care of the R, G and B values exceeding the bounds, Weeks et al. (1995) suggested to normalize (*i.e.*, clipping) each component using $(255)/(max(R, G, B))$.

In Mlsna and Rodriguez (1995), a multivariate contrast enhancement method named "histogram explosion" was proposed. This method aims to explode the *RGB* histogram, *i.e.*, stretch the histogram to its maximum, such that the maximum contrast enhancement can be obtained. The proposed method is indicated to remote sensing imagery, and it can be hue-preserving if the parameters which model the histogram explosion are chosen properly. This method is able to explode nearly the full extent of the *RGB* gamut without clipping, and it is later extended to the *CIELUV* space (Mlsna et al., 1996). The same authors later proposed a recursive algorithm for $3D$ histogram enhancement scheme for color images (Zhang et al., 1996).

Duan and Qiu (2004) proposed a novel histogram processing method for color image contrast enhancement. This method proposes to produce a good balancing between histogram equalization (contrast enhancement) and the maintenance of the image original pixel distribution (to be faithful to the original image visual appearances). Because of its characteristics, it is expected to produce realistic and good-looking pictures. In this method, only the saturation component is enhanced, and it works as follows. The *HSI* color space is divided into A $(a = 1, ..., A)$ hue regions, and each one of these hue regions are divided into B $(b = 1, ..., B)$ luminance regions. For each one of these resulted (a, b) hue-luminance regions, a one-million high resolution saturation histogram is constructed. The method uses a single parameter to control the degree of contrast enhancement, and this parameter is used to recursively divide each one of these hue-luminance images high-dimensional histograms of the range $[0, Sat_{max}(a, b)]$ into K $(k = 1, ..., K)$ intervals, where $Sat_{max}(a, b)$ is the maximum saturation value of the (a, b) hue-luminance region. After the division, the saturations falling into the k-th interval are grouped together, and represented by the same saturation value $k \times Sat_{max}(a, b)/K$. Then the processed *HSI* values are converted back to *RGB* values, and if necessary a clipping or scaling process is performed. Results showed the effectiveness of this method when compared with other previous works in literature, since it improves the contrast and colorfulness of the original image without introducing artifacts, which is caused by traditional equalization processes. Nevertheless, this method is not suitable for real-time applications, since to process a half-million image pixels it takes about one minute in a 2GHz CPU PC.

The luminance quantization error can be significantly magnified by the transformation function, leading to distortion in the processed image a.k.a. the gamut problem (Naik and Murthy, 2003). To decrease the gamut problem, Rodriguez and Yang (1995) proposed the use of high-resolution histograms when transforming the image from the *RGB*

color space to another one, such as the *YIQ* color space[3] (Kuehni and Schwarz, 2008). Experimental results with histogram equalization showed that the use of a higher resolution histogram of the *YIQ* color space luminance leads to reduced distortion, as well as a "flatter" output histogram of the enhanced image.

In Naik and Murthy (2003), a technique to avoid the gamut problem for image processing was formalized. A generalization of linear and nonlinear gray-level contrast enhancement functions to color images is presented as well.

2.4 Conclusions

In this chapter, we presented an overview on image contrast enhancement. In especial, we surveyed histogram specification methods for image contrast enhancement, since they are the core of the method proposed in this work.

In the next chapter, we present our gray-level multi-histogram equalization methods for image contrast enhancement.

[3] *YIQ* is the color space used by the *NTSC* color TV system, employed mainly in North and Central America, and Japan. The Y component represents the luminance information (*i.e.*, the luminance), and is the only component used by black-and-white television receivers - the achromatic part of the signal, whereas I and Q stands for in-phase and quadrature, respectively, referring to the components used in quadrature amplitude modulation, which represent the chrominance information.

Chapter 3

Multi-Histogram Equalization Methods for Gray-Level Images

Histogram equalization is a technique commonly used for image contrast enhancement. It works by redistributing the gray-levels of the input image by using its cumulative density function. Despite its success, this technique has a well-known drawback: it does not preserve the brightness of the input image in the output image. To overcome such drawback, methods based on this technique have proposed to decompose the original image into two sub-images, and then perform the histogram equalization in each sub-image. These methods decompose the original image by using statistical properties, such as the mean gray-level value (Kim, 1997), the equal-area value (Wang et al., 1999) or the level which yields the minimum brightness error between the original and the enhanced images (Chen and Ramli, 2003b).

Although these methods preserve the input brightness in the output image with a significant contrast enhancement, they may produce images which do not look as natural as the input ones. In order to enhance contrast, preserve brightness and still produce natural looking images, this chapter presents a novel technique called multi-histogram equalization, which consists of decomposing the input image into several sub-images, and then applying the classical histogram equalization process to each one of them.

We propose to decompose the image by using two discrepancy functions, conceiving two multi-histogram equalization methods for image contrast enhancement. These discrepancy functions were borrowed from the multithresholding literature (Otsu, 1979; Sezgin and Sankur, 2004; Luessi et al., 2006). A cost function, which takes into account both the discrepancy between the input and enhanced images and the number of decomposed sub-images, is used to automatically decide in how many sub-images the input image will be decomposed on.

Note that several histogram equalization methods proposed in the literature are suitable for real-time applications, because they are quite simple. Our proposed methods, even more sophisticated in the decomposition process of the original image than the others, remain fast and suitable for real-time applications.

The remainder of this chapter is organized as follows. As the proposed methods use many concepts previously introduced in the literature, Section 3.1 presents some basic definitions regarding the gray-level images, which will be referred to throughout this chapter. Section 3.2 describes some previous works in histogram equalization, which are closely related to our proposed methods. The proposed multi-histogram equalization methods are introduced in Section 3.3. Finally, conclusions are drawn in Section 3.4.

3.1 Basic Definitions

In this section, we present some basic definitions for monochromatic image and their probability functions, which will be used throughout this chapter.

Definition 3.1 (Image) *Let $\mathbb{N}$ and $\mathbb{Z}$ denote the set of natural and integer numbers, respectively. Let X^{mn} be a subset of points $(x, y) \in \mathbb{N}^2$, such that $0 \leq x < m$, and $0 \leq y < n$, where m and n denote the dimensions of X^{mn}. Let $||Y||$ denote the the cardinality of a set $Y \subseteq \mathbb{N}^2$. Note that $||X^{mn}|| = m \times n$. A mapping I, from X^{mn} to $\mathbb{Z}_L$, where $\mathbb{Z}_L = \{0, ..., L-1\}$, is called a (*monochromatic*) image. In applications, L is typically 256.*

Definition 3.2 (Level) *For a point $(x, y) \in X^{mn}$, $l = I(x, y)$ is called the* level *of the point (x, y) in I.*

Definition 3.3 (Sub-Image) *Let l_s and l_f be levels of the image I, where $0 \leq l_s \leq l_f < L$. Let $I[l_s, l_f] \subseteq I$ be composed by all mappings from points $(x, y) \in X^{mn}$ to $\{l_s, l_{s+1}, ..., l_{f-1}, l_f\}$,* i.e.*,*

$$I[l_s, l_f] = \{(x, y) \rightarrow I(x, y) | l_s \leq I(x, y) \leq l_f, \forall (x, y) \in X^{mn}\}. \tag{3.1}$$

*The sub-mapping $I[l_s, l_f]$ defines a (*sub-*)*image *of I.*

The definition above was presented to facilitate the definition of a sub-histogram and its probability functions, which are necessary for the definition of bi- and multi-histogram equalization methods. In the following, when the boundaries $[l_s, l_f]$ of the image I are omitted, they are assumed to be $[0, L-1]$.

Definition 3.4 (Histogram) *Let X_l^{mn} be a subset of X^{mn}, such that for all $(x, y) \in X_l^{mn} \subseteq X^{mn}$, we have $I(x, y) = l$. Let H_l^I be the* absolute frequency *of the level l in the image I, where $0 \leq l \leq L-1$,* i.e.*, $H_l^I = ||X_l^{mn}||$. Note that $H_l^I = 0$ if there is no $(x, y) \in X^{mn}$ where $I(x, y) = l$. The mapping H^I from the levels of the image I to their absolute frequency levels,* i.e.*, $H^I : \mathbb{Z}_L \rightarrow \mathbb{N}$, is called the* histogram *of the image I. Note that $\sum_{i=0}^{L-1} H_i^I = m \times n$. Also note that $H_l^I = H_l^{I[l_s, l_f]}$, with $0 \leq l_s \leq l \leq l_f < L$.*

Definition 3.5 (Probability Density Function) *Let* $P_l^{I[l_s,l_f]}$ *be the* relative frequency *(or the probability) of the level* l *in the (sub-)image* $I[l_s, l_f]$, i.e.,

$$P_l^{I[l_s,l_f]} = \frac{H_l^I}{\sum_{i=l_s}^{l_f} H_i^I}, \tag{3.2}$$

where $0 \leq l_s \leq l \leq l_f \leq L-1$. *Note that* $\sum_{i=l_s}^{l_f} P_i^{I[l_s,l_f]} = 1$.

The function $P^{I[l_s,l_f]}$, *which is composed by all* $P_l^{I[l_s,l_f]}$, *is the* probability density function *of the image* $I[l_s, l_f]$.

Definition 3.6 (Probability Distribution Function) *Let* $C_l^{I[l_s,l_f]}$ *be the probability distribution (or the cumulative probability density) of the level* l *in the image* $I[l_s, l_f]$, i.e.,

$$C_l^{I[l_s,l_f]} = \frac{1}{\sum_{i=l_s}^{l_f} H_i^I} \sum_{i=l_s}^{l} H_i^I = \sum_{i=l_s}^{l} P_i^{I[l_s,l_f]}, \tag{3.3}$$

where $0 \leq l_s \leq l \leq l_f \leq L-1$. *Note that* $C_{l_f}^{I[l_s,l_f]} = 1$.

The function $C^{I[l_s,l_f]}$ *composed by all* $C_l^{I[l_s,l_f]}$ *is the* probability distribution function *(or the* cumulative probability density function*) of the image* $I[l_s, l_f]$.

Definition 3.7 (Brightness) *Let* $I[l_s, l_f]$ *be a sub-image of* I. *We define the* mean *(or the* brightness*) of the image* $I[l_s, l_f]$ *as:*

$$l_m(I[l_s, l_f]) = \frac{\sum_{l=l_s}^{l_f} l \times H_l^I}{\sum_{l=l_s}^{l_f} H_l^I} = \sum_{l=l_s}^{l_f} l \times P_l^{I[l_s,l_f]}. \tag{3.4}$$

Definition 3.8 (Contrast) *Let* $I[l_s, l_f]$ *be a sub-image of* I. *We define the* standard deviation *(or the* contrast*) of the image* $I[l_s, l_f]$ *as:*

$$l_\sigma(I[l_s, l_f]) = \sqrt{\frac{\sum_{l=l_s}^{l_f} (l - l_m(I[l_s, l_f]))^2 \times H_l^I}{\sum_{l=l_s}^{l_f} H_l^I}} = \sqrt{\sum_{l=l_s}^{l_f} (l - l_m(I[l_s, l_f]))^2 \times P_l^{I[l_s,l_f]}}. \tag{3.5}$$

Note that this definition of image contrast (standard deviation) is a global one. There are other definitions of contrast based on local properties of the image, *e.g.*, neighbor points in the image (Huang et al., 2005).

3.2 Related Work

This section describes some previous work which make use of the histogram equalization method with the purpose of brightness preserving.

We start by describing the classical histogram equalization (CHE) method in Section 3.2.1. We then present four other methods which are extensions of the CHE, namely BBHE (Kim, 1997), DSIHE (Wang et al., 1999), MMBEBHE (Chen and Ramli, 2003b) and RMSHE (Chen and Ramli, 2003a), which will be later described in this section. These four extensions of the CHE method have one main point in common: they decompose the original image into two or more sub-images, and then equalize the histograms of these sub-images independently. In contrast, the major difference among these methods is the criteria they use to decompose the input image into two or more sub-images.

The first method, described in Section 3.2.2, divides the input image in two by using the mean gray-level value. An extension of this method, which recursively segments the original image, is later described in Section 3.2.5. Section 3.2.3 presents a method which uses the equal-area value to segment the images, whereas the method described in Section 3.2.4 segments images by taking into account the level which yields the minimum brightness error between the input and the enhanced images. Section 3.2.6 presents some final remarks.

Note that, for all the methods described in this section, I and O denote the input (or the original) and the output (or the processed) images, respectively. Both I and O have boundaries which will be denoted by $[l_s, l_f]$, instead of $[0, L-1]$, as previously introduced in Section 3.1. We chose to use this definition because it is more general and, therefore, can be used by other methods which will be presented in this chapter.

3.2.1 Classical Histogram Equalization Method (CHE)

This section describes the classical histogram equalization (CHE) method for monochromatic images (*e.g.*, gray-level ones) in detail, since this method is the core of the methods presented in this chapter. The CHE method for monochromatic images works as follows.

Let the boundaries of the images I and O, represented by $[l_s, l_f]$, be set as $[0, L-1]$. Also, let $H^{I[l_s,l_f]}$ (the image histogram), $P^{I[l_s,l_f]}$ (the image probability density function) and $C^{I[l_s,l_f]}$ (the image probability distribution function) be defined as in Section 3.1. Let $H^{O[l_s,l_f]}$ be the uniform histogram of the output image, where any level l, with $0 \leq l_s \leq l \leq l_f \leq L-1$, has the same amount of pixels, *i.e.*,

$$H_l^{O[l_s,l_f]} = \frac{1}{l_f - l_s + 1} \sum_{l=l_s}^{l_f} H_l^{I[l_s,l_f]}, \tag{3.6}$$

or the same density (probability), *i.e.*,

$$P_l^{O[l_s,l_f]} = \frac{1}{l_f - l_s + 1}. \tag{3.7}$$

The cumulative density function $C^{O[l_s,l_f]}$ is defined in function of l as:

$$C_l^{O[l_s,l_f]} = \frac{1}{\sum_{i=l_s}^{l_f} H_i^{I[l_s,l_f]}} \sum_{i=l_s}^{l} H_i^{I[l_s,l_f]} = \sum_{i=l_s}^{l} P_i^{I[l_s,l_f]} = \frac{i - l_s + 1}{(l_f - l_s + 1)}. \tag{3.8}$$

The l' output level corresponding to the input level l is obtained as the one that minimizes the difference between $C_{l'}^{O[l_s,l_f]}$ and $C_l^{I[l_s,l_f]}$. In other words, the output level l' for the input level l can be computed as the transformation function $T^{I[l_s,l_f]}(l)$, *i.e.*,

$$l' = T^{I[l_s,l_f]}(l) = l_s + \left\langle (l_f - l_s) \times C_l^{I[l_s,l_f]} \right\rangle, \tag{3.9}$$

where $\langle z \rangle$ stands for the nearest integer to $z \in \mathbb{R}$.

To generate the enhanced output image $O[l_s, l_f]$ using this transformation, for any pixel $(x, y) \in X^{mn}$, we obtain its respective output level $O[l_s, l_f](x, y)$ as $l' = T^{I[l_s,l_f]}(l)$, where $l = I(x, y)$, *i.e.*,

$$O[l_s, l_f] = \{O(x, y) = l' | l = I(x, y), l' = T^{I[l_s,l_f]}(l), \forall (x, y) \in X^{mn}\}. \tag{3.10}$$

The high performance of the HE in enhancing the contrast of an image is a consequence of the dynamic range expansion of the gray-level image domain. That is, theoretically the output image enhanced by a HE method uses all the gray-levels in the image domain, *i.e.*, from 0 up to $L - 1$. Besides, the CHE tries to produce an output image with a flatten histogram, *i.e.*, a uniform distribution. Based on information theory, the entropy of a message source will get the maximum value when the message has uniform distribution (Wang et al., 1999). This means that an enhanced image by the CHE method has the maximum information (*i.e.*, entropy) with respect to its original one. However, the CHE method barely satisfies the uniform distribution property in images with discrete gray-level domains.

Despite the advantages offered by the CHE method, it can introduce a significant change in the image brightness, *i.e.*, its mean gray-level. That is, thanks to the uniform distribution specification of the output histogram, the CHE method shift the brightness of the output image to the middle gray-level, *i.e.*, $L/2$. This change in brightness is not desirable when applying the CHE scheme into consumer electronics devices, for instance, TV, camcorders, digital cameras and video surveillance. This is because it may introduce unnecessary visual deterioration to the output image.

3.2.2 Brightness Bi-Histogram Equalization Method (BBHE)

In order to overcome the drawback introduced by the CHE method described in the previous subsection, a brightness preserving bi-histogram equalization (BBHE) method was proposed in Kim (1997). The essence of the BBHE method is to decompose the original image into two

sub-images, by using the image mean gray-level, and then apply the CHE method over each of the sub-images.

Formalizing what we just explained, the input image I is decomposed into two sub-images based on its mean level $l_m(I)$, *i.e.*,

$$I = I[0, \lfloor l_m(I) \rfloor] \cup I[\lfloor l_m(I) \rfloor + 1, L-1], \tag{3.11}$$

where $\lfloor z \rfloor$ stands for the greatest integer not greater than or equal to z (*i.e.*, floor function). Note that in this method description, and in the next ones, the boundaries of the images I and O and their sub-images, will be represented by $[l_s, l_f]$, where $0 \leq l_s \leq l_f < L$ and will be indicated in the equation, *e.g.*, $I[l_s, l_f]$ or $O[l_s, l_f]$.

Each of these decomposed sub-images $I[0, \lfloor l_m(I) \rfloor]$ and $I[\lfloor l_m(I) \rfloor + 1, L-1]$ then have their histograms equalized independently using Equation 3.10. The composition of the resulting processed sub-images constitutes the output image of the BBHE method, *i.e.*,

$$O = O[0, \lfloor l_m(I) \rfloor] \cup O[\lfloor l_m(I) \rfloor + 1, L-1]. \tag{3.12}$$

In Kim (1997), it is mathematically shown that the BBHE method produces an output image with the value of the brightness (the mean gray-level) located in the middle of the mean of the input image and the middle gray-level, *i.e.*,

$$l_m(O) = \frac{1}{2}(l_m(I) + L/2). \tag{3.13}$$

Notice that the output mean brightness of the BBHE method is a function of the input mean brightness $l_m(I)$. This fact clearly indicates that the BBHE preserves the brightness of the image when compared to the case of classical histogram equalization, where the output brightness always tends to the middle gray-level, *i.e.*, $L/2$.

3.2.3 Dualistic Sub-Image Histogram Equalization Method (DSIHE)

Before start describing this method, two useful definitions need to be introduced

Definition 3.9 (Discrete Entropy) *Let $I[l_s, l_f]$ be a sub-image of I. We define the* discrete entropy *of the image $I[l_s, l_f]$ as:*

$$Ent(I[l_s, l_f]) = -\sum_{l=l_s}^{l_f} P_l^{I[l_s,l_f]} \times \log_2 P_l^{I[l_s,l_f]}. \tag{3.14}$$

Note that the discrete entropy of an image can, to some extent, depict the richness of details.

Definition 3.10 (Equal-Area Level) *Let $I[l_s, l_f]$ be a sub-image of I. The level $l_a(I[l_s, l_f])$ which decomposes the image $I[l_s, l_f]$ into two sub-images $I[l_s, l_a(I[l_s, l_f])]$ and $I[l_a(I[l_s, l_f]) + 1, l_f]$ with almost (*i.e.*, in discrete meaning) equal area (*i.e.*, equal density), is called the* equal-area level *of the image $I[l_s, l_f]$, and it is defined as:*

$$l_a(I[l_s, l_f]) = \arg\min_{l_s \leq l \leq l_f} |\sum_{i=l_s}^{l} P_i^{I[l_s,l_f]} - 1/2|, \tag{3.15}$$

where $|z|$ stands for the absolute value of $z \in \mathbb{R}$.

After these definitions, following the same basic ideas used by the BBHE method of decomposing the original image into two sub-images and then equalizing the histograms of the sub-images separately, Wang et al. (1999) proposed the so called equal area dualistic sub-image histogram equalization (DSIHE) method. Instead of decomposing the image based on its mean gray-level, the DSIHE method decomposes the images aiming at the maximization of the Shannon's entropy (Shannon, 1948; Kapur, 1994) of the output image. The method uses the Shannon's entropy because the condition to maximize the average information content (*i.e.*, the entropy) of the processed image can seldom be satisfied for discrete images. For such aim, the input image is decomposed into two sub-images, being one dark and one bright image, respecting the equal area property, *i.e.*,

$$I = I[0, l_a(I)] \cup I[l_a(I) + 1, L - 1], \tag{3.16}$$

where $l_a(I)$ stands for the equal-area level of the image I.

Then the two sub-images $I[0, l_a(I)]$ and $I[l_a(I) + 1, L - 1]$ have their histograms equalized independently using Equation 3.10, and the composition of the resulting processed sub-images constitutes the output image of the DSIHE method, *i.e.*,

$$O = O[0, l_a(I)] \cup O[l_a(I) + 1, L - 1]. \tag{3.17}$$

In Wang et al. (1999), it is shown that the brightness of the output image O produced by the DSIHE method is the average of the equal-area level $l_a(I)$ of the image I and the middle gray-level of the image $L/2$, *i.e.*,

$$l_m(O) = \frac{1}{2}(l_a(I) + L/2). \tag{3.18}$$

The authors claim that the brightness of the output image O generated by the DSIHE method does not present a significant shift in relation to the brightness of the input image, especially for the large area of the image with the same gray-levels (represented by small areas in histograms with great concentration of gray-levels), *e.g.*, images with small objects regarding the great darker or brighter backgrounds.

3.2.4 Minimum Mean Brightness Error Bi-Histogram Equalization Method (MMBEBHE)

Still following the basic principle of the BBHE and DSIHE methods of decomposing an image before applying the CHE method to equalize the resulting sub-images independently, Chen and Ramli (2003b) proposed the minimum mean brightness error bi-histogram equalization (MMBEBHE) method. The main difference between the BBHE and the DSIHE methods and the MMBEBHE one is that the latter searches for a threshold level l_t that decomposes the image I into two sub-images $I[0, l_t]$ and $I[l_t + 1, L - 1]$, such that the minimum brightness difference between the input and output images is achieved, whereas the former methods consider only the input image to perform the decomposition. In this method, the image decomposition process can be described as follows:

$$I = I[0, l_t] \cup I[l_t + 1, L - 1], \tag{3.19}$$

where $l_t(I)$ stands for the threshold level which yields the minimum mean brightness error, *i.e.*,

$$l_t = \underset{0 \leq l \leq L-1}{\arg\min} \langle l_m(I) - l_m(O(l)) \rangle, \tag{3.20}$$

$\langle z \rangle$ stands for the nearest integer value to $z \in \mathbb{R}$, $O(l)$ is the output image for the threshold level l, *i.e.*,

$$O(l) = O[0, l] \cup O[l + 1, L - 1], \tag{3.21}$$

and $O[0, l]$ and $O[l+1, L-1]$ are the enhanced images obtained by the histograms equalization of the images $I[0, l]$ and $I[l + 1, L - 1]$ using Equation 3.10.

The output processed image which generates the minimum mean brightness error is given by:

$$O = O[0, l_t] \cup O[l_t + 1, L - 1]. \tag{3.22}$$

Assumptions and manipulations for finding the threshold level l_t that minimizes the mean brightness error between the input and output images in $\bigcirc(L)$ time complexity were made in Chen and Ramli (2003b). Such strategy allows us to obtain the brightness $l_m(O[0, l_t] \cup O[l_t + 1, L - 1])$ of the output image without generating the output image for each possible threshold level l, and its aim is to produce a method suitable for real-time applications.

3.2.5 Recursive Mean-Separate Histogram Equalization Method (RMSHE)

Recall that the extensions of the CHE method described so far in this chapter were characterized by decomposing the original image into two new sub-images. However, an extended version of the BBHE method (see Section 3.2.2), introduced in Chen and Ramli (2003a), and

named recursive mean-separate histogram equalization (RMSHE), proposes the following. Instead of decomposing the image only once, the RMSHE method proposed to perform image decomposition recursively, up to a scale r, generating 2^r sub-images.

As in the BBHE method, each sub-image $I^{q-1}[l_s, l_f]$ is decomposed based on its mean gray-level $l_m(I^{q-1}[l_s, l_f])$, *i.e.*,

$$I^{q-1}[l_s, l_f] = I^q[l_s, \lfloor l_m(I^{q-1}[l_s, l_f])\rfloor] \cup I^q[\lfloor l_m(I^{q-1}[l_s, l_f])\rfloor + 1, l_f], \tag{3.23}$$

where q stands for the scale of decomposition, with $0 < q \leq r$. Note that $I^0[l_s, l_f]$ stands for $I[0, L-1]$. After the decomposition process, each one of these 2^r sub-images $I^r[l_s, l_f]$ is independently enhanced using the CHE method. The output image O is composed by the union of all the enhanced sub-images $O^r[l_s, l_f]$ obtained by Equation 3.10.

Note that when $r = 0$ (no sub-images are generated) and $r = 1$, the RMSHE method is equivalent to the CHE and BBHE methods, respectively.

In Chen and Ramli (2003a), the authors mathematically showed that the brightness $l_m(O)$ of the output image O is better preserved as r increases following:

$$l_m(O) = l_m(I) + (L/2 - l_m(I))/2^r. \tag{3.24}$$

Note that, computationally speaking, this method presents a drawback: the number of decomposed sub-histograms is a power of two.

3.2.6 An Insight on the Results Produced by HE Methods

The previous sections described methods which use histogram equalization with the purpose of preserving the brightness of gray-level images. Figure 3.1 shows, for the girl image, the output images produced by these HE methods. In turn, Table 3.1 shows values of the brightness and contrast obtained for these images.

Table 3.1: Brightness preserving methods for image contrast enhancement.

Method	Brightness	Contrast
Original	139.20	29.70
HE	133.94	75.47
BBHE	162.78	70.09
DSIHE	131.66	75.42
RMSHE ($r = 2$)	139.77	37.81
MMBEBHE	144.97	68.70

(a) (b) (c) (d) (e) (f)

Figure 3.1: An example of image brightness preserving and contrast enhancement: (a) original image; enhanced images using (a) as input by CHE, BBHE, DSIHE, RMSHE ($r = 2$), and MMBHEBE methods are shown in (b), (c), (d), (e) and (f), respectively.

By analyzing the data in Table 3.1 and the images in Figure 3.1, we observe that the only method which preserves the brightness of the input image and generates a natural looking image is the RMSHE method. Recall that this method is based on multi-histogram decomposition or, in other words, on the recursive decomposition of the image into two sub-images.

From the results in Table 3.1, we can also conclude that the bi-histogram equalization methods are not robust regarding the brightness preserving. To overcome this drawback, Section 3.3 introduces two new robust methods for image contrast enhancement and brightness preserving, also capable of producing natural looking images.

3.3 The Proposed Methods

As mentioned before, the histogram equalization method enhances the contrast of an image but cannot preserve its brightness (which is shifted to the middle gray-level value). As a result, the histogram equalization method can generate unnatural and nonexisting objects in the processed image. In contrast, bi-histogram equalization methods can produce a significative image contrast enhancement and, at some extend, preserve the brightness of the image. However, the images generated might not have a natural appearance. To surmount such drawbacks, the main idea of our generic proposed method is to decompose the image into several sub-images, such that the image contrast enhancement provided by the HE in each sub-image is less intense, leading the output image to have a more natural looking. The conception of this method brings two points.

The first point is how to decompose the input image. As histogram equalization is the focus of the work, the image decomposition process is based on the histogram of the image. The histogram is divided into classes, determined by threshold levels, where each histogram class represents a sub-image. The decomposition process can be seen as an image segmentation process executed through multi-threshold selection (Otsu, 1979; Luessi et al., 2006). The second point is in how many sub-images an image must be decomposed into. This number depends on how the image is decomposed.

In order to answer these questions, Section 3.3.1 presents two cost functions to decompose an image based on threshold levels, whereas the algorithm used to find the optimal threshold levels is presented in Section 3.3.2. These two cost functions conceive two instantiations of the generic MHE method. Finally, a criterion for automatically selecting the number of decomposed sub-images is exposed in Section 3.3.3.

3.3.1 Multi-Histogram Decomposition

Many histogram equalization-based methods have been proposed in the literature to decompose an image into sub-images by using the value of some statistical measure based on the image gray-level value (Kim, 1997; Wang et al., 1999; Chen and Ramli, 2003b,a). These meth-

ods aim to optimize the entropy or preserve the brightness of the image. Here, we will focus our attention on decomposing an image such that the enhanced images still have a natural appearance. For such aim, we propose to cluster the histogram of the image in classes, where each class corresponds to a sub-image. By doing that, we want to minimize the brightness shift yielded by the histogram equalization process into each sub-image. With the minimization of this shift, this method is expected to preserve both the brightness and the natural appearance of the processed image.

From the multi-threshold selection literature point of view, the problem stated above can be seen as the minimization of the within-histogram class variance (Otsu, 1979), where the the within-class variance is the total squared error of each histogram class with respect to its mean value (*i.e.*, the brightness). That is, the decomposition aim is to find the optimal threshold set $T^k = \{t_1^k, ..., t_{k-1}^k\}$ which minimizes the decomposition error of the histogram of the image into k histogram classes (or sub-images) and decomposes the image $I[0, L-1]$ into k sub-images $I[l_s^{1,k}, l_f^{1,k}], ..., I[l_s^{k,k}, l_f^{k,k}]$, where $l_s^{j,k}$ and $l_f^{j,k}$ stand for the lower and upper gray-level boundaries of each sub-image j when the image is decomposed into k sub-images. They are defined as: $l_s^{j,k} = t_{j-1}^k$, if $j > 1$, and $l_s^{j,k} = 0$ otherwise, and $l_f^{j,k} = t_j^k + 1$, if $j \neq k$, and $l_f^{j,k} = L - 1$ otherwise. The discrepancy function for decomposing the original image into k sub-images (or histogram classes) following the minimization of within-class variance can be expressed as:

$$Disc(k) = \sum_{j=1}^{k} \sum_{l=l_s^{j,k}}^{l_f^{j,k}} (l - l_m(I[l_s^{j,k}, l_f^{j,k}]))^2 P_l^{I[0,L-1]}. \tag{3.25}$$

The variant method conceived with this discrepancy function is called Minimum Within-Class Variance MHE method (MWCVMHE).

Note that the mean gray-level (*i.e.*, the brightness) of each sub-image processed by the CHE method is theoretically shifted to the middle gray-level of its range, *i.e.*, $l_m(O[l_s, l_f]) = l_{mm}(I[l_s, l_f]) = l_{mm}(O[l_s, l_f]) = (l_s + l_f)/2$. As we want to minimize the brightness shift of each processed sub-image such that the global processed image has its contrast enhanced and its brightness preserved (creating a natural looking output image), we focus our attention on the brightness of the output image. Hence, instead of using the mean $l_m(I[l_s, l_f])$ of each input sub-image $I[l_s, l_f]$ in the discrepancy function, we propose to use its middle level $(l_s + l_f)/2$, since every enhanced sub-image $O[l_s, l_f]$ will theoretically have its mean value (brightness) on the middle level of the image range - thanks to the specification of a uniform histogram distribution. Therefore, a new discrepancy function is proposed and it is expressed as:

$$Disc(k) = \sum_{j=1}^{k} \sum_{l=l_s^{j,k}}^{l_f^{j,k}} (l - l_{mm}(I[l_s^{j,k}, l_f^{j,k}]))^2 P_l^{I[0,L-1]}, \tag{3.26}$$

Algorithm 3.1: Computing $Disc(k)$ and $PT(k, L-1)$

Data: $\varphi(p,q)$ - discrepancy of sub-image $I[p,q]$
Result: $D(p)_q$ - discrepancy function $Disc(p)$ up to level q
Result: PT - optimum thresholds matrix

```
for q ← 0 ; q < L ; q++ do D(1)_q ← φ(0,q) ;
for p ← 1 ; p ≤ k ; p++ do
    D(p+1)_p ← D(p)_{p-1} + φ(p-1,p-1) ;
    PT(p+1,p) ← p-1 ;
    for q ← p+1 ; q ≤ L-k+p ; q++ do
        D(p+1)_q ← -∞ ;
        for l ← p-1 ; l ≤ q-1 ; l++ do
            if (D(p+1)_q > D(p)_l + φ(l+1,q)) then
                D(p+1)_q ← D(p)_l + φ(l+1,q) ;
                PT(p+1,q) ← l ;
```

where $l_{mm}(I[l_s^{j,k}, l_f^{j,k}])$ stands for the middle value of the image $I[l_s^{j,k}, l_f^{j,k}]$ and it is defined as $\langle (l_s + l_f)/2 \rangle$. The variant method conceived with this discrepancy function is called Minimum Middle Level Squared Error MHE method (MMLSEMHE).

3.3.2 Finding the Optimal Thresholds

The task of finding the optimal $k-1$ threshold levels which segment an image into k classes can be easily performed by a dynamic programming algorithm with $\bigcirc(kL^2)$ time complexity (Otsu, 1980).

Algorithm 3.1 presents this algorithm, where $\varphi(p,q)$ stands for the "discrepancy contribution" of the sub-image $I[p,q]$, *i.e.*,

$$\varphi(p,q) = \sum_{l=p}^{q} (l-\gamma)^2 P_l^{I[0,L-1]}, \tag{3.27}$$

where γ stands for $l_m(I[p,q])$ or $l_{mm}(I[p,q])$ depending on the discrepancy function used (see Equations 3.25 and 3.26).

Once Algorithm 3.1 is run, the optimal threshold vector T^k can be obtained by a back-searching procedure on PT, *i.e.*,

$$t_j^k = PT(j+1, t_{j+1}^{k*}), \tag{3.28}$$

where $1 \leq j < k$, $t_{j+1}^{k*} = L-1$ if $j+1 = k$, and $t_{j+1}^{k*} = t_{j+1}^k$ otherwise.

Remark that, recently, Luessi et al. (2006) proposed a new scheme jointing the matrix search procedure to the dynamic programming one, yielding a faster time complexity algorithm

($\bigcirc(kL)$) to multithresholding. This method can also be employed to perform the image decomposition process described here. Moreover, note that even faster approximated methods based on descendent gradient steps can be employed to find the thresholds (Reddi et al., 1984; Lee and Park, 1990).

3.3.3 Automatic Thresholding Criterium

This section presents an approach for automatically choosing the number of sub-images in which the original image will be decomposed on. This decision is a key point of our work, which has three main aims: 1) contrast enhancement; 2) brightness preserving; 3) natural appearance. Nonetheless, these goals cannot be all maximized simultaneously.

We take into account that, as the number of sub-images in which the original image is decomposed increases, the chance of preserving the image brightness and natural appearance also increases. In contrast, the chances of enhancing the image contrast decrease. Hence, in order to decide in how many sub-images the original image should be decomposed on, this tradeoff should be considered. We propose to use a cost function, initially used in Yen et al. (1995), to automatically select the number of decomposed sub-images. This cost function takes into account both the discrepancy between the original and processed images (which is our own aim decomposition function), and the number of sub-images in which the original image is decomposed on. This cost function is defined as:

$$C(k) = \rho(Disc(k))^{1/2} + (\log_2(k))^2, \tag{3.29}$$

where ρ is a positive weighting constant. The number of decomposed sub-images k is automatically given as the one which minimizes the cost function $C(k)$. It is shown in Yen et al. (1995) that the cost function presented in Equation 3.29 has a unique minimum for practical cases (*i.e.*, $Disc(k)$ is of the form $\alpha \times k^{-\lambda}$, $\alpha > 0$, $\lambda > 0$, $\rho < 4 \ln L \times L^{\lambda/2}/(\lambda \alpha^{1/2} (\ln 2)^2)$ and $0 < k < L$). Hence, instead of finding the value k which minimizes $C(k)$ throughout k values range, it is enough to search for k from 0 up to a value where $C(k)$ starts to increase.

3.4 Conclusions

In this chapter, we introduced two new gray-level multi-histogram equalization methods for image contrast enhancement and brightness preserving. Note that the time complexity of our methods is upper-bounded by the step of finding the optimal thresholds which has $\bigcirc(kL^2)$ time complexity (or even $\bigcirc(kL)$, if Luessi et al. (2006)'s algorithm is employed). These time complexities make our methods fast and suitable for real-time applications, even though they are more sophisticated than the previous ones in the original image decomposition process. Experiments comparing our methods and the ones described in Section 3.2 are presented in Section 5.1.

Chapter 4

Fast Hue-Preserving Histogram Equalization Methods

In the previous chapter we described some classical methods based on histogram equalization which are used to enhance gray-level images, and proposed new ones. Following this same line, in this chapter, we propose a generic fast hue-preserving histogram equalization (HE) method based on the RGB color space for image contrast enhancement and two instantiation of that generic process. The first method uses R-red, G-green and B-blue $1D$ histograms to estimate a RGB $3D$ histogram to be equalized, whereas the second method uses RG, RB, and GB $2D$ histograms.

The proposed methods preserve many of the ideas presented by other methods based on histogram equalization (Gonzalez and Woods, 2002; Trahanias and Venetsanopoulos, 1992). However, they have two main advantages: first, the methods are hue-preserving, *i.e.*, they avoid that new and unrealistic colors appear in the enhanced image. Second, the methods have low time complexity (both instantiations are linear with the image dimension), which makes them suitable for real-time applications, such as contrast enhancement of natural images acquired by mobile phones and PDAs.

This chapter starts with Section 4.1 introducing some basic definitions which will be used in the remaining sections. Following these definitions, in order to give a detailed description of our methods, Section 4.2 describes other methods from which the proposed methods borrow ideas from. Our fast hue-preserving histogram equalization methods for color image contrast enhancement are then introduced in Section 4.3. Section 4.4 discusses the time and space complexities of the described methods and the proposed ones. Finally, conclusions are drawn in Section 4.5.

4.1 Basic Definitions

In a context of discrete variables, the histogram of a variable represents the absolute frequency of each discrete value, whereas the probability density function of a variable constitutes the relative frequency of these values. The probability distribution function (or the cumulative probability density function), in turn, can be seen as the probability of a variable be less or equal to a value. These functions are used to estimate the probability of an event happening.

Considering that a color image is a discrete variable, this section describes its multidimensional histograms and their probability functions, which will be used throughout this chapter.

Definition 4.1 (Color Images) *Let* $\mathbb{N}$ *and* $\mathbb{Z}$ *denote the set of natural and integer numbers, respectively. Let* X^{mn} *be a subset of points* $(x, y) \in \mathbb{N}^2$*, such that* $0 \leq x < m$*, and* $0 \leq y < n$*, where* m *and* n *denote the dimensions of* X^{mn}*. Let* $||Y||$ *denote the cardinality of a set* $Y \subseteq \mathbb{N}^2$*. Note that* $||X^{mn}|| = m \times n$*. A mapping* I*, from* X^{mn} *to* $\mathbb{Z}_L^3$*, is called a (*color*)* image *(*of the *RGB* color space*). By abuse of terminology we denote a color image by* I^{RGB}*.*

Indeed, a color image I^{RGB} *has three mappings from* X^{mn} *to* $\mathbb{Z}_L$*, which are the* red, green *and* blue images, i.e.*,* I^R*,* I^G *and* I^B*, respectively.*

Let us also define three other mappings from X^{mn} *to* $\mathbb{Z}_L^2$, i.e., I^{RG}, I^{RB} I^{GB}*. We call these mappings as* red/green, red/blue *and* green/blue images*, respectively.*

Definition 4.2 (Levels) *For a point* $(x, y) \in X^{mn}$*,* $R_i = I^R(x, y)$*,* $G_i = I^G(x, y)$ *and* $B_i = I^B(x, y)$ *are called the* red, green *and* blue levels *of the point* (x, y) *in* I^{RGB}*, respectively, where* $0 \leq R_i, G_i, B_i < L$*. We can also denote* (R_i, G_i, B_i)*,* (R_i, G_i)*,* (R_i, B_i) *and* (G_i, B_i) *by* $I^{RGB}(x, y)$*,* $I^{RG}(x, y)$*,* $I^{RB}(x, y)$ *and* $I^{GB}(x, y)$*, respectively.*

In the following, we define $1D$, $2D$ and $3D$ histograms and probability density and distribution functions for color images.

For the $1D$ case, we firstly consider the R color channel.

Definition 4.3 ($1D$ Histogram) *Let* $X_{R_i}^{mn}$ *be a subset of* X^{mn}*, such that for all* $(x, y) \in X_{R_i}^{mn} \subseteq X^{mn}$*, we have* $I^R(x, y) = R_i$*. Let* $H_{R_i}^{I^R}$ *be the* absolute frequency *of the level* R_i *in the image* I^R*, where* $0 \leq R_i < L$*,* i.e., $H_{R_i}^{I^R} = ||X_{R_i}^{mn}||$*. Note that* $H_{R_i}^{I^R} = 0$*, if there is no* $(x, y) \in X^{mn}$ *such that* $I^R(x, y) = R_i$*. The mapping* H^{I^R} *from the levels of the image* I^R *to its absolute frequency levels,* i.e., $H^{I^R} : \mathbb{Z}_L \to \mathbb{N}$*, is called the* histogram *of the image* I^R*. Note that* $\sum_{R_i=0}^{L-1} H_{R_i}^{I^R} = m \times n$*.*

Definition 4.4 ($1D$ Probability Density Function) *Let* $P_{R_i}^{I^R}$ *be the* relative frequency *(or the probability) of the level* R_i *in the image* I^R*,* i.e.*,*

$$P_{R_i}^{I^R} = \frac{H_{R_i}^{I^R}}{m \times n}, \tag{4.1}$$

where $0 \leq R_i < L$. *Note that* $\sum_{r_i=0}^{R_i} P_{r_i}^{I^R} = 1$.

The function P^{I^R} *composed by all* $P_{R_i}^{I^R}$ *is the* probability density function *of the image* I^R.

Definition 4.5 (1*D* **Probability Distribution Function**) *Let* $C_{R_i}^{I^R}$ *be the probability distribution (or the cumulative probability density) of the level* R_i *in the image* I^R, i.e.,

$$C_{R_i}^{I^R} = \frac{1}{m \times n} \sum_{r_i=0}^{R_i} H_{r_i}^{I^R} = \sum_{r_i=0}^{R_i} P_{r_i}^{I^R}, \tag{4.2}$$

where $0 \leq R_i < L$. *Note that* $C_{L-1}^{I^R} = 1$.

The function C^{I^R} *composed by all* $C_{R_i}^{I^R}$ *is the* probability distribution function *(or the* cumulative probability density function*) of the image* I^R.

It is immediate to extend the above definitions for the image I^R, *i.e.*, H^{I^R}, P^{I^R} and C^{I^R}, to the images I^G and I^B. Note that the definitions for 1*D* histograms and their probability functions of color images, here introduced, are identical to the ones presented in Section 3.1 for monochrome images. They are again presented for sake of coherence on notation for color images.

For 2*D* histograms and their probability functions, we firstly consider the R and G color channels.

Definition 4.6 (2*D* **Histogram**) *Let* X_{R_i,G_i}^{mn} *be a subset of* X^{mn}, *such that for all* $(x, y) \in X_{R_i,G_i}^{mn} \subseteq X^{mn}$, *we have* $(R_i, G_i) = I^{RG}(x, y)$. *Let* $H_{R_i,G_i}^{I^{RG}}$ *be the* absolute frequency *of the color levels* R_i *and* G_i *in the image* I^{RG}, i.e., $H_{R_i,G_i}^{I^{RG}} = ||X_{R_i,G_i}^{mn}||$. *Note that* $H_{R_i,G_i}^{I^{RG}} = 0$, *if there is no* $(x, y) \in X^{mn}$ *such that* $I^{RG}(x, y) = (R_i, G_i)$. *The mapping* $H^{I^{RG}}$ *from the levels of the image* I^{RG} *to its absolute frequency,* i.e., $H^{I^{RG}} : \mathbb{Z}_L^2 \to \mathbb{N}$, *is called the* histogram *of the image* I^{RG}. *Note that* $\sum_{r_i=0}^{L-1} \sum_{g_i=0}^{L-1} H_{r_i,g_i}^{I^{RG}} = m \times n$.

Definition 4.7 (2*D* **Probability Density Function**) *Let* $P_{R_i,G_i}^{I^{RG}}$ *be the relative frequency (or the probability) of the color levels* R_i *and* G_i *in the image* I^{RG}, i.e.,

$$P_{R_i,G_i}^{I^{RG}} = \frac{H_{R_i,G_i}^{I^{RG}}}{m \times n}, \tag{4.3}$$

where $0 \leq R_i, G_i < L$. *Note that* $\sum_{r_i=0}^{L-1} \sum_{g_i=0}^{L-1} P_{r_i,g_i}^{I^{RG}} = 1$.

The function $P^{I^{RG}}$ *composed by all* $P_{R_i,G_i}^{I^{RG}}$ *is called the* probability density function *of the image* I^{RG}.

Definition 4.8 (2*D* **Probability Distribution Function**) *Let* $C_{R_i,G_i}^{I^{RG}}$ *be the probability distribution (or the cumulative probability density) of the color levels* R_i *and* G_i *in the image* I^{RG}, i.e.,

$$C_{R_i,G_i}^{I^{RG}} = \sum_{r_i=0}^{R_i} \sum_{g_i=0}^{G_i} P_{r_i,g_i}^{I^{RG}}, \tag{4.4}$$

where $0 \leq R_i, G_i < L$. *Note that* $C^{I^{RG}}_{L-1,L-1} = 1$.

The $C^{I^{RG}}$ *function composed by all* $C^{I^{RG}}_{R_i,G_i}$ *is called the* probability distribution function *(or the* cumulative probability density function*) of the image* I^{RG}.

Note that to compute $C^{I^{RG}}$ for all possible R_i and G_i, the above formulation has complexity $\bigcirc(L^4)$. By using a recursive definition, all possible R_i and G_i can be computed in $\bigcirc(L^2)$, *i.e.*,

$$C^{I^{RG}}_{R_i,G_i} = C^{I^{RG}}_{R_i-1,G_i} + C^{I^{RG}}_{R_i,G_i-1} - C^{I^{RG}}_{R_i-1,G_i-1} + P^{I^{RG}}_{R_i,G_i}. \tag{4.5}$$

It is immediate to extend the above definitions for the image I^{RG}, *i.e.*, $H^{I^{RG}}$, $P^{I^{RG}}$ and $C^{I^{RG}}$, to the images I^{RB} and I^{GB}.

For the last scenario, we have a single $3D$ histogram and its probability functions to be defined.

Definition 4.9 ($3D$ **Histogram)** *Let* $X^{mn}_{R_i,G_i,B_i}$ *be a subset of* X^{mn}, *such that for all* $(x, y) \in X^{mn}_{R_i,G_i,B_i} \subseteq X^{mn}$, *we have* $I^{RGB}(x, y) = (R_i, G_i, B_i)$. *Let* $H^{I^{RGB}}_{R_i,G_i,B_i}$ *be the* absolute frequency *of the color levels* R_i, G_i *and* B_i *in the image* I^{RGB}, i.e., $H^{I^{RGB}}_{R_i,G_i,B_i} = ||X^{mn}_{R_i,G_i,B_i}||$. *Note that* $H^{I^{RGB}}_{R_i,G_i,B_i} = 0$, *if there is no* $(x, y) \in X^{mn}$ *such that* $I^{RGB}(x, y) = (R_i, G_i, B_i)$. *The mapping* $H^{I^{RGB}}$ *from the levels of the image* I^{RGB} *to its absolute frequency,* i.e., $H^{I^{RGB}} : \mathbb{Z}^3_L \to \mathbb{N}$, *is called the* histogram *of the image* I^{RGB}. *Note that* $\sum_{r_i=0}^{L-1} \sum_{g_i=0}^{L-1} \sum_{b_i=0}^{L-1} H^{I^{RGB}}_{r_i,g_i,b_i} = m \times n$.

Definition 4.10 ($3D$ **Probability Density Function)** *Let* $P^{I^{RGB}}_{R_i,G_i,B_i}$ *be the relative frequency (or the probability) of the color levels* R_i, G_i, *and* B_i *in the image* I^{RGB}, i.e.,

$$P^{I^{RGB}}_{R_i,G_i,B_i} = \frac{H^{I^{RGB}}_{R_i,G_i,B_i}}{m \times n}, \tag{4.6}$$

where $0 \leq R_i, G_i, B_i < L$. *Note that* $\sum_{r_i=0}^{L-1} \sum_{g_i=0}^{L-1} \sum_{b_i=0}^{L-1} P^{I^{RGB}}_{r_i,g_i,b_i} = 1$.

The function $P^{I^{RGB}}$ *composed by all* $P^{I^{RGB}}_{R_i,G_i,B_i}$ *is the* probability density function *of the image* I^{RGB}.

Definition 4.11 ($3D$ **Probability Distribution Function)** *Let* $C^{I^{RGB}}_{R_i,G_i,B_i}$ *be the probability distribution (or the cumulative probability density) of the color levels* R_i, G_i, *and* B_i *in the image* I^{RGB}, i.e.,

$$C^{I^{RGB}}_{R_i,G_i,B_i} = \sum_{r_i=0}^{R_i} \sum_{g_i=0}^{G_i} \sum_{b_i=0}^{B_i} P^{I^{RGB}}_{r_i,g_i,b_i}, \tag{4.7}$$

where $0 \leq R_i, G_i, B_i < L$. *Note that* $C^{I^{RGB}}_{L-1,L-1,L-1} = 1$.

The function $C^{I^{RGB}}$ *composed by all* $C^{I^{RGB}}_{R_i,G_i,B_i}$ *is called the* probability distribution function *(or the* cumulative probability density function*) of the image* I^{RGB}.

Remark that the above formulation has complexity $\bigcirc(L^6)$ to compute $C^{I^{RGB}}$ for all possible R_i, G_i, and B_i. By using a recursive definition, similarly to the $2D$ case, we can compute all possible R_i, G_i, and B_i in $\bigcirc(L^3)$, *i.e.*,

$$\begin{aligned} C^{I^{RGB}}_{R_i,G_i,B_i} = {} & C^{I^{RGB}}_{R_i-1,G_i-1,B_i-1} + C^{I^{RGB}}_{R_i-1,G_i,B_i} + C^{I^{RGB}}_{R_i,G_i-1,B_i} + C^{I^{RGB}}_{R_i,G_i,B_i-1} \\ & - C^{I^{RGB}}_{R_i-1,G_i-1,B_i} - C^{I^{RGB}}_{R_i-1,G_i,B_i-1} - C^{I^{RGB}}_{R_i,G_i-1,B_i-1} + P^{I^{RGB}}_{R_i,G_i,B_i}. \end{aligned}$$

4.2 Previous Works

In this section, we present two histogram equalization methods directly related to our proposed methods. These methods are particularly important because we borrowed some ideas from them when implementing the methods proposed in this chapter. Note that all the histogram equalization methods described in this chapter work in three phases: (1) they compute the histograms of the image, (2) they compute the density and distribution probability functions of the image from the histograms, and (3) they enhance the image through histogram equalization.

The process carried out to compute the histogram of the image is the same in all methods. With a single scan throughout the image we can compute $1D$, $2D$ or $3D$ histograms, according to the definitions given in Section 4.1.

The second phase, where the density and distribution probability functions are calculated, strongly depends on the dimensions of the probability functions used for the method. It is well known that a typical color image has its R, G and B color channels neither full correlated nor totally independent distributed. Hence, the dimension (*i.e.*, $1D$, $2D$ or $3D$) of the density and distribution probability functions of the images used for the methods has a great impact on the quality of enhanced images and on the time complexity of the methods. In this respect, whereas some methods take into account only the red, green and blue channels separately (calculating $1D$ histograms), others consider the correlation among these channels two at-a-time, or even consider the three of them all together.

Regarding the third phase (the histogram equalization itself), methods can follow very specific rules to achieve it. The classical method processes the $1D$ histograms separately, and then employs the equalized histograms to enhance the image. Other methods process the image pixel by pixel, using an iterative process, in a way that the histogram of the output enhanced image has a uniform distribution, *i.e.*, it is equalized.

In the next subsections, we recall the classical $1D$ histogram equalization method. We then show the $3D$ histogram equalization method proposed by Trahanias and Venetsanopoulos (1992). This last method presents important concepts which will be then incorporated into our methods, described later on in Section 4.3.

4.2.1 Classical 1*D* Histogram Equalization Method

In Section 3.2.1, we described the classical histogram equalization method for enhancing monochromatic images. This classical method can be extended and also applied to enhance color images. However, as the extended version of this method uses a completely different set of notations, in this section we recall what was presented in Section 3.2.1, but using a notation which is more suitable for color images. We focus the description of the method on red images, and then extend it to green and blue images. Putting together these definitions in red, green and blue images, we can perform histogram equalization on the *RGB* color space.

The histogram equalization method for red images is described as follows. Let I^R and O^R be the red input and output images, or the original and equalized images, respectively. Let H^{I^R} (histogram), P^{I^R} (probability density function) and C^{I^R} (cumulative probability density function) be defined as in Section 4.1. The computation of the histogram and the probability functions of the input image constitute the first two phases of the method. Hence, let H^{O^R} be the desired uniform histogram of the output image, where any level R_o of H^{O^R} has the same amount of pixels, *i.e.*,

$$H^{O^R}_{R_o} = \frac{1}{L}(m \times n), \tag{4.8}$$

or the same density (*i.e.*, probability), *i.e.*,

$$P^{O^R}_{R_o} = \frac{1}{L}. \tag{4.9}$$

Thus, the cumulative probability density function C^{O^R} is defined in function of R_o as:

$$C^{O^R}_{R_o} = \frac{1}{m \times n} \sum_{r_o=0}^{R_o} H^{I^R}_{r_o} = \sum_{r_o=0}^{R_o} P^{I^R}_{r_o} = \frac{R_o + 1}{L}. \tag{4.10}$$

The third phase consists of computing the equalized histogram from the cumulative density function of the input image, and then equalizing the image. The R'_o output equalized level corresponding to the input level R_i is obtained as the one that minimizes the difference between $C^{O^R}_{R'_o}$ and $C^{I^R}_{R_i}$. In practice, the output level R'_o for the input level R_i is computed by the transformation function $T^{I^R}(R_i)$, *i.e.*,

$$R'_o = T^{I^R}(R_i) = \left\langle (L-1) \times C^{I^R}_{R_i} \right\rangle, \tag{4.11}$$

where $\left\langle (L-1) \times C^{I^R}_{R_i} \right\rangle$ stands for the nearest integer to $((L-1) \times C^{I^R}_{R_i}) \in \mathbb{R}$. This transformation function was named single mapping law (SML) in Zhang (1992). In this same work, a general mapping law (GML) was also proposed with the purpose of improving the accuracy of a uniform histogram specification. Nonetheless, in this work, we use the SML, *i.e.*, Equation 4.11, because it is simpler and faster to compute.

To generate the output enhanced image with this transformation, for any pixel $(x, y) \in X^{mn}$, we obtain the output value $O^R(x, y)$ as $R'_o = T^{I^R}(R_i)$, where $R_i = I^R(x, y)$.

This method can be easily extended for color image contrast enhancement by applying separately the equalization process described above to the images I^R, I^G and I^B. This extended method presents a well-known problem: it produces unrealistic colors, since it is not hue-preserving (Naik and Murthy, 2003). Note that this method has $\bigcirc(max(m \times n, L))$ and $\bigcirc(L)$ time and space complexities, respectively. From now on, we refer to this extended method as the classical $1D$ histogram equalization method, *i.e.*, C$1D$HE method.

4.2.2 3D Histogram Equalization Method

In this section, we describe the method proposed by Trahanias and Venetsanopoulos (1992), which takes into account the correlation of the three color channels, R, G, and B, simultaneously. It is described as follows.

Let I^{RGB} and O^{RGB} be the input and output color images. Let $H^{I^{RGB}}$, $P^{I^{RGB}}$ and $C^{I^{RGB}}$ be as defined in Section 4.1. Let $H^{O^{RGB}}$ be the uniform histogram of the output image, where any entry (R_o, G_o, B_o) has the same amount of pixels, once a such output histogram is desired, *i.e.*,

$$H^{O^{RGB}}_{R_o,G_o,B_o} = \frac{1}{L^3}(m \times n), \tag{4.12}$$

or the same density, *i.e.*,

$$P^{O^{RGB}}_{R_o,G_o,B_o} = \frac{1}{L^3}. \tag{4.13}$$

Hence, any entry (R_o, G_o, B_o) in $C^{O^{RGB}}$ is computed using $P^{O^{RGB}}$, *i.e.*,

$$\begin{aligned} C^{O^{RGB}}_{R_o,G_o,B_o} &= \sum_{r_o=0}^{R_o}\sum_{g_o=0}^{G_o}\sum_{b_o=0}^{B_o} P^{O^{RGB}}_{r_o,g_o,b_o} \\ &= \sum_{r_o=0}^{R_o}\sum_{g_o=0}^{G_o}\sum_{b_o=0}^{B_o} \frac{1}{L^3} \\ &= \frac{(R_o+1)(G_o+1)(B_o+1)}{L^3}. \end{aligned} \tag{4.14}$$

Note that $C^{O^{RGB}}_{R_o,G_o,B_o}$ can be directly obtained by its own values, *i.e.*, R_o, G_o and B_o.

To yield the output enhanced image, for any input pixel $(x, y) \in X^{mn}$, where $(R_i, G_i, B_i) = I^{RGB}(x, y)$, the smallest (R_o, G_o, B_o) for which the inequality:

$$C^{I^{RGB}}_{R_i,G_i,B_i} - C^{O^{RGB}}_{R_o,G_o,B_o} \geq 0, \tag{4.15}$$

holds.

However, this process of calculating the output image presents an ambiguity, mainly be-

cause there are many solutions for (R_o, G_o, B_o) which satisfy Equation 4.15. This ambiguity is remedied as follows. The computed value of $C^{I^{RGB}}$ at (R_i, G_i, B_i) is initially compared to the value of $C^{O^{RGB}}$ at (R_o, G_o, B_o). If $C^{I^{RGB}}$ is greater (*resp.* less) than $C^{O^{RGB}}$, then the indexes R_o, G_o, and B_o are repeatedly increased (*resp.* decreased), one at-a-time, until Equation 4.15 is satisfied. The obtained (R_o, G_o, B_o) is the output entry to the corresponding input (R_i, G_i, B_i), *i.e.*, if $(x, y) \in X^{mn}$ and $(R_i, G_i, B_i) = I^{RGB}(x, y)$, then $O^{RGB}(x, y) = (R_o, G_o, B_o)$.

From now on, we call the Trahanias and Venetsanopoulos (1992) $3D$ method as TV3DHE method. Note that the TV3DHE method has $\bigcirc(max(m \times n \times L, L^3))$ and $\bigcirc(L^3)$ time and space complexities, respectively.

Note that the methods discussed in this section have drawbacks that make them not suitable for real-world and real-time applications. Whereas the C1DHE method is not hue-preserving, the TV3DHE method is neither hue-preserving nor complies with real-time application requirements.

4.3 The Proposed Methods

In this section, we present a generic method which, in contrast with the methods presented in the previous section, is both hue-preserving and has time and space complexities which complies with real-world and real-time applications. We propose two variants from the generic method, which are characterized by the histograms dimension used to estimate the $3D$ probability functions, *i.e.*, $1D$ or $2D$ histograms - making the variant point of the generic method to be the probability function estimation phase.

4.3.1 Generic Hue-preserving Histogram Equalization Method

In this section, we present our generic method which, as the other ones, is divided in three phases. Initially, let I and O be the input and output images. Let the input $\#D$ histograms and probability functions be defined as in Section 4.1, where # is the histogram dimension used (this is the variant point of our method). Although the proposed method works with $\#D$ histograms, we do not equalize the $\#D$ histograms per say, but a $3D$ pseudo-histogram, *i.e.*, $H'^{I^{RGB}}$. The $H'^{I^{RGB}}$ definition is based on a pseudo $3D$ cumulative density function.

The computation of this cumulative density function, $C'^{I^{RGB}}$, which constitutes the second phase of our method, is performed as the product of the three $\#D$ cumulative functions for any entry (R_i, G_i, B_i). We show in details the variant methods in Section 4.3.2 and 4.3.3.

The third phase works as follows. Unlike the method described in Section 4.2.2, which iteratively increased or decreased the values of R_o, G_o and B_o in order to minimize Equation 4.15, we propose to find the output triplet (R_o, G_o, B_o) for any image pixel, in a single

step, *i.e.*, $\bigcirc(1)$. Thus, from Equations 4.14 and 4.15, we have:

$$C'^{I^{RGB}}_{R_i,G_i,B_i} - \frac{(R_o+1)(G_o+1)(B_o+1)}{L^3} = 0. \tag{4.16}$$

If we take R_o, G_o and B_o as R_i+k, G_i+k and B_i+k, respectively, where k would be the number of iterations required for minimizing Equation 4.15, we obtain:

$$\begin{aligned} &k^3+ \\ &k^2[R'_i+G'_i+B'_i]+ \\ &k[R'_i\times G'_i+R'_i\times B'_i+G'_i\times B'_i]+ \\ &R'_i\times G'_i\times B'_i - L^3\times C'^{I^{RGB}}_{R_i,G_i,B_i} = 0, \end{aligned} \tag{4.17}$$

where R'_i, G'_i, and B'_i mean R_i+1, G_i+1, and B_i+1, respectively. By solving this cubic equation in function of k, we obtain the desired output triplet (R_o, G_o, B_o) as the input one plus the displacement k, *i.e.*, $(R_i+\langle k\rangle, G_i+\langle k\rangle, B_i+\langle k\rangle)$, where $\langle k\rangle$ stands for the nearest integer to $k\in\mathbb{R}$.

Equation 4.17 can be easily solved by the methods proposed in Nickalls (1993) and Cardano (1545). The formed method is faster and mathematically simpler than the latter, which uses transcendental functions. Based on their complexities, in this work, we use the Nickalls (1993)'s method.

Observe that any image pixel is enhanced following a shift transformation by a k factor, *i.e.*, from (R_i, G_i, B_i) to $(R_o, G_o, B_o) = (R_i+\langle k\rangle, G_i+\langle k\rangle, B_i+\langle k\rangle)$, which makes our generic method hue-preserving (Naik and Murthy, 2003).

Having described this generic method, the next subsections show our variant methods, which differ only on the histogram dimension used. By respecting the chronology's conception of our method, the method based on RG, RB and GB $2D$ histograms (Menotti et al., 2006) (from now on HP2DHE method), is firstly described in Section 4.3.2. Then, the method based on $1D$ histograms (Menotti et al., 2007b) (from now on HP1DHE method) is presented in Section 4.3.3.

4.3.2 Hue-preserving $2D$ Histogram Equalization Method

In this section, we present our HP2DHE method which was initially introduced in Melo et al. (2005) and after in Menotti et al. (2006). It uses $2D$ histograms (as defined in Section 4.1) and is based on the correlation of channels two at-a-time to perform the histogram equalization.

The cumulative probability density function, $C'^{I^{RGB}}$, is then computed as the product of the three $2D$ cumulative functions for any entry (R_i, G_i, B_i), *i.e.*,

$$C'^{I^{RGB}}_{R_i,G_i,B_i} = C^{I^{RG}}_{R_i,G_i} \times C^{I^{RB}}_{R_i,B_i} \times C^{I^{GB}}_{G_i,B_i}. \tag{4.18}$$

The main rationale for computing this pseudo-cumulative probability density function as the product of three $2D$ cumulative functions is that the three color channels in an image are usually not simultaneously correlated.

Note that, in Menotti et al. (2006), we proposed to solve Equation 4.15 iteratively, as done in Trahanias and Venetsanopoulos (1992) (TV3DHE method), by using a non hue-preserving transformation. Here, we modify the method originally proposed in Menotti et al. (2006) to use the hue-preserving shift transformation and the solution of Equation 4.15 described in the previous subsection. These two modifications make the HP2DHE method presented here hue-preserving, and reduces its initially time complexity from $\bigcirc(max(m \times n \times L, L^2))$ to $\bigcirc(max(m \times n, L^2))$.

4.3.3 Hue-preserving 1D Histogram Equalization Method

In this section, we present a hue-preserving histogram equalization method based on the RGB color space for image contrast enhancement, which uses $1D$ histograms, and is also a variant of the generic method described in Section 4.3.1. The method is based on the independence assumption of color channels, which is used in a Bayesian framework for computing the cumulative probability density function. We use $1D$ histograms to estimate a $3D$ probability distribution function, and then equalize the conceived histogram through the estimated probability function.

In Data Mining and Knowledge Discovery domains, it is well known that Bayesian classifiers work well, even though the independence assumption is violated (Domingos and Pazzani, 1997). Although it is also well know that this assumption does not hold for the R, G and B channels of color images, we hope that the enhancement produced in color image through histogram equalization will work well.

Hence, the function $C'^{I^{RGB}}$ is estimated for any entry (R_i, G_i, B_i) as the product of every cumulative distribution $C^{I^R}_{R_i}$, $C^{I^G}_{G_i}$, and $C^{I^B}_{B_i}$, following the rule, *i.e.*,

$$C'^{I^{RGB}}_{R_i,G_i,B_i} = C^{I^R}_{R_i} \times C^{I^G}_{G_i} \times C^{I^B}_{B_i}. \tag{4.19}$$

Note that, in Equation 4.19, $C'^{I^{RGB}}$ obeys a Naive Bayesian rule (Stigler, 1983), while in Equation 4.18 (*i.e.*, the one of HP2DHE method) $C'^{I^{RGB}}$ is defined without a mathematical meaning. Nevertheless, the images processed by the HP2DHE method produce similar results to the HP1DHE method, as the experiments reported in the next chapter (Section 5.2) will show.

As we use $1D$ histograms, this method has the time complexity greater than the HP2DHE method, *i.e.*, $\bigcirc(max(m \times n, L))$, and the space complexity is linear, *i.e.*, $\bigcirc(L)$. Moreover, the time and space complexities of HP1DHE are exactly the same of the C1DHE method, which are the best to our knowledge for color image contrast enhancement through histogram

equalization.

4.4 Complexity Analysis

In this section, we present an analysis of the space and time complexities of the histogram equalization methods described in this chapter, including our proposed method (*i.e.*, its variants). As explained before, histogram equalization methods work in three main phases: 1) Histogram computation; 2) Density and Distribution probability functions computation; 3) Image contrast enhancement through histogram equalization. We firstly discuss the time complexity of these methods in each of these three phases.

The first phase is computed with a single scan throughout the image, and hence it has $\bigcirc(m \times n)$ time complexity.

The second phase is dependent on the histograms dimension used. The probability functions for $1D$ histograms can be computed in $\bigcirc(L)$. By using recursive definitions presented in Section 4.1, one can compute the probability functions for $2D$, and $3D$ histograms in $\bigcirc(L^2)$ and $\bigcirc(L^3)$, respectively. Hence, it is confirmed that the time complexity of this second phase is dependent on the dimension of the histograms.

In the third phase, the image is processed pixel by pixel, *i.e.*, $\bigcirc(m \times n)$. The C1DHE method, however, before processing each image, performs a preprocessing in $\bigcirc(L)$ to compute lookup tables, *i.e.*, it computes the transformation function in Equation 4.11 only once for each level of each channel R, G and B. The TV3DHE method executes an iterative process for each pixel in the image, and has $\bigcirc(L)$ time complexity for each one. Note that TV3DHE method can perform $\bigcirc(3(L-1))$ steps in the worst case, since it gives one unitary step at-a-time in only one of the three channels. Our methods have no preprocessing and they perform the third phase in $\bigcirc(1)$ for any image pixel. However, solving the cubic equation described in Equation 4.17 is computationally heavy, making the total run-time performance of our methods worst than the C1DHE one.

Table 4.1 summarizes the time complexity of the methods.

Table 4.1: A summary about time complexity of the histogram equalization methods. $M[x, y]$ stands for $max(x, y)$, and mn stands for $m \times n$.

	C1DHE	TV3DHE method	HP2DHE method	HP1DHE
Histograms	$\bigcirc(mn)$	$\bigcirc(mn)$	$\bigcirc(mn)$	$\bigcirc(mn)$
Probabilities	$\bigcirc(L)$	$\bigcirc(L^3)$	$\bigcirc(L^2)$	$\bigcirc(L)$
Equalization	$\bigcirc(M[mn, L])$	$\bigcirc(mn \times L)$	$\bigcirc(mn)$	$\bigcirc(mn)$
Total	$\bigcirc(M[mn, L])$	$\bigcirc(M[mn \times L, L^3])$	$\bigcirc(M[mn, L^2])$	$\bigcirc(M[mn, L])$

Now, we discuss the space complexity of the methods presented in this chapter. The

space complexity of the methods depends totally on the histograms dimension used, *e.g.*, $\bigcirc(L)$, $\bigcirc(L^2)$ or $\bigcirc(L^3)$. That is, our HP1DHE and the C1DHE methods have linear space complexity with respect to the number of discrete levels, *i.e.*, $\bigcirc(L)$, whilst our HP2DHE and the TV3DHE methods have quadratic and cubic space complexity, *i.e.*, $\bigcirc(L^2)$, $\bigcirc(L^3)$, respectively.

Remark that the HP1DHE and HP2DHE methods have $\bigcirc(max(m \times n, L))$ and $\bigcirc(max(m \times n, L^2))$ time complexities, respectively. And they are linear and quadratic for space complexity, *i.e.*, $\bigcirc(L)$, $\bigcirc(L^2)$, respectively. Hence, such time and space complexities comply with real-time application requirements.

Note that as the term $m \times n$ on the time complexity expression is much more important than the second one[1], on a run-time comparison the methods have similar performance, as will be further illustrated in the next chapter. Observe that especial attention for the run-time of the methods with respect to the image dimension is given in the next chapter in the experiments and is presented in Section 5.2.3.

4.5 Conclusions

In this chapter, we introduced and described two new hue-preserving histogram equalization methods based on the *RGB* color space for image contrast enhancement. In next chapter, we present the experiments for the methods proposed in this chapter and in Chapter 3.

[1]Usually we have $m \times n$ greater than L and the run-time taken on the third phase, where the term $m \times n$ is the only taken into account, is much more heavy

Chapter 5

Experiments

This section reports the results of experiments performed to evaluate the methods introduced in Chapter 3 and 4, and it is divided in two parts. Section 5.1 reports the results concerning the gray-level image contrast enhancement methods introduced in Chapter 3, whereas Section 5.2 presents the results related to the color image contrast enhancement methods proposed in Chapter 4.

5.1 Multi-Histogram Equalization Methods for Gray-level Image Contrast Enhancement and Brightness Preserving

In this section, we report results of experiments comparing our proposed methods in Chapter 3 (Section 3.3) with the other HE methods described in Section 3.2 and the method proposed in Wang and Ye (2005). The input images used in the experiments were the ones previously used in Kim (1997), Wang et al. (1999), Chen and Ramli (2003b), Chen and Ramli (2003a) and Wang and Ye (2005). They are named as they were in the works where they first appeared: arctic hare, bottle, copter, couple, Einstein, F16, girl, hands, house, jet, U2, woman (girl in Wang and Ye (2005)). Images were extracted from the CVG-UGR database (CVG-URG, 2007) and provided by the authors of (Chen and Ramli, 2003b) and (Chen and Ramli, 2003a).

Table 5.1 shows the number of sub-images automatically obtained by the methods MWCVMHE and MMLSEMHE (*i.e.*, the value of the parameter k - see Section 3.3.3), represented by the columns l_m and l_{mm}, respectively. These values were obtained using the threshold criterion for weighting the constant ρ with the value 0.8 (as done in Yen et al. (1995)). In practice, our methods take less than 50 milliseconds to find the number k, decompose and enhance an image on a Pentium IV - 2GHz[1].

To start our analysis, for each image, we compute the brightness (*i.e.*, the mean) and contrast (*i.e.*, the standard deviation) of the original and the output images obtained by the

[1]We take into account the loading and storing time of the image file as well.

Table 5.1: Automatic Selection of the Number of Sub-images - k

Image	l_m	l_{mm}
arctic-hare	5	7
bottle	6	6
copter	6	6
couple	5	6
Einstein	6	7
F16	5	7
girl	5	6
hands	5	6
house	6	6
jet	5	5
U2	4	4
woman	6	7

HE methods. Moreover, in order to assess the appropriateness of the processed images for consumer electronics products, we compute the $PSNR$ measure (Rabbani and Jones, 1991) as well. In the image processing literature, the $PSNR$ has been used as a standard measure to evaluate and compare compression and segmentation algorithms (Rabbani and Jones, 1991). It is well-known that a processed image with good quality (with respect to the original one) presents $PSNR$ values within 30 dB and 40 dB (Rabbani and Jones, 1991).

The values of brightness, contrast and $PSNR$ obtained for each image are presented in Tables 5.2, 5.3 and 5.4. These tables are divided into three parts: 1) The names and the data of original images (for the $PSNR$ table, the values of original images are constant, *i.e.*, ∞); 2) The data values obtained by the Uni-, Bi-HE and Wang and Ye (2005)'s methods, *i.e.*, HE, BBHE, DSIHE, MMBEBHE, and BPHEME; 3) The values obtained by the MHE methods, *i.e.*, RMSHE ($r = 2$), and our proposed MWCVMHE and MMLSEMHE methods.

In Tables 5.2 and 5.3, we firstly compare the data values (image brightness and image contrast, respectively) of each of the 8 processed images with the original image and highlight in gray the best results in parts 2 (*i.e.*, Uni-, Bi-HE and Wang and Ye (2005)) and 3 (*i.e.*, MHE) of the table. In a second step, we compare the best values in parts 2 and 3 of the tables against each other (*i.e.*, Uni-, Bi-HE and Wang and Ye (2005)'s methods against MHE methods). The best value is dark-grayed, the worst light-grayed.

Let us first analyze the results in Table 5.2, regarding the brightness of the original and the processed images. By observing the absolute difference between the value of the brightness in the original and processed images (*i.e.*, the brightness preservation), we state that: 1) The images produced by our proposed methods are better in preserving the brightness of the original images in 8 out of 12 images; 2) Even though our methods are not always the best

Table 5.2: Image's Brightness - Mean ($\mu = \sum_{l=0}^{L-1} l \times p(l)$)

Image	original	HE	BBHE	DSIHE	MMBEBHE	BPHEME	RMSHE ($r = 2$)	MWCVMHE	MMLSEMHE
arctic hare	220.89	139.45	199.18	184.76	209.22	222.92	218.05	217.96	220.13
bottle	78.76	128.35	94.15	97.73	82.36	79.37	81.08	78.94	79.08
copter	191.44	128.69	174.23	164.47	188.57	192.12	188.43	190.20	190.53
couple	33.35	129.83	66.47	77.23	49.79	33.96	43.46	36.54	35.45
einstein	107.75	128.83	126.99	119.78	108.84	109.00	117.85	110.50	108.64
F16	179.20	129.42	180.22	163.24	180.24	180.32	180.40	184.99	178.93
girl	139.20	133.94	162.78	131.66	144.97	145.21	139.77	139.46	140.05
hands	27.99	179.71	52.99	46.64	46.06	38.36	31.75	41.61	31.63
house	68.97	129.86	94.00	95.48	70.48	70.74	77.01	72.68	71.35
jet	201.11	129.33	196.15	174.25	201.51	201.93	200.42	200.75	201.70
U2	32.51	131.33	49.32	74.21	39.78	33.56	37.06	32.66	33.55
woman	113.13	128.52	129.07	124.43	114.17	114.12	113.00	113.84	113.24

Table 5.3: Image's Contrast - Global Standard Deviation ($\sigma = \sqrt{\sum_{l=0}^{L-1} (l - \mu) \times p(l)}$, where $\mu = \sum_{l=0}^{L-1} l \times p(l)$)

Image	original	HE	BBHE	DSIHE	MMBEBHE	BPHEME	RMSHE ($r = 2$)	MWCVMHE	MMLSEMHE
arctic hare	49.07	86.73	71.91	81.29	57.90	34.87	52.76	56.69	49.11
bottle	52.07	73.34	73.47	75.70	59.65	63.65	59.12	55.19	54.83
copter	40.66	73.90	72.70	76.76	52.52	55.89	52.05	44.85	44.48
couple	31.57	71.81	74.13	79.50	48.46	32.98	53.26	35.83	32.02
einstein	37.11	73.56	73.87	73.92	62.33	72.14	57.92	40.05	37.59
F16	45.12	74.57	67.68	77.40	68.79	62.61	61.08	55.30	46.74
girl	29.70	75.47	70.09	75.42	68.70	74.67	37.81	35.37	31.47
hands	54.36	27.29	60.92	75.80	69.39	21.74	59.90	50.51	54.69
house	38.25	73.61	75.14	75.55	55.43	59.66	56.84	41.93	39.72
jet	52.00	74.31	64.71	78.33	54.36	49.70	56.79	57.19	55.92
U2	25.62	72.23	64.58	78.39	50.00	32.14	44.68	36.52	29.63
woman	49.19	73.51	73.62	73.69	66.11	72.80	62.57	52.26	50.69

Table 5.4: $PSNR = 10 \times \log_{10}\left[(L-1)^2/MSE\right]$

Image	HE	BBHE	DSIHE	MMBEBHE	BPHEME	RMSHE ($r = 2$)	MWCVMHE	MMLSEMHE
arctic hare	8.11	16.63	13.09	23.55	22.95	30.74	31.44	40.27
bottle	12.88	18.68	17.53	28.44	25.72	29.68	35.99	36.71
copter	10.61	15.95	14.20	25.50	23.20	25.62	33.83	34.77
couple	7.57	13.18	11.61	19.86	38.54	19.65	30.59	40.16
einstein	15.08	15.15	15.58	18.91	16.21	19.51	31.42	34.53
F16	11.92	20.69	16.02	20.32	21.61	22.72	24.43	37.10
girl	13.03	13.30	12.99	14.03	13.19	28.00	29.39	33.03
hands	4.36	19.58	17.76	19.99	17.18	30.93	24.49	35.82
house	10.82	14.27	14.07	21.41	19.93	21.36	31.81	36.37
jet	9.51	22.50	14.37	30.78	23.99	27.85	29.14	31.74
U2	6.99	15.06	10.94	19.87	27.32	22.12	26.21	31.08
woman	17.83	17.73	18.25	21.60	19.23	23.67	28.83	34.53

brightness preserving ones, their resulting brightness is always very close to the brightness of the original images; 3) The MMLSEMHE method has shown to be more robust than the MWCVMHE method in terms of brightness preservation.

We perform a similar analysis to the one performed in Table 5.2 in Table 5.3. By observing the contrast values, we state that: 1) The method DSIHE produces the best image contrast enhancement in 10 out of 12 images, losing only twice for the classical HE method; 2) The RMSHE (with $r = 2$ - four sub-images) presents the best image contrast enhancement among the MHE methods in 10 out 12 images, losing only twice for our MWCVMHE method; 3) The MMLSEMHE method produces the smallest image contrast enhancement - this is the price to pay to obtain at the same time image contrast enhancement, brightness preserving, and natural looking images. Nonetheless, as will be shown in a further visual analysis of images, the images produced by the MMLSEMHE method are the best ones regarding the natural look.

Finally, we analyze the data presented in Table 5.4. In Table 5.4, the best values of $PSNR$ are highlighted in gray. Recall that the greater the value of the $PSNR$, the better it is. Looking at these figures, we observe that the images processed by the MMLSEMHE method produces the best $PSNR$ values, as they are within the range $[30dB, 40dB]$. Based on this result we argue that the MMLSEMHE method performs image contrast enhancement, preserves the brightness and also produces images with a natural looking. Moreover, this result corroborates, in practice, our hypothesis that the MMLSEMHE method, using the discrepancy function in Equation 3.26, yields image with the best $PSNR$ values among all the HE methods.

Once the images were analyzed considering their brightness, contrast and $PSNR$, we performed an image visual assessment. Remark that all the 12 input images, their histograms, their respective enhanced images and equalized histograms (obtained by all the methods listed in Tables 5.2, 5.3 and 5.4), adding up more than 200 images, can be seen in Menotti (2007). Here we present an analysis of 3 images: girl, Einstein and arctic hare.

Figure 5.1 shows the resulting images obtained by the BPHEME method (Wang and Ye, 2005) and our proposed ones for the girl image. Note that the output images obtained by Bi-HE and the RMSHE methods for the girl image can be observed at Figure 3.1. By visually inspecting the images on these two figures, we can clearly see that only the MHE methods (*i.e.*, RMSHE (with $r = 2$), MWCVMHE and MMLSEMHE methods) are able to generate natural looking images and still offer contrast enhancement.

Figure 5.2 shows the Einstein and the resulting images obtained by the MHE methods, *i.e.*, RMSHE (with $r = 2$), MWCVMHE and MMLSEMHE. By observing the processed images, it is noticeable that our proposed methods are the only ones among the MHE methods that can produce images with a natural looking. Recall that the other methods are worse than MHE methods for producing natural looking images.

(a) (b) (c) (d)

Figure 5.1: Results: (b), (c) and (d) are the enhanced resulting images by BPHEME, MWCVMHE ($k = 5$), and MMLSEMHE ($k = 6$) methods, respectively, using (a) the girl image as input.

Figure 5.3 shows the images obtained by applying the MHE methods to the image arctic hare. We chose this picture because it shows that, even though the image contrast produced by our methods is sometimes limited, they can enhance particular and interesting parts of an image. Observe that on the upper right corner of the images, we can perceive contrast enhancement. Nonetheless, the RMSHE (with $r = 2$) and MWCVMHE methods generate better enhancement on that region than the MMLSEMHE method.

After analyzing the data presented in Tables 5.2, 5.3 and 5.4 and visually observing some processed images, we conclude that: 1) The MMLSEMHE method produces images with better quality than the other methods with respect to the $PSNR$ measure; 2) Nonetheless, a better image contrast enhancement can be obtained by the MWCVMHE method, which also presents satisfactory brightness preserving and natural looking images; 3) The RMSHE

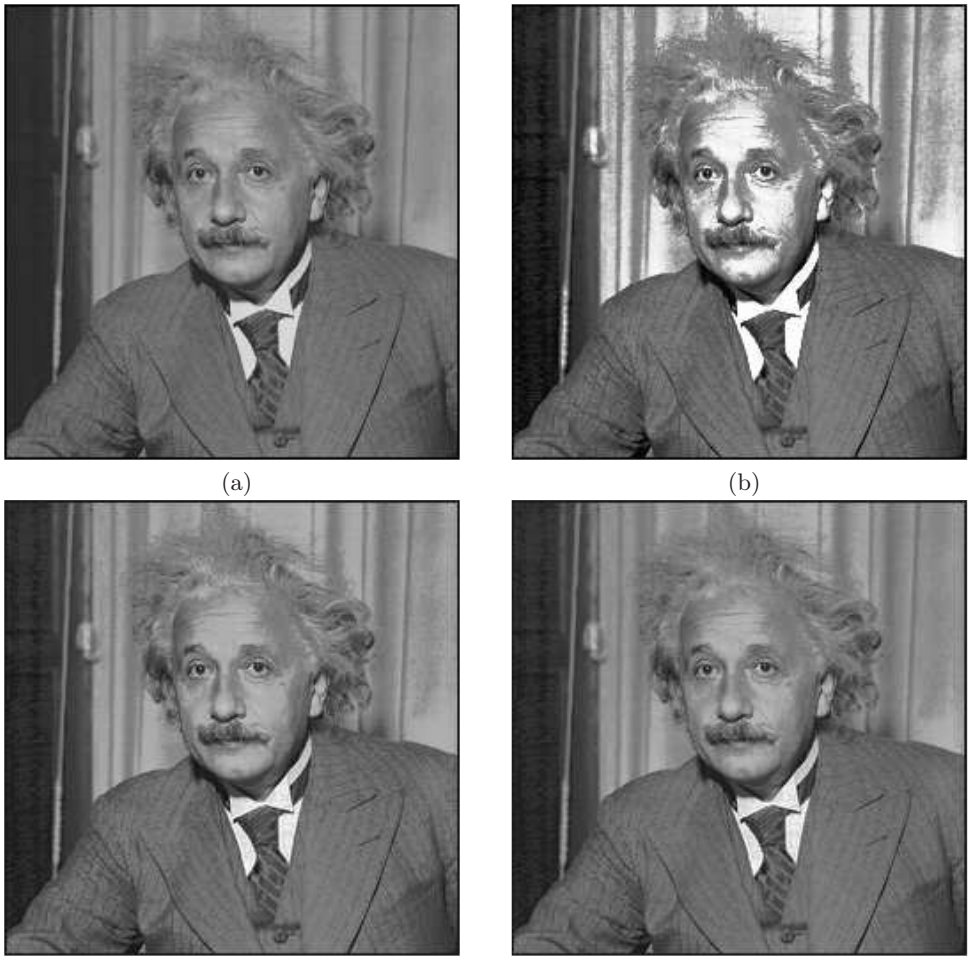

(a) (b)

(c) (d)

Figure 5.2: Results for : (a) original image; (b), (c) and (d) are the enhanced resulting images by RMSHE ($r = 2$), MWCVMHE ($k = 6$), and MMLSEMHE ($k = 7$) methods, respectively, using the einstein image.

method (with $r = 2$) should be employed when better contrast enhancement than the one offered by the MMLSEMHE and MWCVMHE methods is desired. However, in this case, the processed image may present some annoying and unnatural artifacts (for instance Figure 5.2b).

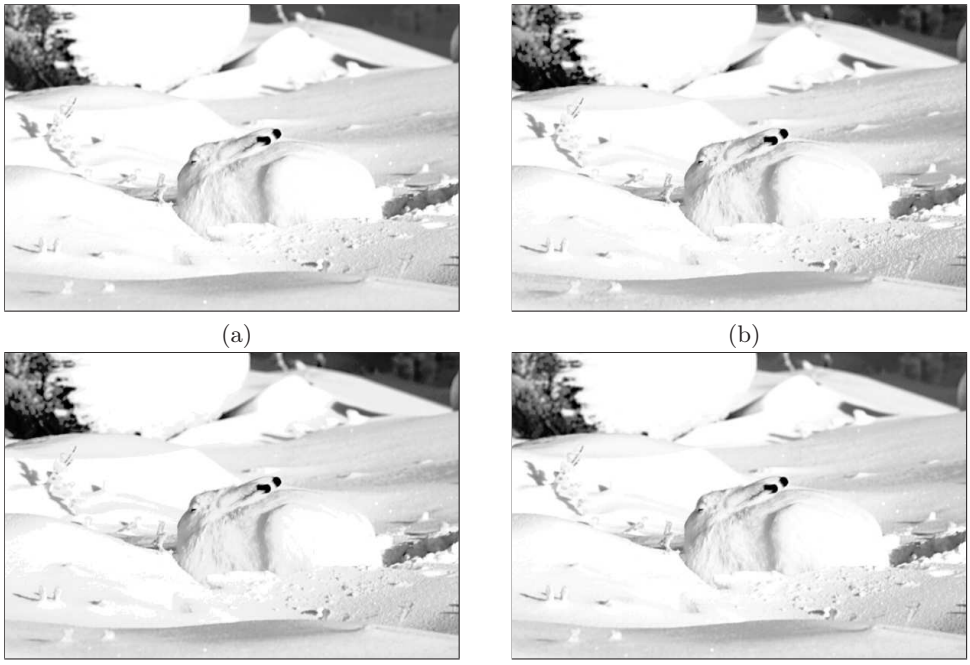

(a) (b) (c) (d)

Figure 5.3: Results for : (a) original image; (b), (c) and (d) are the enhanced resulting images by RMSHE ($r = 2$), MWCVMHE ($k = 5$), and MMLSEMHE ($k = 7$) methods, respectively, using the arctic hare image.

5.2 Histogram Equalization Methods for Color Image Contrast Enhancement based on the *RGB* Color Space

In this section, a comparison among our proposed HE methods for color images and the ones described in Section 4.2 is carried out. Firstly, a subjective assessment is used to compare the visual quality of two images: the beach and the train. After, we define objective measures to compare quantitatively the quality of the yielded images and the contrast improvement obtained for the processed images. Finally, a run-time analysis of the HE methods for color contrast enhancement images is performed.

5.2.1 Subjective Evaluation

In this section, we visually compare the processed images to the original ones, in order to assess the quality of the processed images. The main goal is highlight how delicate it is to evaluate subjectively enhanced images.

Figure 5.4 shows the results for the beach image. Note that unrealistic colors are present in the image generated by the C1*D*HE method (Figure 5.4b). The image produced by the TV3*D*HE method is overenhanced, producing oversaturated and bright colors (Figure 5.4c).

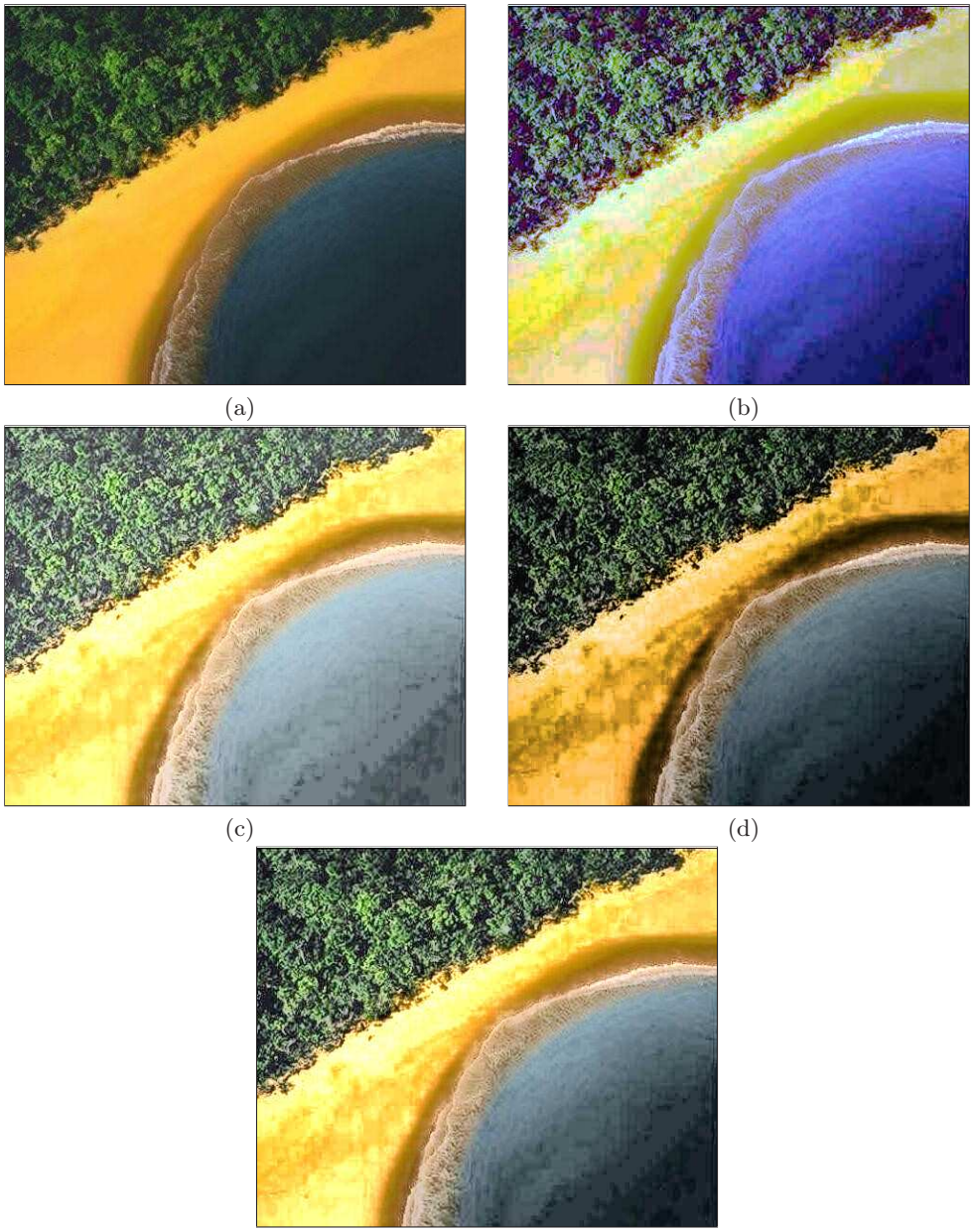

(a) (b) (c) (d) (e)

Figure 5.4: Results for the beach (partial brazilian flag) image: (a) original image; (b) C1DHE; (c) TV3DHE; (d) HP2DHE; (e) HP1DHE.

In turn, the image produced by our HP2DHE method (Figure 5.4d) is more realistic than all the others. However, from another viewpoint, which considers the application in which the methods are used, we can say that the output image of the TV3DHE method has better quality than the others. This is because the water region in this particular image (Figure 5.4c) was better enhanced. Despite these arguments, we can say that our HP1DHE method generates

(a) (b) (c) (d) (e)

Figure 5.5: Results for the train image: (a) original image; (b) C1DHE; (c) TV3DHE; (d) HP2DHE; (e) HP1DHE.

an image (Figure 5.4e) with a good balance between non oversaturated and realistic colors.

Figure 5.5 shows the results for the second image, the train. We observe that the TV3DHE method produces an oversaturated image (Figure 5.5c), as it did for the beach image. The images produced by our methods (Figure 5.5d and Figure 5.5e) are more real than the one obtained by the TV3DHE method. However, some hidden details in dark regions continue to be uncleared. In our opinion, the best enhancement is achieved by the image produced by the C1DHE method (Figure 5.5b). This is because the image produced by the C1DHE method presents colors which are more realistic for the green regions, and have more details than those produced by the other three methods. However, again, note that in the sky portion of the image unrealistic colors are produced by the C1DHE method.

From the discussion above, we claim that our methods produce images (Figures 5.4d, 5.4e, 5.5d, and 5.5e) with the best trade-off between the saturated colors and quality preservation

(*i.e.*, realistic images). That is, our methods produce images with colors that are more realistic than the C1DHE (which is not hue preserving), and the images are not so saturated as the ones produced by the TV3DHE method.

Nonetheless, we notice from the experiments just reported that it is difficult to assess the quality of an enhanced image using only a subjective measure. Ideally, a more objective and quantitative evaluation should be performed, allowing us to draw more clear and solid conclusions.

5.2.2 Objective Evaluation

As noticed above, it is imperative to evaluate the image quality yielded by the HE methods quantitatively, since subjective evaluation can be very application-dependent and not always conclusive. Hence, here, we use quantitative measures to assess the quality of original and processed images produced by the methods described in Section 4.2 and ours (presented in Section 4.3), and then perform an objective comparison among them. We also evaluate the contrast improvement by comparing the processed images to the original one.

The measures used for comparing the methods are defined in Section 5.2.2.1. The numerical results obtained through these quantitative measures in a data set of 300 images taken from the Berkeley University (Martin et al., 2001) are analyzed and discussed in Section 5.2.2.2.

5.2.2.1 Measures for Assessing Color Images Quality and Contrast

This section describes two types of measures that can be used to evaluate color images: a color image quality mesure and a measure of contrast as defined bellow. The defined color image quality measure (CIQM) (Yendrikhovskij et al., 1998b,a) is composed by the color image naturalness and colorfulness indexes (two psycho-physical measures defined according to the human vision system), and is used to verify if the HE methods preserve the quality of the images. These measures are based on the *CIELUV* color space, and are described as follows.

The naturalness is the degree of correspondence between human perception and the reality world. Based on assumptions experimentally proved, the *CIE* a^*b^* or *CIE* $u'v'$ planes are roughly divided into four privileged segments: achromatic, orange-yellow, yellow-green and blue. The *naturalness index* is suggested to be computed as the sum of the naturalness indexes of the privileged segments, weighted by the number of pixels within a privileged segment. In turn, the naturalness index of a privileged segment is defined as a Gaussian density function of the difference between the apparent color of the segment and the prototypical color of that segment category. The colorfulness presents the color vividness degree. The *colorfulness index* can be computed as a linear function of the average saturation of the image and its standard deviation.

The naturalness and colorfulness indexes can be computed for every image without any other additional information, such as a reference image, being provided. Hence, by using these

quantitative measures based on the human vision system, we can compare the performance of various histogram equalization methods for color image contrast enhancement without any subjective evaluation.

In order to define the CIQM, we firstly calculate the color naturalness index (CNI) and the colorfulness index (CCI). These two indices are defined in the *CIELUV* color space (Yendrikhovskij et al., 1998b). Note that even though the conversion required for computing the CIQMs are said to be standard, essential implementation details are no clear in Yendrikhovskij et al. (1998b)

The first index, the CNI, is computed as follows:

1. Converting the image from the *RGB* color space to the *CIELUV* color space. This is done by first converting the image from the *RGB* color space to the XYZ one (using D_{65} white point), *i.e.*,

$$\begin{bmatrix} X \\ Y \\ Z \end{bmatrix} = \begin{bmatrix} 0.4124 & 0.3576 & 0.1805 \\ 0.2126 & 0.7152 & 0.0722 \\ 0.0193 & 0.1192 & 0.9505 \end{bmatrix} \times \begin{bmatrix} d(R) \\ d(G) \\ d(B) \end{bmatrix}, \tag{5.1}$$

where

$$d(K) = \begin{cases} ((K + 0.055)/1.055)^{2.4}, & \text{if } K > 0.04045 \\ K/12.92, & \text{otherwise.} \end{cases} \tag{5.2}$$

Having the image in the XYZ color space, we convert it to the *CIELUV* one, *i.e.*,

$$L^* = \begin{cases} 116(Y/Y_n)^{1/3} - 16, & \text{if } Y/Y_n > 0.008856 \\ 903.3(Y/Y_n), & \text{otherwise,} \end{cases} \tag{5.3}$$

$$u^* = 13L^*(u^{'} - u_n^{'}), \tag{5.4}$$

$$v^* = 13L^*(v^{'} - v_n^{'}), \tag{5.5}$$

where

$$u^{'} = (4X)/(X + 15Y + 3Z), \tag{5.6}$$

$$v^{'} = (9Y)/(X + 15Y + 3Z), \tag{5.7}$$

and $u_n^{'}$ and $v_n^{'}$ are computed using the D_{65} white point - $(X_n, Y_n, Z_n) = (95.047, 100.000, 108.883)$, based on Equations 5.6 and 5.7.

2. Computing the hue (H_{uv}^*) and saturation (S_{uv}^*), *i.e.*,

$$H_{uv}^* = arctan(v^*/u^*), \tag{5.8}$$

$$S^*_{uv} = C^*_{uv}/L^* = \sqrt{(u^*)^2 + (v^*)^2}/L^*. \tag{5.9}$$

3. Thresholding the L^* and S^*_{uv} components, where L^* values between 20 and 80 and S^*_{uv} values over 0.1 are kept.

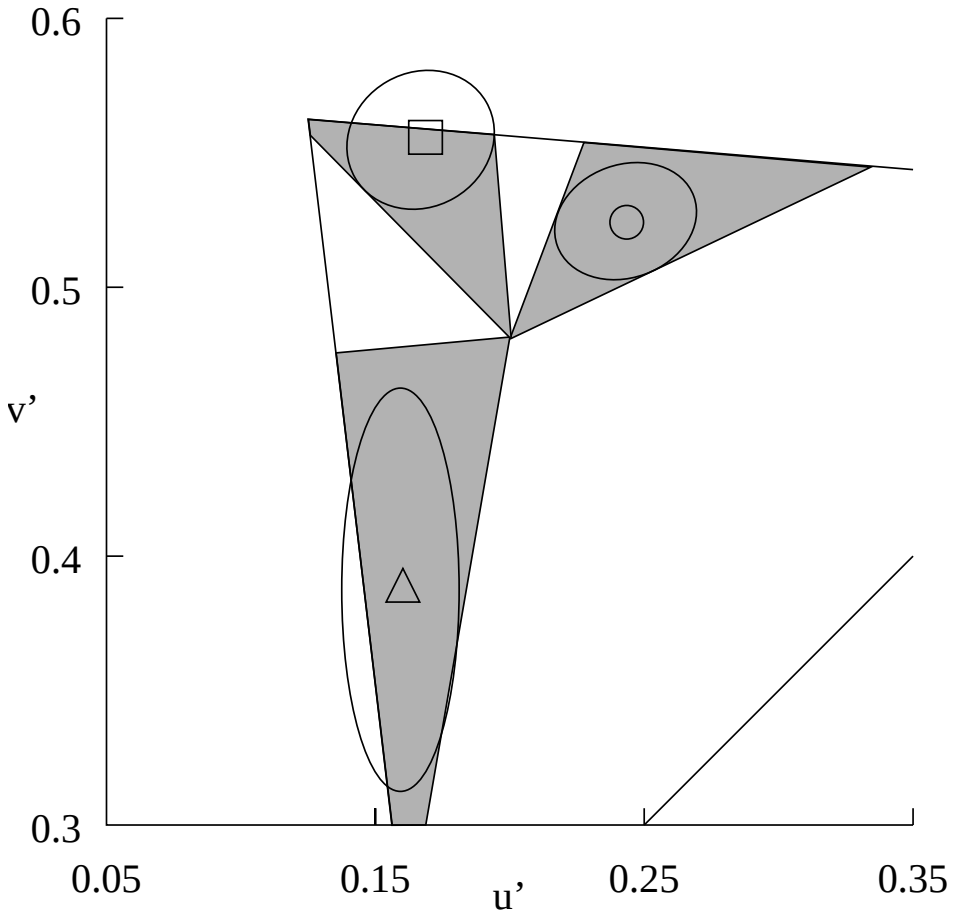

Figure 5.6: The "skin", "grass" and "sky" segments derived from the naturalness judgments of the colors (Yendrikhovskij et al., 1998b). Ellipses: standard deviations of a Gaussian approximation to subject responses. Data are shown in the *CIELUV* color space.

4. Defining three kinds of pixels according to hue value (H^*_{uv}): $25 - 70$ is called "skin" pixels, $95 - 135$ is called "grass" pixels, and $185 - 260$ is called "sky" pixels, following the Yendrikhovskij et al. (1998b)'s psychophysics studies. Note that saturation and hue values are defined based on polar coordinates, and the hue varies from 0 to 360 degrees (see Figure 5.6).

5. Computing the averaged saturation values for "skin" $\overline{S}_{skin}$, "grass" $\overline{S}_{grass}$, and "sky" $\overline{S}_{sky}$ pixels, *i.e.*, respectively.

6. Computing local CNI values for "skin" N_{skin}, "grass" N_{grass}, and "sky" N_{sky} pixels:

$$N_{skin} = exp(-0.5((\overline{S}_{skin} - 0.763)/0.524)^2),^2 \tag{5.10}$$

$$N_{grass} = exp(-0.5((\overline{S}_{grass} - 0.810)/0.528)^2), \tag{5.11}$$

$$N_{sky} = exp(-0.5((\overline{S}_{sky} - 0.432)/0.221)^2). \tag{5.12}$$

7. Finally, computing the global CNI value:

$$CNI = \frac{(n_{skin}N_{skin} + n_{grass}N_{grass} + n_{sky}N_{sky})}{(n_{skin} + n_{grass} + n_{sky})}. \tag{5.13}$$

Note that the conversion described above is in low level of detail such that the numerical results presented in this section can be easily reproduced.

Our second index, the CCI, can be easily computed as:

$$CCI = \mu_{S^*_{uv}} + \sigma_{S^*_{uv}}, \tag{5.14}$$

where $\mu_{S^*_{uv}}$ and $\sigma_{S^*_{uv}}$ stand for the mean and standard deviation of the saturation in $CIELUV$ (S^*_{uv}), defined in Equation 5.9, respectively.

Having calculated these two indexes, we define the color image quality measure Q in terms of CNI and CCI, *i.e.*,

$$Q = wCNI + (1 - w)CCI/CCI_{max}, \tag{5.15}$$

where the weighting parameter w is set to 0.75 as suggested in Yendrikhovskij et al. (1998b), and CCI_{max} is set to 2.8396 following the maximum CCI value found in our experiments. This first measure shows us the quality of both the original and the processed images in terms of color.

The second measure is the image contrast, and is defined as follows. Let us firstly define the regional standard deviation of the luminance, *i.e.*,

$$L^\alpha_\sigma(x, y) = \frac{\sqrt{\sum_{p=x-W}^{x+W}\sum_{q=y-W}^{y+W}(L^\alpha(p, q) - L^\alpha_\mu(x, y))^2}}{(2W + 1)^2}, \tag{5.16}$$

where

$$L^\alpha_\mu(x, y) = \frac{1}{(2W + 1)^2}\sum_{p=x-W}^{x+W}\sum_{q=y-W}^{y+W} L^\alpha(p, q), \tag{5.17}$$

L^α stands either for the luminance L^* in the $CIELUV$ color space (defined as in Equation 5.3), or for the luminance in the RGB color space, which is defined as the average of the three

[2]The values 0.763, 0.810, 0.432, 0.524, 0.528 and 0.221 were determined experimentally (Yendrikhovskij et al., 1998b).

channels R, G and B, *i.e.*, $L^{RGB} = (R_i + G_i + B_i)/3$, and the parameter W is setup to 24 (*i.e.*, blocks of 49×49 pixels as in Jobson et al. (2002)).

From here, we define the overall contrast of an image by the mean of the regional standard deviations of the luminance (Jobson et al., 2002). This measure provides a gross measure of the regional contrast variations, and it has been used by Huang et al. (2005) as a measure of contrast in gray-level images.

Note that we define the contrast for the luminance in both the *CIELUV* and *RGB* color spaces. In the *CIELUV* color space it is done because it is where the color quality image measure is defined, and in the *RGB* color space because it is where our methods work. We do that to highlight that the HE methods improve the contrast for the luminance in both color spaces, as the analysis of the results, in the next section, will confirm.

5.2.2.2 Computational Results

This section presents and discusses the numerical results obtained by using the metrics described in the previous section to evaluate the two proposed methods (HP1*D*HE and HP2*D*HE) and the others described in Section 4.3 (C1*D*HE and TV3*D*HE) in a data set composed of 300 images.

We compute, for both the original and the processed images, the contrast in both the *CIELUV* and *RGB* color spaces, as described in Equation 5.16. We also compute the CIQMs, as described in Equations 5.13, 5.14 and 5.15. Tables 5.5 and 5.6 show these data. Note that the values in both tables are presented in the form $\mu \pm \sigma$, *i.e.*, the mean and standard deviation obtained on the data set of 300 images. All images used and produced in this experiment can be seen in Menotti (2008).

Table 5.5: Contrast for the images in the *CIELUV* and *RGB* color spaces

Method	L^*	L^{RGB}
Original	12.53 ± 15.86	31.13 ± 98.02
C1*D*HE	18.38 ± 14.28	47.11 ± 95.21
HP1*D*HE	18.14 ± 13.75	46.73 ± 92.33
HP2*D*HE	18.55 ± 15.29	47.02 ± 100.20
TV3*D*HE	13.30 ± 8.36	36.44 ± 59.64

Table 5.5 shows the contrast in both the *CIELUV* and *RGB* color space for the original and processed images. From this table, we observe that the images processed by our methods, *i.e.*, HP1*D*HE and HP2*D*HE, have the value of the contrast increased, in average, about 50% in both the *CIELUV* and *RGB* color space. The values of the contrast of images processed by the C1*D*HE method increase in a similar fashion. In contrast, the TV3*D*HE method is the

one which increases the less the contrast. Remark that, in general, the improvement of the value of contrast in the *CIELUV* color space is proportional to the one in the *RGB* space (the range of the *CIELUV* luminance is $[0, 100]$ and the *RGB* luminance is $[0, 255]$ (with $L = 256$)). Confirming what we had hypothesized in the previous section, the HE methods increased the contrast in both color spaces. From this first analysis, we state that our methods and the C1DHE are effective in yielding significant increasing in the value of images contrast.

Table 5.6 shows the Q, CNI and CCI measures for the original and processed images. Note that the first numerical column in this table reports the Q measure values, which are a weighting function of the CNI and CCI measures. We observe that, in average, the images processed by our methods have preserved the values of Q in the processed images close to the value in the original ones. This means that our methods produce images with quality similar to the original images. Also note that the images enhanced by the C1DHE method have obtained similar Q values to the ones obtained by our methods. In contrast, the images produced by the TV3DHE method have Q values quite smaller than the ones calculated from the original images. This shows that the TV3DHE method yields images with deteriorated color quality.

Table 5.6: Color Image Quality Measures

Method	Q	CNI	CCI
Original	0.6754 ± 0.0195	0.8064 ± 0.0332	0.8026 ± 0.1234
C1DHE	0.6780 ± 0.0141	0.7834 ± 0.0260	1.0275 ± 0.1329
HP1DHE	0.6557 ± 0.0205	0.7829 ± 0.0351	0.7779 ± 0.0673
HP2DHE	0.6673 ± 0.0230	0.7828 ± 0.0408	0.9105 ± 0.0987
TV3DHE	0.5831 ± 0.0160	0.7197 ± 0.0247	0.4923 ± 0.0498

On the second numerical column of Table 5.6, we have the values for the CNI measure. Observe that, in average, our methods and the C1DHE keep the naturalness of the produced images close to the one in the original image, whereas the images produced by the TV3DHE method have CCI values significantly smaller than the ones obtained from the original images.

On the third numerical column of Table 5.6, we report the values for the CCI measure. Observe that the CCI measure is based on the mean and standard deviation of the saturation of the image in the *CIELUV* color space. The results reported show that, in average, the C1DHE method is the one that more frequently increases the value of the CCI measure from the original to the processed images. It achieves such result because it equalizes the three R, G and B $1D$ histograms freely and separately. On the other hand, the C1DHE method has the well-known drawback of not being hue-preserving, which will be discussed and illustrated further in this section. The images produced by the TV3DHE method, in average, do not preserve both the CNI and CCI values and, consequently the Q value, close to the values of

the original images. The fact that the TV3DHE method produces images with CCI values quite different from the ones in the original images corroborates the hypothesis previously subjectively stated in Section 5.2.1 (and in Menotti et al. (2006, 2007b)) that the TV3DHE method produces overenhanced/oversatured images. That is, in general the saturation values of the images produced by the TV3DHE method are smaller than the saturation values of the images produced by the other methods, and so are their variances.

From the analysis regarding the contrast and the CIQMs, we claim that: 1) The contrast of the images processed by our HP1DHE and HP2DHE methods is in average 50% greater than the contrast of the original images, whilst the color quality, measured by the naturalness and colorfulness indexes, of the processed images are close to the ones of the original image; 2) The TV3DHE method is the one that shows the smaller improvement on the contrast of the original image. Moreover, it produces images overenhanced, deteriorating the color quality of the images; 3) The results achieved for contrast enhancement and color quality preservation by the C1DHE method are as good as our methods.

Besides the good results that our numerical analysis attributed to the C1DHE method, the C1DHE is not suitable for real-world applications because the images produced by it do not preserve the hue of the original image. As a result, the images produced by the C1DHE method may have unnatural colors, even though the CNI, CCI and, consequently, Q, indicate that the images produced by the C1DHE method have image color quality close to the ones of the original images. These contradictory results show that the CQIMs used in this work have a drawback. They can quantitatively represent the color quality of a image by means of the naturalness and colorfulness indexes, but they do not take into account simultaneously the original and processed images in such assessment.

Note that we could perform changes in the TV3DHE method in order to make it faster and hue-preserving, by applying our shift-hue-preserving transformation. Nonetheless, even after these modifications, the images enhanced by the the TV3DHE method would continue to be overenhanced and the contrast improvement would not be significant.

Despite the good results that our numerical analysis attributed to the C1DHE method and the fact that it is six times faster than our methods, the C1DHE is not suitable for real-world applications: the images produced by this method do not preserve the hue of the original image. As a result, the images produced by the C1DHE method may have unnatural colors, even though the CNI, CCI and, consequently, Q indexes indicate that the images produced by the C1DHE method have image color quality close to the ones of the original images. These contradictory results show that the CQIMs used in this work have a drawback. They can quantitatively represent the color quality of an image by means of the naturalness and colorfulness indexes, but they do not take into account simultaneously the original and processed images in such assessment.

In order to exemplify the conclusions reached, we will carefully analyze one example of an

(a) (b) (c) (d) (e)

Figure 5.7: Results for the landscape image: (a) original image; (b) C1DHE; (c) TV3DHE; (d) our HP1DHE; (e) our HP2DHE.

image extracted out of the 300 presented in the database, namely landscape. Table 5.7 shows the contrast and the CNI, CCI and Q values for the original and processed landscape images in Figure 5.7. Figure 5.7b shows the landscape image processed by the C1DHE method, and highlights the fact that it is not hue-preserving. We observe that the colors present in the image in Figure 5.7b look unnatural with respect to the original image in Figure 5.7a, even through the CNI, CCI and Q values of the processed image is close to the ones in the original image. We can also observe that the image produced by the TV3DHE method in Figure 5.7c is overenhanced, *i.e.*, the colors are oversaturated, as explained before in this section. Moreover, we can see that the increase in the value of the image contrast produced by the TV3DHE method is the smallest among the compared methods, as shown in Table 5.7.

Finally, the claims about our methods are verified in the images in Figures 5.7d and 5.7e and confirmed in Table 5.7. As observed, the images have their contrast value increased by in average 50%, while their color quality measures values are kept close to the ones of the original images. Furthermore, recall that our methods are hue-preserving.

Table 5.7: Color Image Quality and Contrast Measures for the Images in Figure 5.7.

Method	Color Quality			Contrast	
	Q	CNI	CCI	$CIELUV$	RGB
Original	0.7038	0.8540	0.7196	7.00	17.03
C1DHE	0.7681	0.9292	0.8089	12.09	30.32
HP1DHE	0.7210	0.8725	0.7575	11.50	28.98
HP2DHE	0.6504	0.7688	0.8381	11.00	27.59
TV3DHE	0.7140	0.9004	0.4392	8.76	23.68

5.2.3 Run-time Analysis

In this section, we analyze the run-time behavior of the C1DHE, TV3DHE, HP1DHE and HP2DHE methods with respect to the image dimension, in order to confirm the time complexity of the methods as exposed in Section 4.4. Other factors that affect the run-time of the methods are also analyzed. Nonetheless, in the experiments of this section, we consider the number of levels of each channel constant, *i.e.*, $L = 256$.

In order to perform this analysis, we build a setup as follows. We select three images (the train, beach and landscape), and reshape and resize each one of them in seven different image dimensions, starting from 128×128 pixels, and increasing by a multiplicative factor of 2 up to 1024×1024 pixels, *i.e.*, 128×128, 256×128, 256×256, 512×256, 512×512, 1024×512 and 1024×1024. We end up with twenty one images to be used for run-time analysis of the four methods.

In order to collect unbiased run-times, we randomly select and run each one of these images as input for each method ten times. Table 5.8 shows the average run-time measured to run the images for the methods. Note that the time for loading and saving the image files are also take into account.

Although the C1DHE method is in average about five times faster than ours, recall that it is not hue-preserving. In contrast, our HP1DHE and HP2DHE methods are, in average, seven times faster than the TV3DHE method. These last two statements are based on a linear regression on the data presented in Table 5.8. Note that, in average, our methods enhance images of 512×512 pixels in about 100 milliseconds on a Pentium 4 - 2GHz. This run-time complies with real-time applications.

Table 5.8: Average run-time in milliseconds for analysis.

Image Dimension	C1DHE	TV3DHE	HP1DHE	HP2DHE
128×128	4	737	11	20
256×128	8	786	18	28
256×256	10	876	32	41
512×256	15	1049	52	61
512×512	24	1399	95	104
1024×512	38	2068	181	193
1024×1024	66	3272	350	371

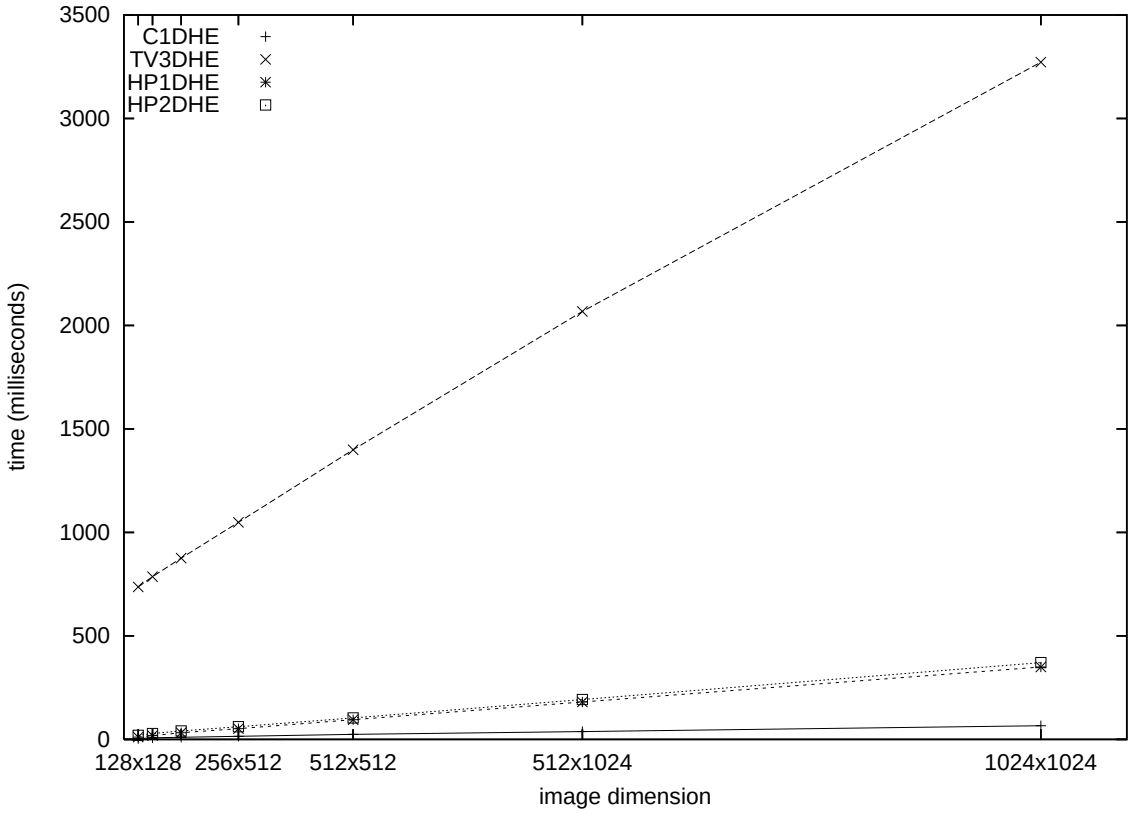

Figure 5.8: Run-time curves of the C1DHE, TV3DHE, HP1DHE and HP2DHE methods.

Figure 5.8 shows the run-time curves of the four methods built based on the data in Table 5.8. As we can observe, the slant (*i.e.*, the angular coefficient) of the TV3DHE curve is much bigger than the others. This fact can be explained by the slow, iterative and not hue-preserving third step of the TV3DHE, *i.e.*, the histogram equalization step - $\bigcirc(3(L-1))$.

Also observe that the linear coefficient of the run-time curves of the methods based on $1D$ and $2D$ histograms (our HP1DHE and HP2DHE methods and the C1DHE one) is much lower than the one based on $3D$ histograms (TV3DHE method). This difference is clearly explained by the cost of storing/computing the $3D$ histograms.

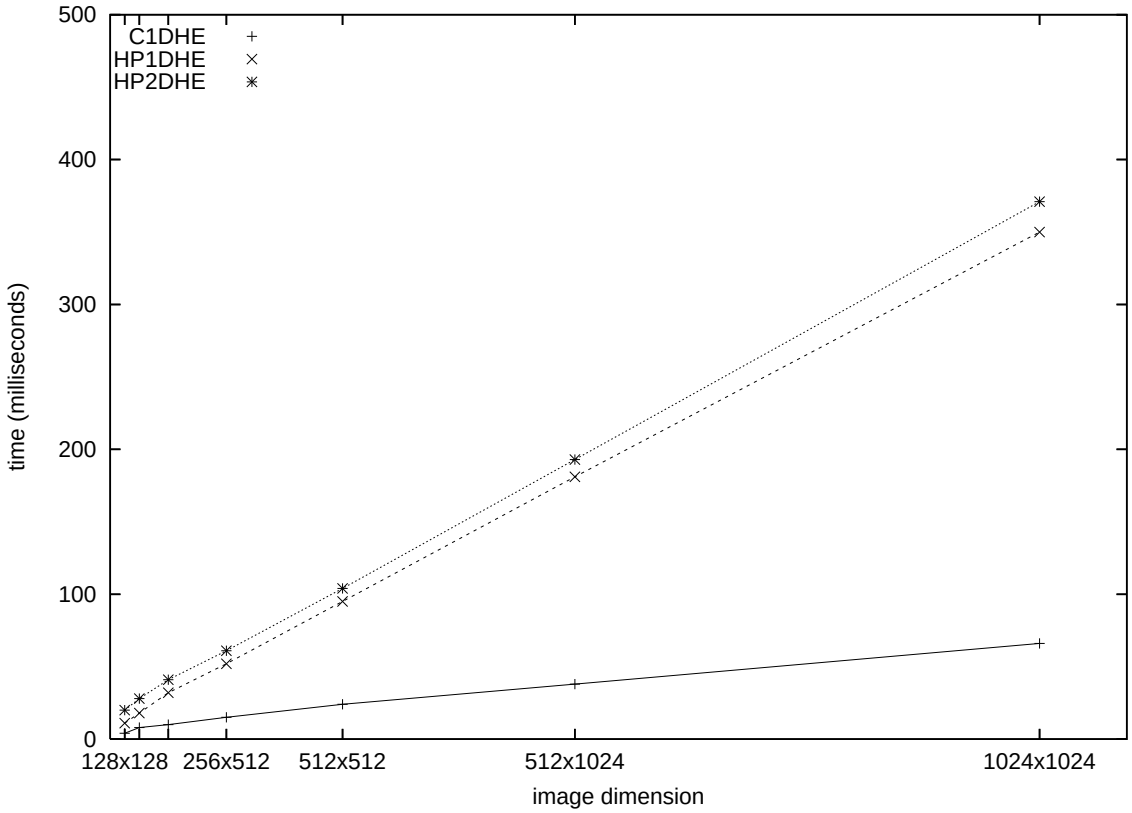

Figure 5.9: Run-time curves of the C1DHE, HP1DHE and HP2DHE methods.

In order to highlight the difference among the run-time curves of the methods based on $1D$ and $2D$ histograms, Figure 5.9 shows the run-time curves of the C1DHE, HP1DHE and HP2DHE methods. We note that the computational time of the HP2DHE method is slightly more expensive than the HP1DHE one. This is because the HP2DHE method uses $2D$ histograms instead of $1D$ histograms - this is the only difference on the implementation of these methods. In the graph of Figure 5.9, it is clear that the C1DHE method is faster than ours. Nonetheless, once more, note that the C1DHE is not hue-preserving.

5.3 Conclusion

In this chapter, we firstly showed results of experiments regarding the multi-histogram equalization methods for gray-level image contrast enhancement. These experiments showed that our methods are better on preserving the brightness of the processed image (in relation to the original one) and yielding images with natural appearance, at the cost of contrast enhancement. These experiments bring two major contributions to the current literature: 1) An objective comparison among all the HE studied methods using quantitative measures, such as the $PSNR$, brightness and contrast; 2) An analysis showing the boundaries of the HE technique and its variations (*i.e.*, Bi- and Multi-HE methods) for contrast enhancement, brightness preserving and natural appearance.

In the second part of this chapter, we presented experiments regarding the histogram equalization methods for color image contrast enhancement. We firstly performed an subjective assessment on the quality of the processed images with respect to the original one, which was not conclusive. After, we evaluated the processed images objectively by using measures of contrast, naturalness and colorfulness on a database composed of 300 images, such that a quantitative comparison could be performed. The analysis of the experiments showed that the value of the contrast of the images produced by our methods is in average 50% greater than the original value. Simultaneously, our HP1DHE and HP1DHE methods keep the quality of the image in terms of naturalness and colorfulness close to the quality of the original image. The same results are achieved by the C1DHE method. However, this classical method does not preserve the hue and produces images that are not realistic with respect to the original image. Finally, we performed a runtime analysis confirming the time and space complexities of the methods for color image contrast enhancement.

In the next chapter, we point out the conclusions of this work.

Chapter 6

Conclusion and Future Work

This work presented two new types of methods for image contrast enhancement through histogram equalization. The main motivation to use methods based on histogram equalization to improve contrast in images was their simplicity and appropriateness for real-time applications (Woods and Gonzalez, 1981; Reza, 2004). Whereas the first type of proposed methods is suitable for gray-level images, the second type can be applied to color images.

The gray-level multi-histogram equalization methods, introduced in Chapter 3, differ from other methods previously proposed in the literature in one major point. They segment the image into several sub-images based on discrepancy functions borrowed from the multithresholding literature, instead of using image statistical features. As showed by experiments reported in Section 5.1, the proposed methods are successful in enhancing the contrast of images while preserving their brightness and avoiding the appearance of unnatural artifacts. Furthermore, although the proposed methods used a more sophisticated technique to decompose the original image than the other methods described in this thesis, they are still fast and, consequently, suitable to be applied to real-time problems.

The fast hue-preserving histogram equalization methods for color image contrast enhancement, proposed in Chapter 4, also showed to be able to produce images with colors which are more realistic than the ones produced by methods which are not hue-preserving. Besides, the produced images were also not as saturated as the ones produced by other histogram equalization methods we compared them to.

We also performed an objective and quantitative evaluation of the output images using measures based on the human vision system, such as the naturalness and the colorfulness indexes. The motivation for it was that subjective assessment carried out to judge the quality of the color images produced by contrast enhancement methods is not very effective. Indicating the best method over all the compared ones is not a straightforward task.

It is important to note that, to the best of our knowledge, this is the first work to evaluate histogram equalization methods with a well-known database of 300 images by using measures such as naturalness and colorfulness.

6.1 Future Work

In this section we present future work as possible extensions of this thesis.

6.1.1 Polar Color Spaces

The histogram equalization method for color images proposed in Chapter 4 is based on the *RGB* color space. However, the *RGB* color space is not the only one which can be used when working with images. In special, there is a set of color spaces called polar spaces. Polar spaces, introduced in the late seventies (Smith, 1978), are transformations of the *RGB* color space, and include the *HSV* (hue, saturation, value) color space – also known as *HSB* (hue, saturation, brightness), and the *HSL* (hue, saturation, lightness/luminance) color space – also known as *HLS* or *HSI* (hue, saturation, intensity). The main difference between the *HSL* and the *HSV* color spaces is that the brightness of a pure color is equal to the brightness of white, whereas the lightness of a pure color is equal to the lightness of a medium gray-level.

The polar spaces are often used by artists instead of the *RGB* color space because it is often more natural to think about a color in terms of hue and saturation, instead of in terms of additive or subtractive color components. With this in mind, we plan to develop a method for image contrast enhancement using the polar color space. This method would also be based on histogram equalization techniques, as the two other methods proposed in this work.

However, note that the polar spaces were not conceived neither for processing purposes nor for the current computing facilities. For this reason, these color spaces are not coherent with the theory of synthesis of colors (Newton's Disk) (Newton, 1672). In other words, these colors spaces are not able to perform image processing transformations such that coherent colors are yielded (*e.g.*, according to the Newton theory of synthesis, summing up the colors red and blue should result in the color magenta). Hence, Serra (2005) proposed $L1 - L2$ norms to correct this problem, and make the polar color spaces adequate to perform color transformations.

Recently, Angulo (2007) started analyzing the impact of these corrections proposed by Serra (2005) while performing image contrast enhancement through spatial smoothing using morphological operators. In future work, we also propose to make a similar analyze to the one done by Angulo (2007), but using histogram equalization methods. The main motivation for that is to verify the impact of the correction on polar color spaces when applied to color image contrast enhancement.

6.1.2 Color Quality Measures

The drawbacks pointed out in Chapter 5, regarding the proposed color quality measures, should be considered for future work. We plan to modify the current measures by taking into account the original and processed images simultaneously, in order to define new measures of color image quality measure.

Appendix A

Other Research Studies

During the doctorate period, the PhD student worked in parallel on other research subjects. Some of them are briefly shown in the followings.

A.1 1D Component Tree in Linear Time and Space and its Application to Gray-Level Image Multithresholding

The upper-weighted sets of a signal are the sets of points with weight above a given threshold. The components of the upper-weighted sets, thanks to the inclusion relation, can be organized in a tree structure, which is called the component tree. In Menotti et al. (2007a), we present a linear time and space algorithm to compute the component tree of one-dimensional signals.

From this algorithm we derive an efficient gray-level image multithresholding method, which is based on the hypothesis that objects which appear on an image can be represented by salient classes present in the histogram of this image. These classes are modelled as the most significative components of the histogram's component tree, where the importance corresponds to the volume attribute. We show results of the proposed method and compare it with classical methods.

A.2 Segmentation of Envelopes and Address Block Location

Although nowadays there are working systems for sorting mail in some constrained ways, segmenting gray-level images of envelopes and locating address blocks in them is still a difficult problem. Pattern Recognition research has contributed greatly to this area since the problem concerns feature design, extraction, recognition, and also the image segmentation if one deals with the original gray-level images from the beginning.

The problem consists of segmenting and locating the address block in postal envelopes. The aim is to automatically separate in postal envelopes the regions related to background,

stamps, rubber stamps, and the address blocks. We worked with three different approaches for solve the problem.

The first one is based on statistical hypothesis testing and feature selection in the wavelet space (Menotti and Borges, 2007; Menotti et al., 2004b, 2003b,a). First, a typical image of a postal envelope is decomposed using Mallat algorithm and Haar basis. High frequency channel outputs are analyzed to locate salient points in order to separate the background. A statistical hypothesis test is taken to decide upon more consistent regions in order to clean out some noise left. The selected points are projected back to the original gray-level image, where the evidence from the wavelet space is used to start a growing process to include the pixels more likely to belong to the regions of stamps, rubber stamps, and written area.

We also proposed two other approaches which are based on fractal dimension (Eiterer et al., 2004b,a,c) and lacunarity (Facon et al., 2005). These approaches are variants of the first approach on the feature selection step, *i.e.*, instead of using the wavelet space, we use fractal dimension and lacunarity as features to solve the problem.

We evaluate all these works by a pixel to pixel accuracy measure (Menotti et al., 2004a) using a ground truth database composed of 200 real images with different layouts and backgrounds. Success rate for address block location reached is over 90%.

A.3 Statistical Hypothesis Testing and Wavelet Features for Region Segmentation

In Menotti et al. (2005), we introduce a novel approach for region segmentation. In order to represent the regions, we devise and test new features based on low and high frequency wavelet coefficients which allow to capture and judge regions using changes in brightness and texture. A fusion process through statistical hypothesis testing among regions is established in order to obtain the final segmentation. The proposed local features are extracted from image data driven by global statistical information. Preliminary experiments show that the approach can segment both texturized and regions cluttered with edges, demonstrating promising results. Hypothesis testing is shown to be effective in grouping even small patches in the process.

A.4 A New Algorithm for Constructing Minimal Perfect Hash Functions

In Botelho et al. (2004), we present a three-step algorithm for generating minimal perfect hash functions which runs very fast in practice. The first step is probabilistic and involves the generation of random graphs. The second step determines the order in which hash values are assigned to keys. The third step assigns hash values to the keys. We give strong evidences that first step takes linear random time and the second and third steps take deterministic

linear time. We improve upon the fastest known method for generating minimal perfect hash functions. The total time to find a minimal perfect hash function in a PC computer took approximately 175 seconds for a collection of 20 million keys. The time to compute a table entry for any key is also fast because it uses only two different hash functions that are computable in time proportional to the size of the key. The amount of space necessary to store the minimal perfect hash function is approximately half the space used by the fastest known algorithm.

Bibliography

Abdou, I. and Pratt, W. (1979). Quantitative design and evaluation of enhancement/thresholding edge detectors. *Computer*, 9(5):28–37.

Anderson, G. and Netravali, A. (1976). Image restoration based on a subjective criterion. *IEEE Transactions on Systems, Man and Cybernetics*, SMC-6:845–859.

Andrews, H., Tescher, A., and Kruger, R. (1972). Image processing by digital computer. *IEEE Spectrum*, 9:20–32.

Angulo, J. (2007). Morphological colour operations in totally ordered lattices based on distances: Application to image filtering, enhancement and analysis. *Computer Vision and Image Understading*, pages 1–18. in press, doi:10.1016/j.cviu.2006.11.008.

Arcese, A., Mengert, P., and Trombini, W. (1970). Image detection through bipolar correction. *IEEE Transactions on Information Theory*, IT-16:534–543.

Beghdadi, A. and Le-Negrate, A. (1989). Contrast enhancement technique based on local detection of edges. *Computer Vision, Graphics, and Image Processing*, 46:162–174.

Berns, R., Billmeyer, F., and Saltzaman, M. (2000). *Billmeyer and Saltzaman's Principles of Color Technology*. Wiley, New York, 3rd edition.

Bockstein, I. (1986). Color equalization method and its application to color image processing. *Journal of the Optical Society of America*, 3(5):735–737.

Botelho, F., Menotti, D., and Ziviani, N. (2004). A new algorithm for constructing minimal perfect hash functions. Technical Report TR004/04, Department of Computer Science, Universidade Federal de Minas Gerais.

Brown, D. (1966). Digital computer analysis and display of the radionuclide scan. *Journal of the Nuclear Medicine*, 7:740–745.

Cardano, G. (1545). *Artis magnae, sive de regulis algebraicis*. Nuremberg. (also known as Ars magna).

Castleman, K. (1979). *Digital Image Processing*. Prentice-Hall, Englewood Cliffs, NJ.

Chang, D.-C. and Wu, W.-R. (1998). Image contrast enhancement based on a histogram transformation of local standard deviation. *IEEE Transactions on Medical Imaging*, 17(4):518–531.

Chen, S.-D. and Ramli, A. (2003a). Contrast enhancement using recursive mean-separate histogram equalization for scalable brightness preservation. *IEEE Transactions on Consumer Electronics*, 49(4):1301–1309.

Chen, S.-D. and Ramli, A. (2003b). Minimum mean brightness error bi-histogram equalization in contrast enhancement. *IEEE Transactions on Consumer Electronics*, 49(4):1310–1319.

Chitwong, S., Cheevasuvit, F., Dejhan, K., and Mitatha, S. (2000). Color image enhancement based on segmentation region histogram equalization. In *Proceedings of the Asian Conference on Remote Sensing ACRS'2000*, pages 1–3.

Coltuc, D., Bolon, P., and Chassery, J.-M. (2006). Exact histogram specification. *IEEE Transactions on Image Processing*, 15(5):1143–1152.

Cooley, J. and Tukey, T. (1965). An algorithm for machine calculation of complex fourier series. *Math. Comp.*, 19:297.

CVG-URG (2007). Image database. `http://decsai.ugr.es/cvg/dbimagenes/`.

de A. Araújo, A. (1985). Sum of the absolute grey level differences: an edge-preserving smoothing approach. *Electronics Letters*, 21(25/26):1219–1220.

de A. Araújo, A. (1989). *Filtragem Espacial*. SBC/JAI/UFU, Uberlândia-MG, Brazil. brochure.

Domingos, P. and Pazzani, M. (1997). On the optimality of the simple bayesian classifier under zero-one loss. *Machine Learning*, 29(2-3):103–130.

Duan, J. and Qiu, G. (2004). Novel histogram processing for colour image enhancement. In *Proceedings of the Thrid International Conference on Image and Graphics (ICIG'04)*, pages 55–58. IEEE.

Duda, R. and Hart, P. (1973). *Pattern Classification and Scene Analysis*. Wiley, New York.

Eiterer, L. F., Facon, J., and Menotti, D. (2004a). Envelope address block segmentation through fractal-based approach. In *9th Iberoamerican Congress on Pattern Recognition (CIARP 2004), LNCS 3287*, pages 454–461, Puebla, Mexico.

Eiterer, L. F., Facon, J., and Menotti, D. (2004b). Postal envelope address block location by fractal-based approach. In *XVII Brazilian Symposium on Computer Graphics and Image Processing, (SIBGRAPI 2004)*, pages 90–97, Curitiba, PR, Brasil.

Eiterer, L. F., Facon, J., and Menotti, D. (2004c). Segmentation of envelope address blocks through fractal-based approach. In *Iberoamericam Meeting on Optics (RIAO) and Optics Lasers and Their Aplications (OPTILAS)*, pages 1–6, Porlamar, Venezuela.

Facon, J., Menotti, D., and de Albuquerque Araújo, A. (2005). Lacunarity as a texture measure for address block segmentation. In *10th Iberoamerican Congress on Pattern Recognition (CIARP 2005), LNCS 3773*, pages 112–119, Havana, Cuba.

Frei, W. (1977). Image enhancement by histogram hyperbolization. *Computer Graphics Image Processing*, 6:286.

Gabor, D. (1965). Information theory in electron microscopy. *Lab. Invest.*, 14:801–809.

Gonzalez, R. and Woods, R. (2002). *Digital Image Processing.* Prentice Hall, 2nd edition.

Graham, R. (1962). Snow removal – a noise-stripping process for picture signals. *IRE Transactions on Information Theory*, IT-8:129–134.

Hall, E. (1971). A survey of preprocessing and feature extraction techniques for radiographic images. *IEEE Transactions on Computers*, C-20:1032–1044.

Hall, E. (1974). Almost uniform distributions for computer image enhancement. *IEEE Transactions on Computers*, C-23(2):207–208.

Hanmandlu, M. (2006). An optimal fuzzy system for color image enhancement. *IEEE Transactions on Image Processing*, 15(10):380–393.

Hasler, S. and Susstrunk, S. (2003). Measuring colorfulness in real images. In *Proceedings of the Human Vision and Electronic Imaging VIII*, volume 5007, pages 87–95. SPIE.

Huang, K.-Q., Wang, Q., and Wu, Z.-Y. (2006). Natural color image enhancement and evaluation algorithm based on human visual system. *Computer Vision and Image Understanding*, 103:52–63.

Huang, K.-Q., Wu, Z.-Y., and Wang, Q. (2005). Image enhancement based on the statistics of visual representation. *Image and Vision Computing*, 23:51–57.

Huang, T. (1975). *Picture Processing and Digital Filtering.* Springer, New York.

Hummel, R. (1975). Histogram modification techniques. *Computer Graphics and Image Processing*, 4:209–224.

Hummel, R. (1977). Image enhancement by histogram transformation. *Computer Graphics and Image Processing*, 6(2):184–195.

Ibrahim, H. and Kong, N. (2007). Brightness preserving dynamic histogram equalization for image contrast enhancement. *IEEE Transactions on Consumer Electronics*, 53(4):1752–1758.

Jain, A. (1989). *Fundamentals of Digital Image Processing*. Prentice Hall, Englewood Cliff, NJ.

Jin, Y., Fayad, L., and Laine, A. (2001). Contrast enhancement by multi-scale adaptive histogram equalization. In *Proceedings of Wavelets: Applications in Sigal and Image Processing IX*, volume 4478, pages 206–213. SPIE.

Jobson, D., Rahman, Z.-U., and Woodell, G. (2002). The statistics of visual representation. In *Visual Information Processing XI*, volume 4736, pages 25–35. SPIE.

Kapur, N. (1994). *Measures of Information and Their Applications*. J. Wiley & Sons.

Kim, J., Kim, L., and Hwang, S. (2001). An advanced contrast enhancement using partially overlapped sub-block histogram equalization. *IEEE Transactions on Circuits and systems for Video Technolog*, 11(4):474–484.

Kim, S.-Y., Han, D., Choi, S.-J., and Park, J.-S. (1999). Image contrast enhancement based on the piecewise-linear approximation of cdf. *IEEE Transactions on Consumer Electronics*, 45(3):828–834.

Kim, T., Paik, J., and Kang, B. (1998). Contrast enhancement system using spatially adaptive histogram equalization with temporal filtering. *IEEE Transactions on Consumer Electronics*, 44(1):82–87.

Kim, Y.-T. (1997). Contrast enhancement using brightness preserving bi-histogram equalization. *IEEE Transactions on Consumer Electronics*, 43(1):1–8.

Klette, R. and Zamperoni, P. (1996). *Handbook of Image Processing Operators*. John Wiley & Sons, Chichester - New York - Brisbane - Toronto - Singapore.

Kober, V. (2006). Robust and efficient algorithm of image enhancement. *IEEE Transactions on Consumer Electronics*, 52(2):655–6594.

Kuehni, R. and Schwarz, A. (2008). *Color Ordered: A Survey of Color Systems from Antiquity to the Present*. Oxford University Press Inc., USA, 1st edition.

Kundu, S. (1998). A solution to histogram-equalization and other related problems by shortest path methods. *Pattern Recognition*, 31(3):231–234.

Kuwahara, M., Hachimuar, K., Eiho, S., and Kinoshita, M. (1976). Processing of ri-angiocardiographics images. In Preston, K. and Onoe, M., editors, *D*igital Processing of Biomedical Images. Plenum, New York.

Lamberti, F., Montrucchio, B., and Sanna, A. (2006). Cmbfhe: A novel contrast enhancement technique based on cascaded multistep binomial filtering histogram equalization. *IEEE Transactions on Consumer Electronics*, 52(3):966–974.

Lee, H. and Park, R.-H. (1990). Comments of "an optimal multiple threshold scheme for image segmentation". *IEEE Transactions on Systems, Man and Cybernetics*, 20(3):741–742.

Lee, J. (1976). An approach for the space variant restoration and enhancement of images. In *Proceedings of Symposium on Current Math. Prob. in Image Science*.

Lee, J. (1980). Digital image enhancement and noise filtering by use of local statistics. *IEEE Transactions on Pattern Analysis and Machine Intelligence*, 2:165–174.

Lee, J. (1981). Redefined filtering of image noise using local statistics. *Computer Graphics and Image Processing*, 15:380–389.

Lillesand, T. and Kiefer, R. (1994). *Sensing and Photo Interpretation*. John Wiley & Sons, New York, 3rd edition.

Luessi, M., Eichmann, M., Schuster, G., and Katsaggelos, A. (2006). New results on efficient optimal multilevel image thresholding. In *IEEE International Conference on Image Processing*, pages 773–776.

Luft, T., Colditz, C., and Deussen, O. (2006). Image enhancement by unsharp masking the depth buffer. *ACM Transactions on Graphics*, 25(3):1206–1213.

Martin, A. (1962). *Technical Television*. Prentice-Hall, Englewood Cliffs, NJ, USA.

Martin, D., Fowlkes, C., Tal, D., and Malik, J. (2001). A database of human segmented natural images and its application to evaluating segmentation algorithms and measuring ecological statistics. In *Proc. 8th International Conference on Computer Vision*, volume 2, pages 416–423.

Mascarenhas, N. and Velasco, F. (1989). *Processamento Digital de Imagens*. EBAI, 2nd edition.

Melo, A. P., Menotti, D., Facon, J., Sgarbi, E. M., and de Albuquerque Araújo, A. (2005). Realce de imagens coloridas através da equalização de histogramas 2D. In *Workshop of Undergraduate Students - XVIII Brazilian Symposium on Computer Graphics and Image Processing (SIBGRAPI 2005)*, pages 1–8, Natal, Brazil.

Menotti, D. (2007). NPDI repository: Test images of multi-histogram equalization methods for gray-level image contrast enhancement. `http://wavelet.dcc.ufmg.br/MHE`.

Menotti, D. (2008). NPDI repository: Test images of fast hue-preserving histogram equalization methods for color image contrast enhancement. `http://wavelet.dcc.ufmg.br/FHPHEM/`.

Menotti, D. and Borges, D. L. (2007). Segmentation of envelopes and address block location by salient features and hypothesis testing. *INFOCOMP Journal of Computer Science*, 6(1):66–79.

Menotti, D., Borges, D. L., and de Albuquerque Araújo, A. (2005). Statistical hypothesis testing and wavelets features for region segmentation. In *10th Iberoamerican Congress on Pattern Recognition (CIARP 2005), LNCS 3773*, pages 671–678, Havana, Cuba.

Menotti, D., Borges, D. L., Facon, J., and de Souza Britto-Jr, A. (2003a). Salient features and hypothesis testing: Evaluating a novel approach for segmentation and address block location. In *DIAR'2003 IEEE Document Image Analysis and Retrieval Workshop, part of CVPR'2003*, pages 41–48, Madison, USA.

Menotti, D., Borges, D. L., Facon, J., and de Souza Britto-Jr, A. (2003b). Segmentation of postal envelopes for address block location: an approach based on feature selection in wavelet space. In *ICDAR'2003 IEEE International Conference on Document Analysis and Recognition*, pages 699–703, Edinburgh, Scotland.

Menotti, D., Facon, J., Borges, D. L., and de Souza Britto-Jr, A. (2004a). A quantitative evaluation of segmentation results through the use of ground-truth images: an application to postal envelope segmentation. In *Eletronical (CD-ROM) Proceedings of SIBGRAPI'2004, Technical Poster IEEE Brazilian Symposium on Computer Graphics and Image Processing*, page 1, Curitiba, Paraná, Brazil.

Menotti, D., Facon, J., Borges, D. L., and de Souza Britto-Jr, A. (2004b). Segmentacao de envelopes postais para localizacao do bloco endereco: uma abordagem baseada em selecao de caracter1sticas no espaco *Wavelet*. In *III Workshop of Theses and Dissertations on Computer Graphics and Image Processing (WTDCGPI), part of SIBGRAPI'2004*, page 8, Curitiba, Paraná, Brazil.

Menotti, D., Melo, A. P., de Albuquerque Araújo, A., Facon, J., and Sgarbi, E. M. (2006). Color image enhancement throught 2D histogram equalization. In *13th International Conference on Systems, Signals and Image Processing (IWSSIP 2006)*, pages 235–238, Budapest, Hungry.

Menotti, D., Najman, L., and de Albuquerque Araújo, A. (2007a). 1d component tree in linear time and space and its application to gray-level image multithresholding. In *8th International Symposium on Mathematical Morphology (ISMM)*, pages 437–448, Rio de Janeiro, Brazil.

Menotti, D., Najman, L., de Albuquerque Araújo, A., and Facon, J. (2007b). A fast hue-preserving histogram equalization method for color image enhancement using a bayesian framework. In *14th International Workshop on Systems, Signals and Image Processing (IWSSIP 2007)*, pages 414–417, Maribor, Slovenija. IEEE Catalog Number: 07EX1858C, ISBN: 978-961-248-029-5, CIP 621.391(082).

Menotti, D., Najman, L., de Albuquerque Araújo, A., and Facon, J. (2008). Fast hue-preserving histogram equalization methods for color image contrast enhancement. *IEEE Transaction on Consumer Electronics*. submitted on January 15, 2008.

Menotti, D., Najman, L., Facon, J., and de Albuquerque Araújo, A. (2007c). Multi-histogram equalization methods for contrast enhancement and brightness preserving. *IEEE Transaction on Consumer Electronics*, 53(3):1186–1194.

Meylan, L. and Süsstrunk, S. (2004). Bio-inspired color image enhancement. In *Proceedings of the Human Vision and Electronic Imaging IX*, volume 5293, pages 1–5. IS&T/SPIE.

Mlsna, P. and Rodriguez, J. (1995). A multivariate contrast enhancement technique for multispectral images. *IEEE Transactions on Geoscience and Remote Sensing*, 33(10):212–216.

Mlsna, P., Zhang, Q., and Rodriguez, J. (1996). 3-d histogram modification of color images. In *Proceedings of the International Conference on Image Processing*, volume 3, pages 1015–1018. IEEE.

Mukherjee, D. and Chatterji, B. (1995). Adaptive neighborhood extended contrast enhancement and its modifications. *Graphical Models and Image Processing*, 57(3):254–265.

Nagao, M. and Matsuyama, T. (1979). Edge preserving smoothing. *Computer Graphics and Image Processing*, 9:394–407.

Naik, S. and Murthy, C. (2003). Hue-preserving color image enhancement without gamut problem. *IEEE Transactions on Image Processing*, 12(12):1591–1598.

Newton, I. (1672). Theory about light and colors. *Philosophical Transactions of the Royal Society*, 71(80):3075–3087.

Ni, Y., Devos, F., Boujrad, M., and Guan, J. (1997). Histogram-equalization-based adaptive image sensor for real-time vision. *IEEE Jounral of Solid-State Circuits*, 32(7):1027–1036.

Niblack, W. (1986). *An Introduction to Digital Image Processing*. Prentice Hall.

Nickalls, R. (1993). A new approach to solving the cubic: Cardan's solution revealed. *The Mathematical Gazette*, 77:354–359.

Oppenheim, A. and Schaefer, R. (1975). *Digital Signal Processing*. Prentice Hall, Englewood Cliffs, N.J.

Otsu, N. (1979). A threshold selection method from grey-level histograms. *IEEE Transactions on Systems, Man and Cybernetics*, 9(1):41–47.

Otsu, N. (1980). An automatic threshold selection method based on discriminant and least squares criteria. *IEEE Transactions of the IECE of Japan*, 64-D(4):349–356.

Paranjape, R., Morrow, W., and Rangayyan, R. (1992). Adaptive-neighborhood histogram equalization for image enhancement. *Computer Graphics and Image Processing*, 54(3):259–267.

Pichon, E., Niethammer, M., and Sapiro, G. (2003). Color histogram equalization through mesh deformation. In *Proceedings of the International Conference on Image Processing (ICIP)*, volume 2, pages 117–120. IEEE.

Pitas, I. and Kiniklis, P. (1996). Multichannel techniques in color image enhancement and modeling. *IEEE Transactions on Image Processing*, 5(1):168–171.

Pizer, S., Amburn, E., Austin, J., Cromartie, R., Geselowitz, A., Greer, T., ter Haar Romeny, B., Zimmerman, J., and Zuiderveld, K. (1987). Adaptive histogram equalization and its variations. *Computer Vision, Graphics and Image Processing*, 39(3):355–368.

Pizer, S., Johnston, R. E., Ericksen, J., Yankaskas, B., and Muller, K. (1990). Contrast-limited adaptive histogram equalization: Speed and effectiveness. In *The First Conference on Visualization in Biomedical Computing*, pages 337–345.

Pizer, S., Zimmerman, J., and Staab, E. (1984). Adaptive grey level assingment in ct scan display. *Journal of Computer Assisted Tomography*, 8:300–308.

Pratt, W. (1978). *Digital Image Processing*. Wiley, New York.

Prewitt, J. (1970). Object enhancement and extraction. In Lipkin, B. and Rosenfeld, A., editors, *P*icture Processing and Psycopictorics, page 70. Academic Press, New York.

Rabbani, M. and Jones, P. (1991). *Digital Image Compression Techniques*. Society of Photo-Optical Instrumentation Engineers (SPIE), Bellingham, WA, USA, 1st edition.

Reddi, S., Rudin, S., and Keshavan, H. (1984). An optimal multiple threshold scheme for image segmentation. *IEEE Transactions on Systems, Man and Cybernetics*, 14(4):661–665.

Reza, A. (2004). Realization of the contrast limited adaptive histogram equalization (clahe) for real-time image enhancement. *Journal of VLSI Siginal Processing*, 38:35–44.

Rodriguez, J. and Yang, C. (1995). High-resolution histogram modification of color images. *Graphical Models and Image Processing*, 57(5):432–440.

Rosenfeld, A. and Kak, A. (1976). *Digital Picture Processing.* Academic Press, New York.

Schreiber, W. (1990). Wirephoto quality improvement by unsharp masking. *Pattern Recognition*, 2:171–180.

Serra, J. (2005). Morphological segmentations of colour images. In *Proceedings of the 7th International Symposium on Mathematical Morphology - ISMM'2005*, pages 151–176. Kluwer.

Sezgin, M. and Sankur, B. (2004). Survey over image thresholdintg techniques and quantitative performance evaluation. *Journal of Electronic Imaging*, 13(1):146–165.

Shannon, C. (1948). A mathematical theory of communication. *Bell Syst. Tech. J.*, 27:379–423.

Singleton, R. (1967). On computing the fast fourier transform. *Commun. Assoc. Comput. Mach.*, 10:647.

Singleton, R. (1968). An algol procedure for the fast fourier transform with arbitrary factors. *Commun. Assoc. Comput. Mach.*, 11:776.

Smith, A. (1978). Color gammet transform pairs. *Computer Graphics*, 12(3):12–19.

Soha, J. and Schwartz, A. (1978). Multidimensional histogram normalization contrast enhancement. In *Proceedings of the 5th Canadian Symposium on Remote Sensing*, pages 86–93.

Stark, J. (2000). Adaptive image constrast enhancement using generalizations of histogram equalization. *IEEE Transactions on Image Processing*, 9(5):889–896.

Stigler, S. (1983). Who discovered bayes' theorem? *The American Statistician*, 37(4):290–296.

Strickland, R., Kim, C., and McDonel, W. (1987). Digital color image enhancement based on the saturation component. *Optical Engineering*, 26(7):609–616.

Tang, J. (2003). Image enhancement using a contrast measure in the compressed domain. *IEEE Signal Signal Processing Letters*, 10(10):289–292.

Tomita, F. and Tsuji, S. (1977). Extraction of multiple regions by smoothing in selected neighborhoods. *IEEE Transactions on Systems, Man and Cybernetics*, SMC-7:107–111.

Trahanias, P. and Venetsanopoulos, A. (1992). Color image enhancement through 3-d histogram equalization. In *Proceedings of 11th International Conference on Pattern Recognition (ICPR)*, pages 545–548. IAPR.

Trusell, J. (1977). A fast algorithm for noise smoothing based on a subjective criterion. *IEEE Transactions on Systems, Man and Cybernetics*, SMC-7:677–681.

Tukey, J. (1977). *Exploratory Data Analysis*. Addision-Wesley, Massachusetts, reading edition.

Wallis, R. (1976). An approach for the space variant restoration and enhancement of images. In *Proceedings of Symposium on Current Math. Prob. in Image Science*.

Wang, C. and Ye, Z. (2005). Brightness preserving histogram equalization with maximum entropy: A variational perspective. *IEEE Transactions on Consumer Electronics*, 51(4):1326–1334.

Wang, D., Vagnucci, A., and Li, C. (1983). Digital image enhancement: A survey. *Computer Vision, Graphics, and Image Processing*, 24(3):363–381.

Wang, Y., Chen, Q., and Zhang, B. (1999). Image enhancement based on equal area dualistic sub-image histogram equalization method. *IEEE Transactions on Consumer Electronics*, 45(1):68–75.

Wang, Z. and Bovik, A. (2006). *Modern Image Quality Assessment*. Morgan & Claypool Publishers.

Weeks, A., Hague, G., and Myler, H. (1995). Histogram specification of 24-bit color images in the color difference (c-y) color space. *Journal of Electronic Imaging*, 4(1):15–22.

Williams, B., Hung, C., Yen, K., and Coleman, T. (2001). Image enhancement using the modified cosine function and semi-histogram equalization for gray-scale and color images. In *Proceedings of the International Conference on Systems, Man and Cybernetics*, volume 1, pages 518–523. IEEE.

Woods, R. and Gonzalez, R. (1981). Real-time digital image enhancement. *Proceedings of IEEE*, 69(5):643–654.

Wyszecki, G. and Stiles, W. (1967). *Color Science*. Wiley, New York.

Yang, C. and Rodriguez, J. (1995). Efficient luminance and saturation processing techniques for bypassing color coordinate transformations. In *Proceedings of the International Conference on Systems, Man and Cybernetics*, volume 1, pages 667–672. IEEE.

Yen, J.-C., Chang, F.-J., and Chang, S. (1995). A new criterion for automatic multilevel thresholding. *IEEE Trans. Image Processing*, 4(3):370–378.

Yendrikhovskij, S., Blommaert, F., and de Ridder, H. (1998a). Optimizing color reproduction of natural images. In *Proceedings of the Sixth Color Imaging Conference: Color Sicence Systems and Applications*, volume 6, pages 140–145. IS&T/SID.

Yendrikhovskij, S., Blommaert, F., and de Ridder, H. (1998b). Perceptually optimal color reproduction. In *Proceedings of the Human Vision and Electronic Imaging III*, volume 3299, pages 274–281. SPIE.

Zhang, Q., Mlsna, P., and Rodriguez, J. (1996). 3-d histogram modification of color images. In *Proceedings of the Southwest Symposium on Image Analysis and Interpretation*, pages 218–223. IEEE.

Zhang, Y. (1992). Improving the accuracy of direct histogram specification. *Electronics Letters*, 28(3):213–214.

Zhu, H., Chan, F., and Lam, F. (1999). Image contrast enhancement by constrained local histogram equalization. *Computer Vision and Image Understanding*, 73(2):281–290.

Zimmerman, J., Pizer, S., Staab, E., Perry, J., McCartney, W., and Brenton, B. (1988). An evaluation of the effectiveness of adaptive histogram equalization for contrast enhancement. *IEEE Transactions on Medical Imaging*, 7(4):304–312.

Zuiderveld, K. (1994). Contrast limited adaptive histogram equalization. In Heckbert, P., editor, *G*raphics Gems IV, chapter VIII.5, pages 474–485. Academic Press, Cambridge, MA.